National Technical University of Athens

School of Mechanical Engineering

Machine Design Laboratory

Diploma Thesis

Michael A. Kremmydas

Analytical and Stochastic Modeling and Design of Optimal Performance FSAE Gearbox

Supervisor: Dr. V. Spitas

Professor NTU Athens

Athens

March 2019

Abstract

In motorsports, developing well engineered solutions is essential for designing a competitive race car. The need for reaching the limits of engineering is even more intense in Formula Student applications. This work deals with the complete development of a gearbox for a single-cylinder powered Formula Student vehicle. The optimal solution for a set of gear ratios is examined using both an analytical and a simulation-based approach. A stochastic optimization method is employed for the latter. The contribution of gear upshift and downshift engine speeds is also taken under consideration. Results are being extracted and combined from different Formula Student tracks and generalized conclusions are made for selecting appropriate gear ratios. The gearbox mechanical design is also being analyzed. Finally, choosing a non-conventional manufacturing method enabled designing beyond the existing gear module standards.

Περίληψη

Το κιβώτιο ταχυτήτων αποτελεί ένα τμήμα του συστήματος μετάδοσης κίνησης ενός οχήματος, ο σχεδιασμός του οποίου αποσκοπεί στο να επιτύχει την κατάλληλη σχέση μεταξύ στροφών κινητήρα και ταχυτήτων οχήματος. Καθότι κάθε κινητήρας συνήθως έχει διαφορετική συμπεριφορά συναρτήσει των στροφών του και κάθε όχημα διαφορετικό εύρος ταχυτήτων αναλόγως με το πεδίο χρήσης του, είναι προφανές ότι ο σχεδιασμός ενός κιβωτίου ταχυτήτων πρέπει να είναι άρρητα συνδεδεμένος με τον εκάστοτε συνδυασμό κινητήρα-οχήματος.

Αυτή η εργασία πραγματεύεται τον σχεδιασμό ενός κιβωτίου ταχυτήτων για το αγωνιστικό μονοθέσιο του 2019 της φοιτητικής ομάδας Prom Racing του Εθνικού Μετσόβιου Πολυτεχνείου. Το κιβώτιο αυτό προορίζεται να αντικαταστήσει την υπάρχουσα λύση που προσφέρει ο κατασκευαστής για τον μονοκύλινδρο κινητήρα KTM 500 EXC, με τον οποίο είναι εξοπλισμένο το μονοθέσιο της ομάδας.

Η εν λόγω ομάδα σχεδιάζει και κατασκευάζει ένα πλήρως λειτουργικό μονοθέσιο, με σκοπό την συμμετοχή στους διαγωνισμούς Formula Student. Λαμβάνοντας υπ όψιν τους κανονισμούς των διαγωνισμών, όλα τα συμμετέχοντα μονοθέσια σχεδιάζονται κάτω από κοινά πλαίσια.

Η μελέτη της επίδρασης των σχέσεων μετάδοσης στις επιδόσεις του μονοθέσιου πραγματοποιήθηκε μέσα από δύο διαφορετικές προσεγγίσεις. Κατ αρχήν, εξετάστηκε αναλυτικά το σενάριο επιτάχυνσης σε ευθεία γραμμή. Με αυτόν τον τρόπο διαπιστώθηκε πως, πέραν από τις σχέσεις μετάδοσης, σημαντικό ρόλο παίζουν οι στροφές του κινητήρα στις οποίες πραγματοποιούνται ανεβάσματα και κατεβάσματα ταχυτήτων. Επιδιώκοντας ελαχιστοποίηση του χρόνου επιτάχυνσης, αναπτύχθηκαν διάφορες αναλυτικές αναδρομικές σχέσεις για την εύρεση των βέλτιστων στροφών ανεβάσματος ταχυτήτων και των βέλτιστων σχέσεων μετάδοσης.

Μέσα από την προηγηθείσα ανάλυση διαπιστώθηκε πως διάφορα σενάρια οδήγησης μέσα σε μια πίστα αγώνων ταχύτητας δεν καλύπτονται από μια απλή επιτάχυνση σε ευθεία γραμμή. Κατά συνέπεια, σε μια δεύτερη προσέγγιση, διαμορφώθηκε ένα μοντέλο προσομοίωσης για το μονοθέσιο, ώστε να εξεταστεί με μεγαλύτερη ακρίβεια ο χρόνος πίστας. Στην μοντελοποίηση αυτή, χρησιμοποιήθηκε ένα καμπυλόγραμμο σύστημα συντεταγμένων για την τοπολογία της πίστας και της επιθυμητής τροχιάς εντός αυτής. Έπειτα, με βάση ένα full-car model, διαμορφώθηκαν οι δυναμικές εξισώσεις ισορροπίας δυνάμεων και ροπών. Για τον προσδιορισμό των κάθετων δυνάμεων στα ελαστικά, πραγματοποιήθηκε μια ανάλυση της λειτουργίας της ανάρτησης και διαμορφώθηκε ένα σύστημα δύο διαφορικών εξισώσεων για την κλίση (pitch) και την περιστροφή (roll) του αμαξώματος. Η συμπεριφορά των ελαστικών μοντελοποιήθηκε σύμφωνα με την Magic Formula που αναπτύχθηκε από τον Pacejka.

Πέραν από την προαναφερθείσα κύρια μοντελοποίηση, πραγματοποιήθηκε ανάλυση της λειτουργίας και των υπολοίπων υποσυστημάτων του μονοθέσιου. Αυτά περιλαμβάνουν το σύστημα μετάδοσης κίνησης και το διαφορικού περιορισμένης ολίσθησης, το σύστημα πέδησης και το σύστημα αλλαγής ταχυτήτων. Επιπλέον, διαμορφώθηκε ένα μοντέλο για τον οδηγό, κύρια στοιχεία του οποίου αποτελούν ο περιορισμός των πλευρικών και εγκάρσιων επιταχύνσεων μέσω ενός μοντέλου friction ellipse, η διαμόρφωση μιας επιθυμητής τροχιάς στην πίστα και ενός PID ελεγκτή για το σύστημα διεύθυνσης με στόχο την ακολούθηση αυτής της τροχιάς.

Τα αποτελέσματα χρόνου πίστας των προσομοιώσεων χρησιμοποιήθηκαν για την εύρεση του συνδυασμού σχέσεων μετάδοσης. Μια στοχαστική τεχνική βελτιστοποίησης αναπτύχθηκε και εφαρμόστηκε για αυτόν τον σκοπό.

Τα αποτελέσματα της αναλυτικής προσέγγισης και της στοχαστικής βελτιστοποίησης για τρεις διαφορετικές πίστες διαγωνισμών Formula Student συγκρίνονται, διακρίνοντας κάποια γενικά συμπεράσματα στον βέλτιστο σχεδιασμό του κιβωτίου ταχυτήτων. Τα αποτελέσματα για κάθε μια ανάλυση προκύπτουν διαφορετικά, όμως με κατάλληλο συνδυασμό επιτυγχάνεται ένα αρκετά ικανοποιητικό αποτέλεσμα για όλες τις περιπτώσεις.

Τέλος, πραγματοποιείται ο μηχανολογικός σχεδιασμός του κιβωτίου. Κάθε βαθμίδα μετάδοσης υλοποιείται με κατάλληλο υπολογισμό των οδοντώσεων, λαμβάνοντας υπ όψιν θέματα κατασκευασιμότητας και αντοχής. Η διάταξη των ταχυτήτων και ο τρόπος εναλλαγής τους εξετάζεται για τον σχεδιασμό ενός τμήματος του συστήματος αλλαγής ταχυτήτων. Η αντοχή του κυρίως σώματος των οδοντωτών τροχών μελετάται με χρήση πεπερασμένων στοιχείων.

Table of Contents

List of figures

List of tables

1. Introduction

1.1 Problem Statement

The general purpose of a gearbox is to be a part of the powertrain connecting the engine of a vehicle and its wheels, while facilitating a certain or a multiple number of drive ratios. The presence of drive ratios is necessary since a vehicle's engine and the vehicle itself always operate within a certain range of speeds. Moreover, the behavior of an engine, for example its efficiency and output torque, usually differs according to its rotational speed. These two simple aspects outline a significant outcome; the design of a gearbox must be performed so as to produce a tailor-made solution for a given engine and the desired vehicle performance.

The design presented in this work is to be implemented in the race car of the Formula-Student team Prom Racing (figure 1). Prom Racing is a team of the National Technical University of Athens that was founded in 2008 and has been active ever since, having designed and manufactured three race cars up to this time. Therefore, all the design efforts are placed upon maximizing the performance of the vehicle that this team develops and, more specifically, of the new fourth vehicle to be designed and manufactured in the team's history, dedicated to participate in Formula Student competitions of 2019.

Figure 1: The Logo of Prom Racing

As a first general assumption, it can be said that the purpose of the gearbox to be designed within this work, is such that maximizes the performance of a Formula-Student type racing vehicle. However, even though all vehicles of this type seem to share similar concepts, they do not share the same characteristics. The main reason is that, even though restrictions are posed upon the engine from the regulations of the competition, the number of cylinders is not specified. Single, double, triple and four cylinder engines are all very popular in Formula Student vehicles. With that being said, the rotational speed range, as well as the amount of torque produced, can vary significantly from vehicle to vehicle.

Usually, multi-cylinder vehicles are heavier but more powerful, while single cylinder ones are lighter but less powerful. This is a very distinct difference between Formula

Student vehicles. For example, the 2018 race car of Prom Racing (figure 2) is using a single cylinder KTM engine, while CAT Racing (figure 3), a very competitive team from the University of Coburg, is using a 4 cylinder Yamaha engine. Both vehicles seem to be very similar and build upon the same concept. However, this is comparison is not close to reality, should the difference of engine and possibly vehicle dynamics be taken under consideration.

Figure 2: A Formula Student vehicle by Prom Racing

Figure 3: A Formula Student vehicle by CAT Racing

Therefore, the scope of the gearbox to be designed is such that serves the needs of the specific car designed by the team. That being said, engine performance and vehicle dynamics, influencing the speeds of the car on the track, should be taken under consideration.

1.2 About Formula Student competitions and their regulations

Formula Student competitions are fully defined, both in their organizational aspects, as well as in the engineering design and limitations of the participant vehicles, by a series of regulations. Up to the year of 2016, these regulations were written and published by the Formula SAE (Society of Automotive Engineers) and hence were referred to as FSAE rules. Competitions were held worldwide and organized by different committees, but all adhered to those rules. Usually, most of them would make minor changes to those rules, which would be active in the specific competition only.

As of 2017, the German based competition FSG (Formula Student Germany) announced they would be establishing their own set of rules. Quickly, most European competitions also announced that they would follow the FSG [1] instead of the FSAE rules. From that period and onwards, both set of regulations exist, having mainly minor differences between each other. However, since Prom Racing team has, up to the present year, plans for participating at European competitions, the vehicle to be designed adheres to the FSG rules.

According to the FSG rules, the competition objective is to challenge "[…] *teams of university students to conceive, design, fabricate, develop and compete with small, formula style, race cars".* In addition "*The competition is split into the following classes:*

• *Internal Combustion Engine Vehicle (CV)*

• *Electric Vehicle (EV)*

• *Driverless Vehicle (DV) (which are either CV or EV) "*

The vehicles that have been designed by the team, as well as the new vehicle to be designed, are all combustion vehicles.

All competitions include, as described by the rules, Static and Dynamic events. During the Static events, the car is stationary and participants are tested for their knowledge mainly upon, but not only limited to, different engineering fields. During the Dynamic events, the vehicle races in a series of tracks and is evaluated mainly based on its times. Points are being extracted out of each event and the ranking is

based upon those points. The maximum points that can be gathered can be seen at Table 1.

	CV & EV	DV
Static Events:		
Business Plan Presentation	75 points	75 points
Cost and Manufacturing	100 points	100 points
Engineering Design	150 points	300 points
Dynamic Events:		
Skid Pad	75 points	75 points
Acceleration	75 points	75 points
Autocross	100 points	100 points
Endurance	325 points	-
Efficiency	100 points	75 points
Trackdrive	-	200 points
Overall	1000 points	1000 points

Table 1: Maximum points for each event

Concerning the dynamic events, the points are granted using different calculation formulas containing the time taken to accomplish each event. A brief explanation of each dynamic event, as well as its scoring can be seen at Table 2. It must be mentioned that details such as penalties and special cases of the rules are not mentioned in this table.

Concerning the vehicle itself, FSG rules specify that the *"[…] vehicle must be open-wheeled, single seat and open cockpit (a formula style body) with four wheels that are not in a straight line".* Many technical regulations and limitations concerning the design and strength of several components of the vehicle, such as the chassis, suspension and aerodynamic devices, are also present within the rules.

The engine of combustion vehicles is also restricted. The rules state that *"The engine(s) used to power the vehicle must be piston engine(s) using a four-stroke primary heat cycle with a displacement not exceeding 710 cm^3 per cycle. Hybrid powertrains, such as those using electric motors running off stored energy, are prohibited".* It is also stated that a single circular restrictor must be placed at the air intake system so that all air passes through it. The diameter of the restrictor should be 20mm or 19mm, depending on whether gasoline or E85 fuel blend is used.

Event	Track	Brief Explanation	Scoring Formula*
Skid Pad	Two circles in a figure of eight pattern	Driver performs 2 laps at each circle, with the 2nd being timed	$71.5\frac{\left(\frac{T_{max}}{T_{team}}\right)^2 - 1}{0.5625} + 3.5$
Acceleration	Straight of 75m	Driver accelerates fully in a straight line	$71.5\frac{\frac{T_{max}}{T_{team}} - 1}{0.5} + 3.5$
Autocross	Closed track, less than 1.5km	Driver performs a single timed lap	$95.5\frac{\frac{T_{max}}{T_{team}} - 1}{0.25} + 4.5$
Endurance	Closed track (similar or the same with the Autocross track)	2 Drivers perform multiple timed laps, 11 km driven per driver, includes non-timed driver change	$300\frac{\frac{T_{max}}{T_{team}} - 1}{0.333} + 25$
Efficiency	Endurance track	Measured fuel burnt during the endurance event	$100\frac{\frac{E_{min}}{E_{team}} - 1}{\frac{E_{min}}{E_{max}} - 1}$

Table 2: Description of Dynamic events

***T_{team} is the team's time**

*** T_{max} is the time of the fastest vehicle multiplied by a factor different for each event**

***E_{min} , E_{team} and E_{max} are the minimum, the team's and the maximum efficiency factors recorded respectively, where the efficiency factor calculated as $E = \frac{T_{min} \cdot V_{min}}{T_{team} \cdot V_{team}}$, where V_{min} and V_{team} are the minimum and the team's used fuel volume respectively**

1.3 The Motivation

The main reason why the original gearbox of the engine does not perform in the most effective way for Formula Student applications is the speed range the vehicle is expected to attain. As mentioned earlier, FSG rules limit the displacement of the vehicle's engine to 710 cm^3. This makes performance motorcycle engines be the first, if not the only choice for Formula Student teams. Usually the weight of those motorcycles is not far from that of a Formula Student vehicle. This makes the first gear ratio usually adequate for both applications. Most of the motorcycles however, are expected to reach at least 150 km/h, whereas top speeds for combustion vehicles in Formula Student competitions rarely exceed 105 km/h. Therefore, the last gear ratio cannot satisfy both requirements.

The teams that do not change the engine's standard gearbox change the final drive ratio of the transmission, so as to improve the inadequate last gear ratio. With this technique, all the gear ratios increase, therefore giving more torque to the wheels,

rendering this modification beneficial. Even in this case though, usually the matching of the final gear ratio to the desired top speed alters some of the rest of the gear ratios in a non-beneficial way. One reason justifying this fact is that, at some gear ratios, the resultant engine speed might be at a range where the output torque is low. The driver might decide to downshift a gear, but the next lower gear results in too high engine speed.

Another significant reason more usual than the one mentioned earlier, is the presence of too many gear shifts. A gear shift takes a non-negligible amount of time so as to be completed. Within this period, no engine torque is transferred to the wheels. If this dead time appears for example during a gear upshift, but the resultant torque at the wheels is not adequately increased in comparison to the torque before the gear change, then the gear change is not beneficial. Of course, the gear change must be performed as the engine always has a maximum speed limitation.

Besides the improvement in the performance of the car, a gearbox design is also a significant study than can be presented at the Engineering Design event of the competitions. Usually, most of the well reputed teams perform this design; therefore the absence of such a study is usually a negative aspect for the design judges.

1.4 Project Constraints

As mentioned earlier, the gearbox that will be designed is designated for the fourth vehicle of the Formula Student team Prom Racing. Consequently, the project is constrained to serve the design of the aforementioned vehicle, as well as the resources and capabilities of the team. All those constraints can be easily concentrated and are presented at Table 3.

Constraint	Description
Time	The project started in February 2018 and should be completed before the testing period of the vehicle in April 2019.
Budget	The money to be spent for outsourced manufacturing services should not exceed 5000€.
Engine	The engine of the vehicle will be a 2012 KTM 500 EXC motorcycle engine. Output torque and engine speed relation is known and will not change significantly. The gearbox should replace the already existing gearbox of the engine.
Shifting System	Electronically controlled shifting system, capable of receiving data from multiple sensors. Mean shifting time is approximately to 0.2 sec, measured from the previous year's vehicle.
Vehicle	Chassis, suspension and aerodynamic package as designed by the team, according to the FSG rules.

Table 3: Project Constraints

1.5 Literature Review

In the automotive industry, the design of a gearbox is a study that usually focuses on fuel economy. Both analytical work, as well as algorithms based on vehicle simulation, have been published for the optimization of fuel consumption. However, as far as the design of a gearbox for improved racing performance, little published work exists. Optimization algorithms using vehicle dynamics simulation, given a certain vehicle and race track, are most common. Savaresi et al. [2] have used a simple one dimensional simulator performing acceleration and braking in a specified track. Using this, they run a set of possible gear ratios of a 6-speed gearbox, for determining the optimal solution as the one that minimizes lap time.

More specific work focusing on Formula Student applications is also seldomly published. Most of the projects that deal with transmission design for combustion vehicles mainly focus on the mechanical design, rather than on the selection of gear ratios. Avgerinos (Αυγερινός) [3] used the design of progressive and geometrical gearbox architecture, to define multiple different concepts for the gear ratios. These were tested for their performance in multiple Formula Student events using the commercial vehicle dynamics software CAR MAKER [4].

In this work, an effort to combine already existing knowledge and a new approach will be integrated. An analytical optimization will be used as a first approach. Conclusions will be taken from this analysis and a vehicle dynamics simulation will be used for determining the most suitable gear ratios.

2. Methods used for determining gear ratios

2.1 The influence of multiple competition events

Given a description of the overall concept of Formula Student through the respective rules and regulations, it is clear that a measure of the performance of a Formula Student vehicle is the number of points it receives in a competition. Concerning the Static events, it is evident that a well justified gearbox design will result to extra points in the Engineering Design event. The rest of the static events are not directly connected with such a project. Any indirect influence to those events will not be taken under consideration. As a result, the development of the gearbox should aim at increasing the performance of the vehicle in the Dynamic events.

Concerning the Dynamic events, again not all get influenced by the gearbox design. Particularly, the Skidpad event should be considered as a traction limited and not engine power limited race. The vehicle should perform small radius cornering as fast as possible. This means that relatively low speeds are attained, allowing the usage of a drive ratio that can provide the wheels with more than sufficient torque.

Another example is the Fuel Efficiency event. In general, Formula Student is mainly a race and not a fuel efficiency competition. This is clear, as 325 points are granted for the best time in the Endurance event, whereas only 100 points will be gained for best fuel efficiency in the Endurance track. In addition, the fuel efficiency competition is only a 10% of the overall points, whereas all the rest of the dynamic competitions can add up to 57.5% of the total score.

Besides that fact, when a large radius in a track is encountered, a race driver will always decide to accelerate using the entire engine load capacity. This prevents almost any fuel economy to be achieved in straight lines. Therefore, only near-steady speed parts of the track will have a chance of better fuel economy. This fact significantly limits the extent up to which fuel consumption can be decreased by designing a new gearbox.

Nevertheless, if a gearbox would be designed so as to improve fuel economy, design efforts would be placed on using an appropriate gear ratio for partial engine load conditions. For this reason, it is necessary to know the relationship between engine speed and fuel consumption for the power output of the engine, also known as brake specific fuel consumption (BSFC). An example of a BSFC map can be seen in figure 4. Unfortunately, given the limited time the team has for tuning the engine on a dynamometer, full load conditions are mainly tuned. Partial load is also examined, but in a limited number of engine speed and engine load combinations. This practice results to decent fuel economy, but does not provide enough information so as to construct a BSFC map.

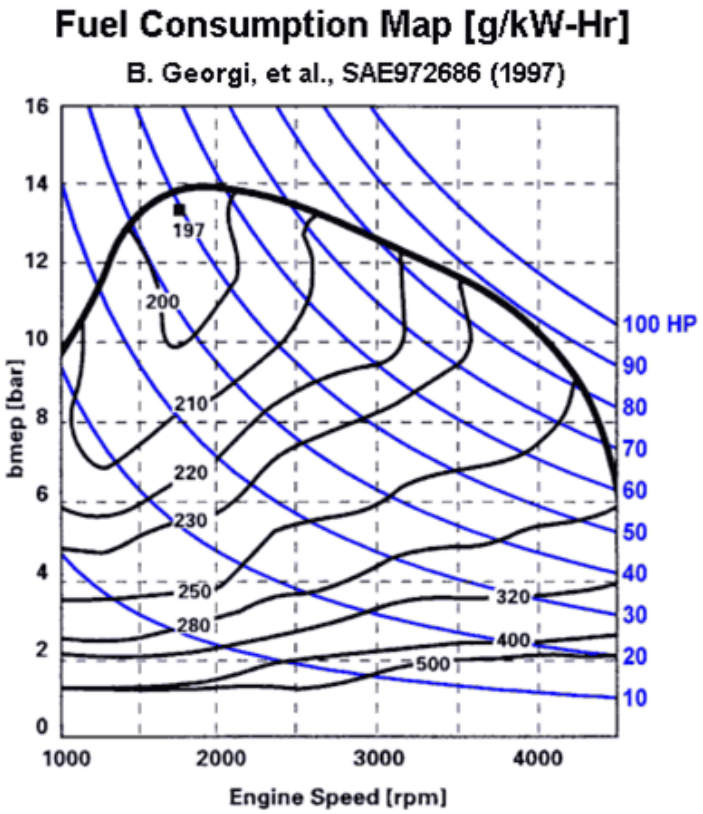

Figure 4: Typical BSFC map

Concluding, the performance in only three Dynamic events will be considered in the process of selecting gear ratios. Those are the Autocross, Endurance and Acceleration events. The points granted by those events are given by the FSG rules to be:

$$\text{Acceleration Score} = 71.5\frac{\frac{1.5 \cdot T_{min}}{T_{team}} - 1}{0.5} + 3.5 \quad (1)$$

$$Autocross\ Score = 95.5\frac{\frac{1.25 \cdot T_{min}}{T_{team}} - 1}{0.25} + 4.5 \quad (2)$$

$$Endurance\ Score = 300\frac{\frac{1.333 \cdot T_{min}}{T_{team}} - 1}{0.333} + 25 \quad (3)$$

where T_{min} is the time of the fastest vehicle and T_{team} is the team's time recorded for each event.

In general, if the behavior of the vehicle and the driver can be modeled and simulated, an approach of searching for the drive ratios that maximize the sum of the points for the three events can be adopted. This is a classic case of optimization. However, as every method of this kind, an initial point is required. Moreover, a solution that might

come as result which is considered to be an optimum is likely to be a localized optimum, as it is far from some generally acceptable guidelines for the design of a gearbox.

At this point, it is evident that there is a need of calculating a set of gearbox gear ratios that can be considered as a generally fair design and decent starting point. For this reason, before executing a simulation so as to maximize the points, a more analytical and simplified approach will be used.

2.2 The analytical method

Lap performance of the vehicle can be modeled as a series of straight lines with acceleration and braking and turns at constant speed or with acceleration under torque, limited by tire traction. Within this modeling, an important assumption has been made. More specifically, it was assumed that the engine is not under full load during turning. This is because, at each turn, significant values of lateral acceleration will be achieved and traction will be greatly limited by the tires, due to combined lateral and longitudinal acceleration. Therefore, as a first approach, it is logical that only the time spent during straight line acceleration is examined.

Considering the acceleration of the engine rotational masses negligible compared to the mass of the vehicle and neglecting tire rolling friction, the equation of motion in the case of straight line acceleration is:

$$m\ddot{x} = \frac{i_k T_{(n)}}{R} - \frac{1}{2}\rho C_D A(\dot{x})^2 \tag{4}$$

where n is the engine speed, m is the total vehicle mass, T is the engine crankshaft effective torque as measured at the wheels, i_k are the final transmission ratios of each gear (k) (k=1,2,…,m), R is the loaded rolling radius of the tire and $\frac{1}{2}\rho C_D A(\dot{x})^2$ is the aerodynamic drag.

Neglecting any tire slippage, the engine speed in rpm is coupled with the vehicle speed as:

$$\dot{x} = \frac{\pi}{30}\frac{R}{i_k}n \tag{5}$$

Therefore, eq. (5) can be rewritten as:

$$\dot{n} = f_k(n) \tag{6}$$

where the function:

$$f_k(n) = \frac{1}{m}\left[\frac{30}{\pi}\frac{{i_k}^2}{R^2}T_{(n)} - \frac{\pi}{30}\frac{1}{2}\rho C_D A\frac{R}{i_k}n^2\right] \tag{7}$$

is different for each gear (k).

Let $n_{1,k}$ and $n_{2,k}$ (figure 5) be the range of engine speeds for which the engine is operating at each gear (k). Then the time spent at each gear (k) can be found by integration of eq. (6):

$$\Delta T_{1\to 2} = \int_{n_{1,k}}^{n_{2,k}} \frac{dn}{f_k(n)} \tag{8}$$

It is now obvious that the total lap-time spend during straight line acceleration is:

$$\Delta T = \sum_{s} (\Delta T_s) = F(n_{1,k,s}\,, n_{2,k,s}\,,\, i_k) \tag{9}$$

where the indicator (s) changes for each straight line.

The preceding analysis reveals that, except for gear ratios i_k for each gear (k), there are more parameters to be examined. These are the engine speeds $n_{1,k,s}\,, n_{2,k,s}$ for each gear (k) and straight line (s). Therefore, in an attempt to minimize straight line lap-time ΔT, the engine speeds and gear ratios are examined separately.

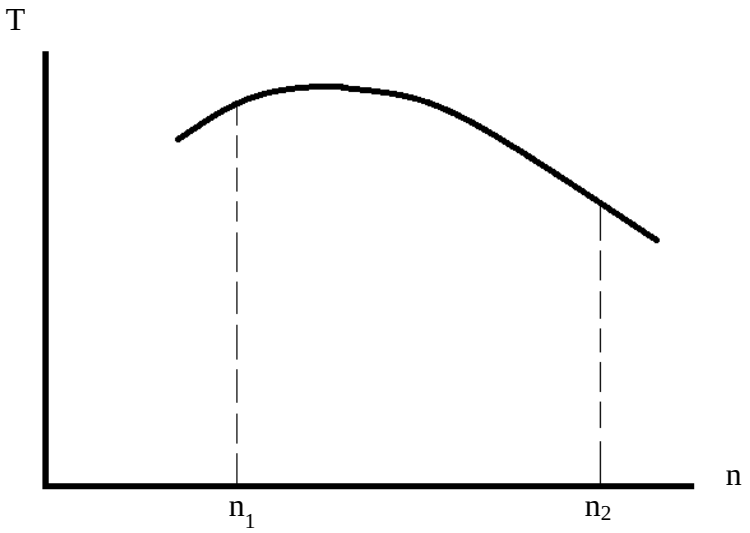

Figure 5: Engine speed range

As mentioned earlier, engine speed is coupled with vehicle speed. The track speeds of the vehicle are dependent upon:

- The length of the straight lines
- The radius of the turns
- The way turns of different radius, or turns and straight lines, are being interchanged between each other

Therefore, it can be understood that the shape of the track will influence engine speeds $n_{1,k,s}\,, n_{2,k,s}$ at each straight line (s). To waive this constraint, it will be

attempted to examine each straight line separately. Therefore, at each individual straight line, the acceleration time can be calculated as:

$$\Delta T_s = \int_{n_{1,g_s,s}}^{n_{2,g_s,s}} \frac{dn}{f_{g_s}(n)} + \sum_{j=g_s+1}^{G_s-1} \int_{n_{1,j,s}}^{n_{2,j,s}} \frac{dn}{f_j(n)} + \int_{n_{1,G_s,s}}^{n_{2,G_s,s}} \frac{dn}{f_{G_s}(n)} \tag{10}$$

where g_s and G_s is the first and final ratio used at each straight line (s).

During each gear upshift, from gear (k) to gear (k+1), the shifting system will 'kill' the engine load by disabling ignition and fuel delivery. Due to friction the engine speed will decrease and, over the shift time, the car speed will remain approximately steady. Using this assumption, from eq. (5) it follows that:

$$n_{1,k+1,s} = n_{2,k,s} \frac{i_{k+1}}{i_k} \tag{11}$$

Substituting to eq. (10) yields:

$$\Delta T_s = \int_{n_{1,g_s,s}}^{n_{2,g_s,s}} \frac{dn}{f_{g_s}(n)} + \sum_{j=g_s+1}^{G_s-1} \int_{\frac{i_j}{i_{j-1}} n_{2,j-1,s}}^{n_{2,j,s}} \frac{dn}{f_j(n)} + \int_{n_{1,G_s,s}}^{n_{2,G_s,s}} \frac{dn}{f_{G_s}(n)} \tag{12}$$

It is obvious that all engine start speeds $n_{1,k,s}$ are dependent upon $n_{2,k-1,s}$, except for $n_{1,g_s,s}$, which cannot be changed. Also, the speed $n_{2,G_s,s}$ cannot be changed. Therefore, the speeds $n_{2,k,s}$ can be optimized for k=g_s, g_{s+1},…, Gs-1 by finding the root of the derivative of eq. (12):

$$\frac{\partial \Delta T_j}{\partial n_{2,k,j}} = 0 \Rightarrow \frac{\partial}{\partial n_{2,k,s}} \int_{n_{1,g_s,s}}^{n_{2,g_s,s}} \frac{dn}{f_{g_s}(n)} + \sum_{j=g_s+1}^{G_s-1} \left[\frac{\partial}{\partial n_{2,k,s}} \int_{\frac{i_j}{i_{j-1}} n_{2,j-1,s}}^{n_{2,j,s}} \frac{dn}{f_j(n)} \right] = 0 \Rightarrow$$

$$\xrightarrow{\substack{the\ terms\ not\ containing \\ n_{2,k,s}\ vanish}} \frac{\partial}{\partial n_{2,k,s}} \left[\int_{\frac{i_k}{i_{k-1}} n_{2,k-1,s}}^{n_{2,k,s}} \frac{dn}{f_k(n)} + \int_{\frac{i_{k+1}}{i_k} n_{2,k,s}}^{n_{2,k+1,s}} \frac{dn}{f_{k+1}(n)} \right] = 0 \Rightarrow$$

$$\Rightarrow \frac{1}{f_k(n_{2,k,s})} - \frac{i_{k+1}}{i_k} \frac{1}{f_{k+1}\left(\frac{i_{k+1}}{i_k} n_{2,k,s}\right)} = 0 \Rightarrow$$

$$\Rightarrow f_k(n_{2,k,s}) = \frac{i_k}{i_{k+1}} f_{k+1}\left(\frac{i_{k+1}}{i_k} n_{2,k,s}\right) \tag{13}$$

It is now obvious that the problem is the same for every straight line (s). Eliminating the indicator s, the relationship above can be rearranged and rewritten as:

$$T(n_{2,k}) = \frac{i_{k+1}}{i_k} T\left(\frac{i_{k+1}}{i_k} n_{2,k}\right) \tag{14}$$

Eq. (14) leads to valid solutions only for $n_{2,k}$<n_{max}, where n_{max} is the maximum speed of the engine. Additionally, to obtain a minimum for the time ΔT, the derivative $\frac{\partial \Delta T}{\partial n_{2,k}}$ must be negative for every speed bellow the selected $n_{2,k}$. Equivalently:

$$T(n) > \frac{i_{k+1}}{i_k} T\left(\frac{i_{k+1}}{i_k} n\right) \text{ for every speed n} < n_{2,k} \tag{15}$$

It can be noted that, by multiplying both sides of eq. (14) with $n_{2,k}$, a more compact relation arises using only the engine effective output power P, measured again at the wheels:

$$P(n_{2,k}) = P\left(\frac{i_{k+1}}{i_k} n_{2,k}\right) \tag{16}$$

Eq. (16) indicates that, in an ideal engine maintaining constant power, there is no need for gear shifting. However, engine power usually increases for all engine speeds and decreases only slightly, if not at all, close to the engine maximum speed n_{max}. Since $i_{k+1} < i_k$, eq. (16) evidently shows that there is no need for shifting into another gear at an engine speed where output power has yet not started decreasing. As a result, the optimal gear shift speed will usually coincide with n_{max}.

Since the selection of shift speeds becomes independent for every track straight line (s), from this point onward the indicator (s) will be eliminated when referring to shift speeds $n_{2,k}$ and $n_{1,k}$. It is also evident that the selection of shift speeds becomes independent from the aerodynamic drag.

Examining the gear ratios now, should the same methodology be used as before, it is evident that the derivative of eq. (12) with respect to the gear ratios is:

$$\frac{\partial \Delta T_j}{\partial i_k} = \frac{\partial}{\partial i_k} \int_{n_{1,g_s}}^{n_{2,g_s}} \frac{dn}{f_{g_s}(n)} + \sum_{j=g_s+1}^{G_s-1} \left[\frac{\partial}{\partial i_k} \int_{\frac{i_j}{i_{j-1}} n_{2,j-1}}^{n_{2,j}} \frac{dn}{f_j(n)} \right] + \frac{\partial}{\partial i_k} \int_{n_{1,G_s}}^{n_{2,G_s}} \frac{dn}{f_{G_s}(n)} \tag{17}$$

differs in the cases k=g_s, g_s+1<G_s-2, k= G_s-1 and k= G_s. Therefore, each straight line cannot be directly examined independently. To once again eliminate this constraint, the following percentages-frequencies of usage are employed:

- $P_{1,k}$: the usage frequency of ratio i_k so as to begin accelerating with a mean engine speed of $\overline{n_{1,k}} > \frac{i_k}{i_{k-1}} n_{2,k-1}$, while within the straight line there is a satisfactory gear change from gear (k) to gear (k+1)
- $P_{2,k}$: the usage frequency of ratio i_k so as to begin accelerating with a mean engine speed $\overline{n_{1,k}} > \frac{i_k}{i_{k-1}} n_{2,k-1}$, while within the straight line no gear change occures

- $P_{3,k}$: the usage frequency of ratio i_k as an intermediate gear ratio, so as to accelerate from $n_{1,k} = \frac{i_k}{i_{k-1}} n_{2,k-1}$ to $n_{2,k}$
- $P_{4,k}$: the usage frequency of ratio i_k as an intermediate gear ratio, so as to accelerate from $n_{1,k} = \frac{i_k}{i_{k-1}} n_{2,k-1}$ to a mean engine speed of $\overline{n_{2,k}} < n_{2,k}$
- P_{start}: the usage frequency of ratio i_1 as a starting gear from n_{start} to $n_{2,1}$

Taking the percentages-frequencies of usage under consideration, instead of expressing the straight line lap-time for each straight line separately, the total straight line lap-time can be rewritten as:

$$\begin{aligned} \Delta T = P_{start} \int_{n_{start}}^{n_{2,1}} \frac{dn}{f_1(n)} + P_{1,1} \int_{\overline{n_{1,1}}}^{n_{2,1}} \frac{dn}{f_1(n)} + P_{2,1} \int_{\overline{n_{1,1}}}^{\overline{n_{2,1}}} \frac{dn}{f_1(n)} \\ + \sum_{j=2}^{m} \left[P_{1,j} \int_{\overline{n_{1,j}}}^{n_{2,j}} \frac{dn}{f_j(n)} + P_{2,j} \int_{\overline{n_{1,j}}}^{\overline{n_{2,j}}} \frac{dn}{f_j(n)} \right. \\ \left. + P_{3,j} \int_{\frac{i_j}{i_{j-1}} n_{2,j-1}}^{n_{2,j}} \frac{dn}{f_j(n)} + P_{4,j} \int_{\frac{i_j}{i_{j-1}} n_{2,j-1}}^{\overline{n_{2,j}}} \frac{dn}{f_j(n)} \right] \end{aligned} \tag{18}$$

where m is the number different gear ratios. It is evident that for the first and last gear:

$$\left\{ \begin{matrix} P_{3,1} = P_{4,1} = 0 \\ P_{3,m} = P_{1,m} = 0 \end{matrix} \right\} \tag{19}$$

The percentages $P_{1,k}$, $P_{2,k}$, $P_{3,k}$, $P_{4,k}$ and P_{start} will mainly depend upon the race-track. Even if it is considered that they are independent from the gear ratio selection, the relations resulting the equation $\frac{\partial \Delta T}{\partial i_k} = 0$ will depend upon those percentages. Also, it is essential that the speeds $\overline{n_{1,k}}$ and $\overline{n_{2,k}}$ are known. This indicates the need for a lap-time simulation.

However, as a first approximation, it may be considered that at each turn, due to the fact that the driver has reached the speed that describes the maximum lateral acceleration, the corner speeds are approximately constant. Therefore, the acceleration from each entry in a corner, continues from the same point after the exit from the corner. This enables the simplification of the problem above as being a single straight line acceleration problem. In this case the following sets of equations arise:

$$\left\{ \begin{matrix} k = 1 \Rightarrow P_{1,1} = P_{2,1} = 0 \; and \; P_{start} = 1 \\ k = 2,3, \dots, m-1 \Rightarrow P_{1,k} = P_{2,k} = P_{4,k} = 0 \; and \; P_{3,k} = 1 \\ k = m \Rightarrow P_{2,m} = 0 \; and \; P_{4,m} = 1 \end{matrix} \right\} \tag{20}$$

This simplifies straight line lap-time as:

$$\Delta T = \int_{n_{start}}^{n_{2,1}} \frac{dn}{f_1(n)} + \sum_{j=2}^{m-1} \left[\int_{\frac{i_j}{i_{j-1}} n_{2,j-1}}^{n_{2,j}} \frac{dn}{f_j(n)} \right] + \int_{\frac{i_m}{i_{m-1}} n_{2,m-1}}^{\overline{n_{2,m}}} \frac{dn}{f_m(n)} \tag{21}$$

Differentiating eq. (21) with respect to the gear ratios i_k for k=2,3,…,m-1 yields:

$$\frac{\partial \Delta T}{\partial i_k} = \sum_{j=2}^{m-1} \left[\frac{\partial}{\partial i_k} \int_{\frac{i_j}{i_{j-1}} n_{2,j-1}}^{n_{2,j}} \frac{dn}{f_j(n)} \right] + \frac{\partial}{\partial i_k} \int_{\frac{i_m}{i_{m-1}} n_{2,m-1}}^{\overline{n_{2,m}}} \frac{dn}{f_m(n)} \xrightarrow{\substack{the\ terms\ not\ containing \\ n_{2,k,s}\ vanish}}$$

$$\Rightarrow \frac{\partial \Delta T}{\partial i_k} = \frac{\partial}{\partial i_k} \int_{\frac{i_k}{i_{k-1}} n_{2,k-1}}^{n_{2,k}} \frac{dn}{f_k(n)} + \frac{\partial}{\partial i_k} \int_{\frac{i_{k+1}}{i_k} n_{2,k}}^{n_{2,k+1}} \frac{dn}{f_{k+1}(n)} \Rightarrow$$

$$\Rightarrow \frac{\partial \Delta T}{\partial i_k} = -\left[\frac{n_{2,k-1}}{i_{k-1}} \frac{1}{f_k\left(\frac{i_k}{i_{k-1}} n_{2,k-1}\right)} + \int_{\frac{i_k}{i_{k-1}} n_{2,k-1}}^{n_{2,k}} \frac{\partial f_k(n)}{\partial i_k} \frac{dn}{f_k^2(n)} \right] + \frac{i_{k+1}}{{i_k}^2} \frac{n_{2,k}}{f_{k+1}\left(\frac{i_{k+1}}{i_k} n_{2,k}\right)} \tag{22}$$

For $\frac{\partial \Delta T}{\partial i_k} = 0$ the following recursive relationship can be obtained:

$$\frac{i_{k+1}}{{i_k}^2} \frac{n_{2,k}}{f_{k+1}\left(\frac{i_{k+1}}{i_k} n_{2,k}\right)} - \frac{n_{2,k-1}}{i_{k-1}} \frac{1}{f_k\left(\frac{i_k}{i_{k-1}} n_{2,k-1}\right)} = \int_{\frac{i_k}{i_{k-1}} n_{2,k-1}}^{n_{2,k}} \frac{\partial f_k(n)}{\partial i_k} \frac{dn}{f_k^2(n)} \tag{23}$$

Note that with differentiation of eq. (7):

$$\frac{\partial f_k(n)}{\partial i_k} = \frac{1}{m} \left[\frac{60}{\pi} \frac{i_k}{R^2} T_{(n)} + \frac{\pi}{30} \frac{1}{2} \rho C_D A \frac{R}{{i_k}^2} n^2 \right] \tag{24}$$

Differentiating eq. (21) with respect to the first gear ratio i_1 yields:

$$\frac{\partial \Delta T}{\partial i_1} = \frac{\partial}{\partial i_1} \int_{n_{start}}^{n_{2,1}} \frac{dn}{f_1(n)} + \frac{\partial}{\partial i_1} \int_{\frac{i_2}{i_1} n_{2,1}}^{n_{2,2}} \frac{dn}{f_2(n)} \Rightarrow$$

$$\Rightarrow \frac{\partial \Delta T}{\partial i_1} = -\left[\frac{dn_{start}}{di_1} \frac{1}{f_1(n_{start})} + \int_{n_{start}}^{n_{2,1}} \frac{\partial f_1(n)}{\partial i_1} \frac{dn}{f_1^2(n)} \right] + \frac{i_2}{{i_1}^2} \frac{n_{2,1}}{f_2\left(\frac{i_2}{i_1} n_{2,1}\right)} \tag{25}$$

For minimizing the lap-time in respect to the first gear ratio $\frac{\partial \Delta T}{\partial i_1} = 0$, hence:

$$\frac{i_2}{{i_1}^2}\frac{n_{2,1}}{f_2\left(\frac{i_2}{i_1}n_{2,1}\right)} - \frac{dn_{start}}{di_1}\frac{1}{f_1(n_{start})} = \int_{n_{start}}^{n_{2,1}} \frac{\partial f_1(n)}{\partial i_1}\frac{dn}{f_1^2(n)} \tag{26}$$

The torque at the wheels while the 1st gear is engaged usually reaches the maximum torque due to tire traction $T_{r,max}$. The subscript (r) refers to the rear wheels, since the vehicle is rear-wheel driven. This means that the inequality $i_1 T_{(n)} > T_{r,max}$ is being satisfied for certain engine speeds n. Then, during starting, the following strategy is adopted:

- Maintaining constant torque $T_{r,max}$ at the wheels, using the clutch, up to the engine speed n for which $i_1 T_{(n)} = T_{r,max}$
- Full clutching up to n_{max}

The strategy above supposes that $T_{(n_{Tmax})} > \frac{T_{r.max}}{i_1} > T_{(n_{max})}$, where n_{Tmax} is the engine speed at maximum output torque.

What follows from the assumptions above is that the starting engine speed can be calculated as:

$$T_{(n_{start})} = \frac{T_{r.max}}{i_1} \tag{27}$$

Usually, the torque in the engine speed range of $n_{Tmax} < n < n_{max}$ does not have any other local maximum or minimum. Therefore, the derivative of the engine torque with respect to the engine speed does not change sign and so, if eq. (27) is satisfied, the following calculation can take place:

$$\frac{dn_{start}}{di_1} = \frac{dn_{start}}{dT_{(n_{start})}}\frac{dT_{(n_{start})}}{di_1} = \frac{dT_{(n_{start})}}{di_1}\frac{1}{\frac{dT}{dn}|n = n_{start}} \overset{(27)}{\Longrightarrow}$$

$$\frac{dn_{start}}{di_1} = -\frac{T_{r.max}}{{i_1}^2}\frac{1}{\frac{dT}{dn}|n = n_{start}} \tag{28}$$

If the gear ratio i_1 is too big, then $\frac{T_{r.max}}{i_1} < T_{(n_{max})}$ and eq. (27) cannot be satisfied. In this case, an appropriate choice for the starting engine speed would be $n_{start} = n_{max}$. Likewise, if the gear ratio i_1 is too small, then $\frac{T_{r.max}}{i_1} > T_{(n_{Tmax})}$ and the starting engine speed should be chosen as $n_{start} = n_{Tmax}$. In both cases above, it is evident that $\frac{dn_{start}}{di_1} = 0$.

Finally, differentiating eq. (21) with respect to the final gear ratio i_m yields:

$$\frac{\partial \Delta T}{\partial i_m} = \frac{\partial}{\partial i_m}\int_{\frac{i_m}{i_{m-1}}n_{2,m-1}}^{\overline{n_{2,m}}} \frac{dn}{f_m(n)} \Rightarrow$$

$$\Rightarrow \frac{\partial \Delta T}{\partial i_m} = -\left[\frac{n_{2,m-1}}{i_{m-1}} \frac{1}{f_m\left(\frac{i_m}{i_{m-1}} n_{2,m-1}\right)} + \int_{\frac{i_m}{i_{m-1}} n_{2,m-1}}^{\overline{n_{2,m}}} \frac{\partial f_m(n)}{\partial i_m} \frac{dn}{f_m^2(n)}\right] \quad (29)$$

It is evident that $\frac{\partial \Delta T}{\partial i_m} < 0$. This indicates that lap-time always decreases as the final gear ratio increases**.** One constraint that can be imposed to the design is that of maximum speed U_{max}. Therefore, given a maximum speed, the final gear ratio is calculated as:

$$i_m = \frac{\frac{\pi}{30} R n_{max}}{U_{max}} \quad (30)$$

The set of eq. (14), (23), (26), (27) and (30) can be solved as a system for finding the gear ratios and corresponding shift engine speeds.

2.3 Lap-time simulation: equations of motion, suspension and tire modeling

As mentioned previously, a simulation of the behavior of the vehicle and the driver can be combined with an optimization approach, aiming to maximize the sum of the points for the Dynamic events of interest. The basic vehicle modeling analysis performed for this method is examined in this section. All the implementation of the simulation is performed in Matlab [5]. An accountable portion of the modeling is taken from Tremlett et al. [6].

2.3.1 Coordinate system and transformations

The coordinate system of the vehicle body frame is placed on the center of gravity, with the z axis pointing towards the ground, as seen in figure 6. It is evident that the vehicle is considered to be symmetrical around the longitudinal x axis, directed towards the front of the vehicle. The corresponding x, y and yaw velocity can also be seen in this figure.

A curvilinear coordinate system is adopted for the race track and the desired trajectory to be followed. The track coordinate system will follow the centerline of the edges of the track and will in general not coincide with the desired trajectory. Therefore, the equation describing the curvature (κ) as a function of the distance (s) on the curve will be different for the two systems.

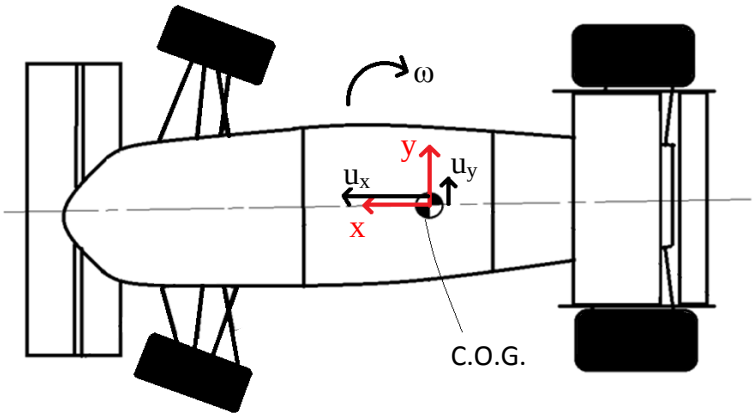

Figure 6: Vehicle coordinate system

As seen in figure 7, to define the position of a frame in relation to the curvilinear system, the following set of numbers is required:

- The length (s) along the curve of the curvilinear system
- The offset distance (s_n) from the curve of the curvilinear system
- The angle (β) of the frame relative to the tangent of the curve of the curvilinear system

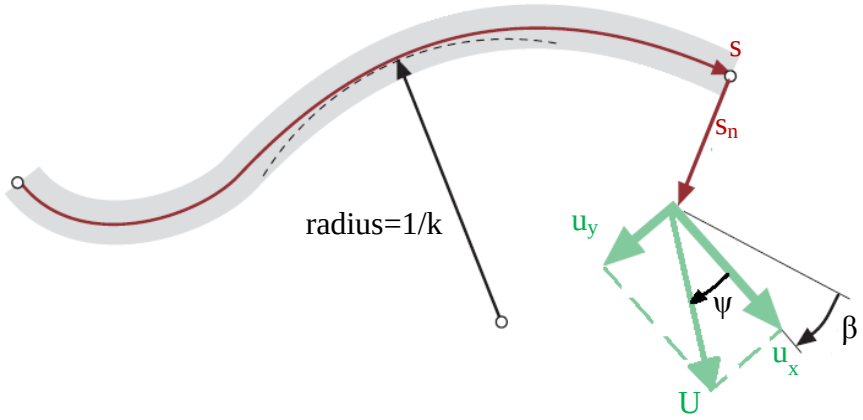

Figure 7: Curvilinear coordinate system

The position of the vehicle frame will be determined in relation to the curvilinear system of the desired trajectory to be followed. The differential equations relating the vehicle motions to the coordinate system can be described by:

$$\dot{s} = \frac{u_x cos\beta - u_y sin\beta}{1 - \kappa s_n} = U \frac{cos(\beta + \psi)}{1 - \kappa s_n} \quad (31)$$

$$\dot{s}_n = u_x sin\beta + u_y cos\beta = U sin(\beta + \psi) \quad (32)$$

$$\dot{\beta} = \omega - k \frac{u_x cos\beta - u_y sin\beta}{1 - \kappa s_n} = \omega - kU \frac{cos(\beta + \psi)}{1 - \kappa s_n} \quad (33)$$

where U is the total vehicle speed and ψ is the side slip angle that can be calculated as:

$$U = \sqrt{{u_x}^2 + {u_y}^2} \quad (34)$$

$$\tan\psi = {u_x}/{u_y} \quad (35)$$

2.3.2 Equations of motion - Force and moment equilibrium

Different simplifications exist for describing the equations of motion. The simplest model consists of only one mass and therefore one degree of freedom, on which longitudinal and lateral forces are exerted. The steering and suspension dynamics are not taken under consideration, as no moments are calculated. This model has a fair performance on general motorsport applications. However, in Formula Student where the tracks involve rapidly changing turn radii, results might be inadequate from a simulation utilizing this approach.

Another very common model is the half car, or bicycle car model. This is a two dimensional approach, where the vehicle width is considered negligible. Steering and suspension dynamics are also involved in this analysis. This enables the model to simulate the transitional phases of entering and exiting a turn. It is a well performing model and has been used to simulate Formula Student vehicles quite frequently. Criens et al. [7] as well as Singh & Palanivelu [8] used a bicycle car model to build a Formula Student vehicle simulator.

Having introduced steering dynamics, the bicycle car model adds an extra input to the vehicle as a system. Steering in a manner that keeps the vehicle under control and on a specified track, is a difficult but essential parameter of the simulation. The weak point of this analysis is the absence of roll dynamics and the influence of the different speeds at the inner and outer wheels during turning. These parameters can have some effect, especially in Formula Student tracks where the track radius is often comparable with the width of the car.

A step ahead into including these features is introducing a full car model. This model includes all four tires of the car and all equations of motion. The difficulty of performing this change can be considered less than the one required to create a

steering control. Therefore, the implementation of a full car model provides the simulation with greater accuracy, without requiring excessive additional analysis. This model is also very common within Formula Student applications. Dos Santos [9] used a full car model in a simulation accounting for suspension compliance. Brown [10] used a full car model so as to design an all-wheel torque vectoring system. Harsh [11] used a full car model so as to create a simulation and evaluate the influence of different systems of the vehicle ON its performance.

Concerning the vehicle model utilized in this work, a full car model is used. The top view defining the forces and distances required to express the longitudinal, lateral and yaw motion equations can be seen in figure 8.

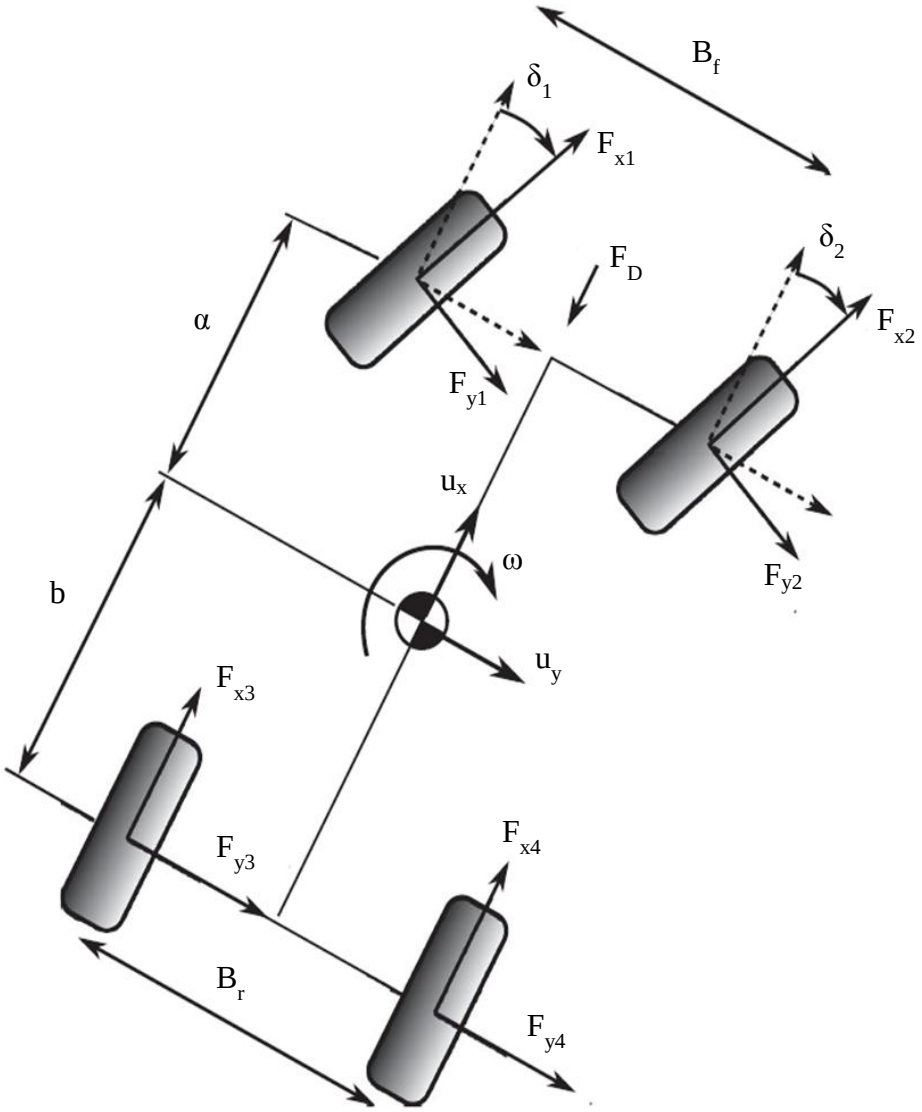

Figure 8: Top view of the vehicle

The equations of motion of the vehicle rigid body frame can be written as:

$$m(\dot{u}_x - \omega u_y) = \Sigma F_{x,external} \tag{36}$$
$$m(\dot{u}_y + \omega u_x) = \Sigma F_{y,external} \tag{37}$$
$$I_z \dot{\omega} = \Sigma M_{z,external} \tag{38}$$

Using figure 8, the external sum of forces and moments can be expressed as:

$$\Sigma F_{x,ext} = cos\delta_1 F_{x1} + cos\delta_2 F_{x2} - sin\delta_1 F_{y1} - sin\delta_2 F_{y2} + F_{x3} + F_{x4} + F_D \tag{39}$$
$$\Sigma F_{y,ext} = sin\delta_1 F_{x1} + sin\delta_2 F_{x2} + cos\delta_1 F_{y1} + cos\delta_2 F_{y2} + F_{y3} + F_{y4} \tag{40}$$
$$\begin{aligned}\Sigma M_{z,ext} = {} & (cos\delta_1 F_{x1} - cos\delta_2 F_{x2})\frac{B_f}{2} - (sin\delta_1 F_{y1} + sin\delta_2 F_{y2})\frac{B_f}{2} \\ & + (F_{x3} - F_{x4})\frac{B_r}{2} + a(sin\delta_1 F_{x1} + sin\delta_2 F_{x2}) \\ & + a(cos\delta_1 F_{y1} + cos\delta_2 F_{y2}) - b(F_{y3} + F_{y4})\end{aligned} \tag{41}$$

2.3.3 Tire vertical loads and suspension modeling

Concerning roll and pitch motions of the vehicle, the steady state weight transfer will be examined first. Further definition of the forces and distances in a side view of the vehicle can be seen in figure 9. Any change in the distances due to suspension movement will be considered negligible. Requesting for $\Sigma F_{z,external} = 0$ and $\Sigma M_{x,external} = \Sigma M_{y,external} = 0$, the steady-state tire loads are easily calculated as:

$$\begin{cases} F_{z1,s} = 0.5m\left(\frac{b}{L}g + \frac{F_L}{m}\frac{b}{L}\right) + \Delta F_{z1,s} \\ F_{z2,s} = 0.5m\left(\frac{b}{L}g + \frac{F_L}{m}\frac{b}{L}\right) + \Delta F_{z2,s} \\ F_{z3,s} = 0.5m\left(\frac{a}{L}g + \frac{F_L}{m}\frac{a}{L}\right) + \Delta F_{z3,s} \\ F_{z4,s} = 0.5m\left(\frac{a}{L}g + \frac{F_L}{m}\frac{a}{L}\right) + \Delta F_{z4,s} \end{cases} \tag{42}$$

where the values $\Delta F_{z1,s}$, $\Delta F_{z2,s}$, $\Delta F_{z3,s}$, $\Delta F_{z4,s}$ express the steady-state variation of the tire normal loads due to pitch and roll moments and are equal to:

$$\begin{cases} \Delta F_{z1,s} = 0.5\left(-\frac{h}{L}\Sigma F_{x,external} + 2\xi\frac{h}{B_f}\Sigma F_{y,external} - F_D\frac{h_a}{L} + F_L\frac{b_a - b}{L}\right) \\ \Delta F_{z2,s} = 0.5\left(-\frac{h}{L}\Sigma F_{x,external} - 2\xi\frac{h}{B_f}\Sigma F_{y,external} - F_D\frac{h_a}{L} + F_L\frac{b_a - b}{L}\right) \\ \Delta F_{z3,s} = 0.5\left(\frac{h}{L}\Sigma F_{x,external} + 2(1-\xi)\frac{h}{B_r}\Sigma F_{y,external} + F_D\frac{h_a}{L} + F_L\frac{a_a - a}{L}\right) \\ \Delta F_{z4,s} = 0.5\left(\frac{h}{L}\Sigma F_{x,external} - 2(1-\xi)\frac{h}{B_r}\Sigma F_{y,external} + F_D\frac{h_a}{L} + F_L\frac{a_a - a}{L}\right) \end{cases} \tag{43}$$

where ξ is the front distribution of the vehicle torsional stiffness, also referred to as front mechanical balance.

The aerodynamic drag and downforce are expressed as:

$$F_D = \frac{1}{2}\rho C_D A {u_x}^2 \tag{44}$$

$$F_L = \frac{1}{2}\rho C_L A {u_x}^2 \tag{45}$$

respectivelly.

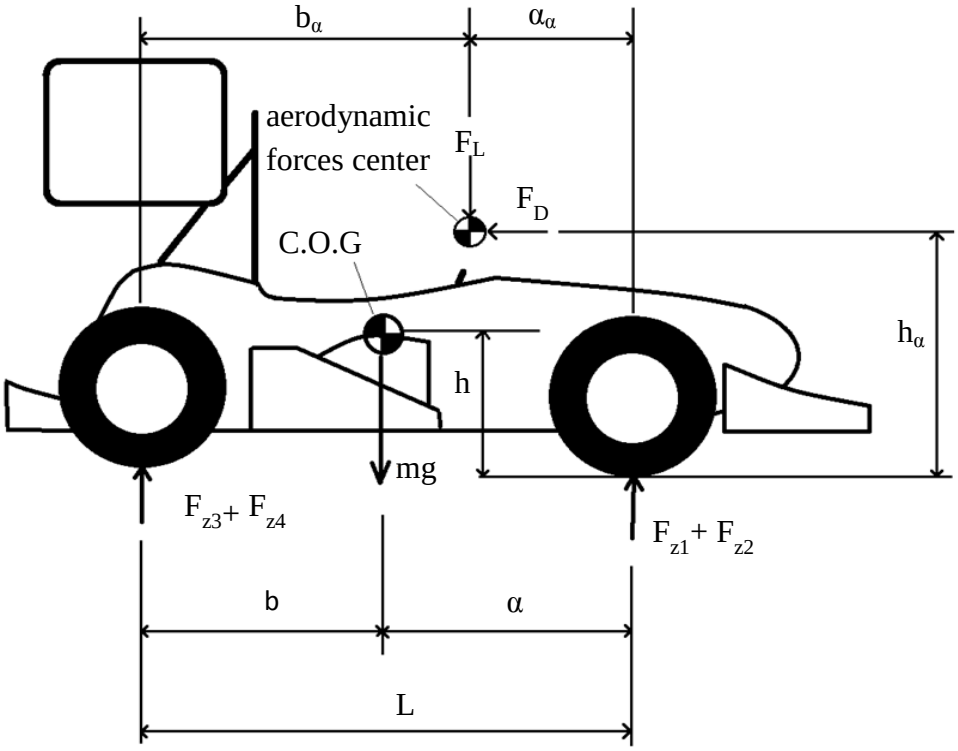

Figure 9: Right view of the vehicle

The heave motion of the vehicle will now be ignored and therefore tire loads are expressed as:

$$\begin{cases} F_{z1} = 0.5m\left(\frac{b}{L}g + \frac{F_L}{m}\frac{b}{L}\right) + \Delta F_{z1} \\ F_{z2} = 0.5m\left(\frac{b}{L}g + \frac{F_L}{m}\frac{b}{L}\right) + \Delta F_{z2} \\ F_{z3} = 0.5m\left(\frac{a}{L}g + \frac{F_L}{m}\frac{a}{L}\right) + \Delta F_{z3} \\ F_{z4} = 0.5m\left(\frac{a}{L}g + \frac{F_L}{m}\frac{a}{L}\right) + \Delta F_{z4} \end{cases} \tag{46}$$

Following the modeling proposed by Vilela & Barbosa [12], the suspension can be modeled as a torsional spring for roll angles. The roll moment exciting the suspension at steady state is the lateral force $-\Sigma F_{y,external}$, multiplied by the distance of the center of gravity and the roll axis. This distance creating a leverage, can be seen in figure 10. The roll axis of the suspension can be defined as the geometrical instant axis of roll rotation. Since the left and right suspension stiffness is the same, any torque exerted around the roll axis results to rotation and not translation.

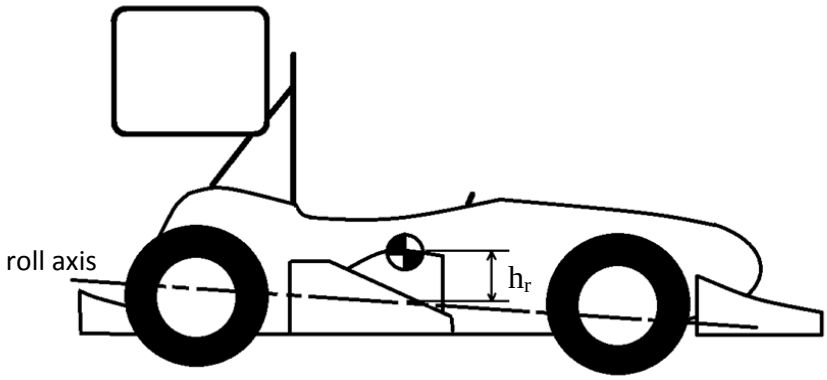

Figure 10: Roll axis and roll axis leverage

Likewise, the pitch moment is the longitudinal force $\Sigma F_{x,external}$, multiplied by the distance of the center of gravity and the pitch axis. However, in pitch, the front and rear suspension stiffness might be different. This means that a torque exerted around an arbitrary pitch axis can result to a combined rotation and translation. To deal with this problem, for pitch only, the lateral position of the pitch axis will be considered such that upon exerted torque, only rotation occurs. Following the distances seen in figure 11, the position of the pitch axis can be calculated as:

$$k_{front} a_p = k_{rear} b_p \tag{47}$$

where k_{front} and k_{rear} are the front and rear axle suspension vertical stiffness, including tire compliance.

Considering the dynamic conditions of roll and pitch, damping and moment of inertia acceleration should be taken under consideration. Therefore, the motion equations for pitch and roll can be written as:

$$I_{roll}\dot{r} + c_{roll}\dot{r} + k_{roll} r = -h_r \Sigma F_{y,external} \tag{48}$$

$$I_{pitch}\ddot{p} + c_{pitch}\dot{p} + k_{pitch} p = h_p \Sigma F_{x,external} \tag{49}$$

where I_{roll} and I_{pitch} are the roll and pitch moments of inertia round the roll and pitch axis, c_{roll}, k_{roll} and c_{pitch}, k_{pitch} are the roll and pitch damping and stiffness coefficients of the suspension and h_r and h_p are the roll and pitch moment leverages respectively.

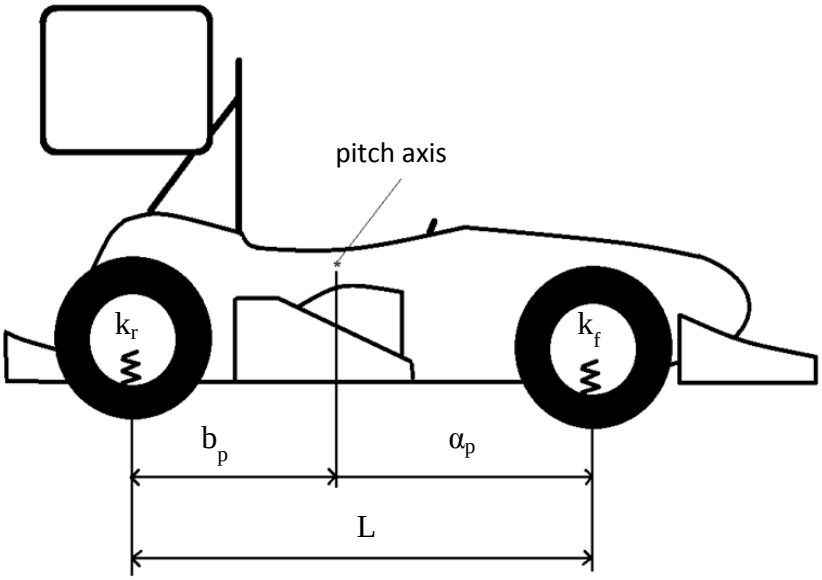

Figure 11: Position of pitch axis

The wheel vertical load variation due to pitch can be found considering the suspension stiffness and damping:

$$\begin{cases} \Delta F_{z1,pitch} = -\dfrac{k_{front}}{2} a_p p - \dfrac{c_{front}}{2} a_p \dot{p} \\ \Delta F_{z2,pitch} = -\dfrac{k_{front}}{2} a_p p - \dfrac{c_{front}}{2} a_p \dot{p} \\ \Delta F_{z3,pitch} = \dfrac{k_{rear}}{2} b_p p + \dfrac{c_{rear}}{2} b_p \dot{p} \\ \Delta F_{z4,pitch} = \dfrac{k_{rear}}{2} b_p p + \dfrac{c_{rear}}{2} b_p \dot{p} \end{cases} \tag{50}$$

where c_{rear} and c_{front} are the damping coefficients of the rear and the front axle of the suspension. It is evident now that there will be a translation for every pitch speed $\dot{p}$ around the pitch axis since $(\Delta F_{z1pitch} + \Delta F_{z2,pitch}) - (\Delta F_{z3,pitch} + \Delta F_{z4,pitch}) \neq 0$. This is true, unless the suspension damping follows the relationship:

$$c_{front} a_p = c_{rear} b_p \Rightarrow \frac{c_{front}}{k_{front}} = \frac{c_{rear}}{k_{rear}} \tag{51}$$

Therefore, for simplifying this analysis, eq. (51) will be considered as satisfied. In this case, pitch stiffness and damping can be calculated as:

$$k_{pitch} = k_{front} {a_p}^2 + k_{rear} {b_p}^2 \overset{(47)}{\Longrightarrow}$$

$$\Rightarrow k_{pitch} = \frac{L^2}{\frac{1}{k_{front}} + \frac{1}{k_{rear}}} \tag{52}$$

$$c_{pitch} = c_{front}{a_p}^2 + c_{rear}{b_p}^2 \overset{(51)}{\Longrightarrow}$$

$$\Rightarrow c_{pitch} = \frac{L^2}{\frac{1}{c_{front}} + \frac{1}{c_{rear}}} \tag{53}$$

Using the equations above, wheel load variation due to pitch can be simplified as:

$$\begin{cases} \Delta F_{z1,pitch} = -\frac{1}{2}\Delta F_{z,p} \\ \Delta F_{z2,pitch} = -\frac{1}{2}\Delta F_{z,p} \\ \Delta F_{z3,pitch} = \frac{1}{2}\Delta F_{z,p} \\ \Delta F_{z4,pitch} = \frac{1}{2}\Delta F_{z,p} \end{cases} \tag{54}$$

where

$$\Delta F_{z,p} = \frac{k_{pitch}}{L}p + \frac{c_{pitch}}{L}\dot{p} \tag{55}$$

The wheel vertical load variation due to roll can be found as:

$$\left.\begin{aligned} (\Delta F_{z2,roll} - \Delta F_{z1,roll})B_f &= k_{roll,front}r + c_{roll,front}\dot{r} \\ \Delta F_{z2,roll} &= -\Delta F_{z1,roll} \\ (\Delta F_{z4,roll} - \Delta F_{z3,roll})B_r &= k_{roll,rear}r + c_{roll,rear}\dot{r} \\ \Delta F_{z3,roll} &= -\Delta F_{z4,roll} \end{aligned}\right\} \Rightarrow$$

$$\Rightarrow \begin{cases} \Delta F_{z1,roll} = -\frac{1}{2}\frac{k_{roll,front}}{B_f}r - \frac{1}{2}\frac{c_{roll,front}}{B_f}\dot{r} \\ \Delta F_{z2,roll} = \frac{1}{2}\frac{k_{roll,front}}{B_f}r + \frac{1}{2}\frac{c_{roll,front}}{B_f}\dot{r} \\ \Delta F_{z3,roll} = -\frac{1}{2}\frac{k_{roll,rear}}{B_r}r - \frac{1}{2}\frac{c_{roll,rear}}{B_r}\dot{r} \\ \Delta F_{z4,roll} = \frac{1}{2}\frac{k_{roll,rear}}{B_r}r + \frac{1}{2}\frac{c_{roll,rear}}{B_r}\dot{r} \end{cases} \tag{56}$$

As with the case of pitch, damping in roll motions is considered to follow the relationship:

$$\frac{c_{roll,front}}{k_{roll,front}} = \frac{c_{roll,rear}}{k_{roll,rear}} \tag{57}$$

In this case, considering the definition of the roll stiffness distribution:

$$\xi = \frac{k_{roll,front}}{k_{roll,front} + k_{roll,rear}} \tag{58}$$

wheel vertical load variation due to roll can be simplified as:

$$\begin{cases} \Delta F_{z1,roll} = -\frac{1}{2}\xi \frac{B_f + B_r}{B_f} \Delta F_{z,r} \\ \Delta F_{z2,roll} = \frac{1}{2}\xi \frac{B_f + B_r}{B_f} \Delta F_{z,r} \\ \Delta F_{z3,roll} = -\frac{1}{2}(1-\xi) \frac{B_f + B_r}{B_r} \Delta F_{z,r} \\ \Delta F_{z4,roll} = \frac{1}{2}(1-\xi) \frac{B_f + B_r}{B_r} \Delta F_{z,r} \end{cases} \tag{59}$$

where

$$\Delta F_{z,r} = \frac{k_{roll}}{B_f + B_r} r + \frac{c_{roll}}{B_f + B_r} \dot{r} \tag{60}$$

The roll stiffness can be calculated using a parallel and series spring connection model:

$$\frac{1}{k_{roll,front}} = \frac{1}{k_{tire,front} \frac{{B_f}^2}{2}} + \frac{1}{k_{susp,front} \frac{{B_f}^2}{2} + k_{rollbar,front}} \tag{61}$$

$$\frac{1}{k_{roll,rear}} = \frac{1}{k_{tire,rear} \frac{{B_f}^2}{2}} + \frac{1}{k_{susp,rear} \frac{{B_f}^2}{2} + k_{rollbar,rear}} \tag{62}$$

$$k_{roll} = k_{roll,front} + k_{roll,rear} \tag{63}$$

The total wheel vertical load variation can be expressed as the superposition of the loads from roll and pitch:

$$\left.\begin{aligned} \Delta F_{z1} &= \Delta F_{z1,pitch} + \Delta F_{z1,roll} \\ \Delta F_{z2} &= \Delta F_{z2,pitch} + \Delta F_{z2,roll} \\ \Delta F_{z3} &= \Delta F_{z3,pitch} + \Delta F_{z3,roll} \\ \Delta F_{z4} &= \Delta F_{z4,pitch} + \Delta F_{z4,roll} \end{aligned}\right\} \Rightarrow$$

$$\Rightarrow \begin{cases} \Delta F_{z1} = -\frac{1}{2}\Delta F_{z,p} - \frac{1}{2}\xi\frac{B_f + B_r}{B_f}\Delta F_{z,r} \\ \Delta F_{z2} = -\frac{1}{2}\Delta F_{z,p} + \frac{1}{2}\xi\frac{B_f + B_r}{B_f}\Delta F_{z,r} \\ \Delta F_{z3} = \frac{1}{2}\Delta F_{z,p} - \frac{1}{2}(1-\xi)\frac{B_f + B_r}{B_r}\Delta F_{z,r} \\ \Delta F_{z4} = \frac{1}{2}\Delta F_{z,p} + \frac{1}{2}(1-\xi)\frac{B_f + B_r}{B_r}\Delta F_{z,r} \end{cases} \quad (64)$$

Proper combination of eq. (64) yields:

$$\Delta F_{z,p} = \frac{1}{2}(\Delta F_{z3} + \Delta F_{z4}) - \frac{1}{2}(\Delta F_{z1} + \Delta F_{z2}) \quad (65)$$

$$\Delta F_{z,r} = (\Delta F_{z2} - \Delta F_{z1})\frac{B_f}{B_f + B_r} + (\Delta F_{z4} - \Delta F_{z3})\frac{B_r}{B_f + B_r} \quad (66)$$

The final step in this analysis is finding the dynamic equations for the roll and pitch quantities $\Delta F_{z,r}$ and $\Delta F_{z,p}$. This can be done by starting from eq. (48) and (49). More specifically, for roll motions it is calculated that:

$$I_{roll}\ddot{r} + c_{roll}\dot{r} + k_{roll}r = -h_r\Sigma F_{y,external} \overset{(60)}{\Longrightarrow}$$

$$\overset{(60)}{\Longrightarrow} \frac{I_{roll}}{B_f + B_r}\ddot{r} + \Delta F_{z,r} = -\frac{h_r\Sigma F_{y,external}}{B_f + B_r} \quad (67)$$

In steady state $\ddot{r} = 0$ and therefore:

$$\Delta F_{z,r,s} = -\frac{h_r\Sigma F_{y,external}}{B_f + B_r} \quad (68)$$

Substituting to the eq. (67) yields:

$$\ddot{r} = \frac{B_f + B_r}{I_{roll}}\left(\Delta F_{z,r,s} - \Delta F_{z,r}\right) \quad (69)$$

From eq. (60) it follows that:

$$\Delta F_{z,r} = \frac{k_{roll}}{B_f + B_r}r + \frac{c_{roll}}{B_f + B_r}\dot{r} \Rightarrow \Delta\ddot{F}_{z,r} = \frac{k_{roll}}{B_f + B_r}\ddot{r} + \frac{c_{roll}}{B_f + B_r}\dddot{r} \overset{(69)}{\Longrightarrow}$$

$$\overset{(69)}{\Longrightarrow} \Delta\ddot{F}_{z,r} = \frac{k_{roll}}{I_{roll}}\left(\Delta F_{z,r,s} - \Delta F_{z,r}\right) + \frac{c_{roll}}{I_{roll}}\left(\Delta\dot{F}_{z,r,s} - \Delta\dot{F}_{z,r}\right) \Rightarrow$$

$$\Rightarrow I_{roll}\Delta\ddot{F}_{z,r} + c_{roll}\Delta\dot{F}_{z,r} + k_{roll}\Delta F_{z,r} = c_{roll}\Delta\dot{F}_{z,r,s} + k_{roll}\Delta F_{z,r,s} \quad (70)$$

Likewise, the corresponding equation for pitch becomes:

$$I_{pitch}\Delta\ddot{F}_{z,p} + c_{pitch}\Delta\dot{F}_{z,p} + k_{pitch}\Delta F_{z,p} = c_{pitch}\Delta\dot{F}_{z,p,s} + k_{pitch}\Delta F_{z,p,s} \quad (71)$$

The preceding analysis results to a separate differential equation for the quantities $\Delta F_{z,r}$ and $\Delta F_{z,p}$, involved in wheel vertical load variations described in eq. (64). The steady state quantities $\Delta F_{z,r,s}$ and $\Delta F_{z,p,s}$ can be obtained using subscript (s) in eq. (65) and (66).

2.3.4 Tire modeling

The x and y coordinates of the forces appearing in eq. (39) to (41) refer to forces resulting the friction of the tires and the road. A tire model links those forces with the dimensionless slip quantities of slip ratio K and slip angle α. These are defined as:

$$K = \frac{R_e\omega_{tire}}{u_{x,tire}} - 1 \quad (72)$$

$$tana = \frac{u_{y,tire}}{u_{x,tire}} \quad (73)$$

where the x and y axis are defined in the tire coordinate system as shown in figure 12 and R_e is the tire loaded rolling radius.

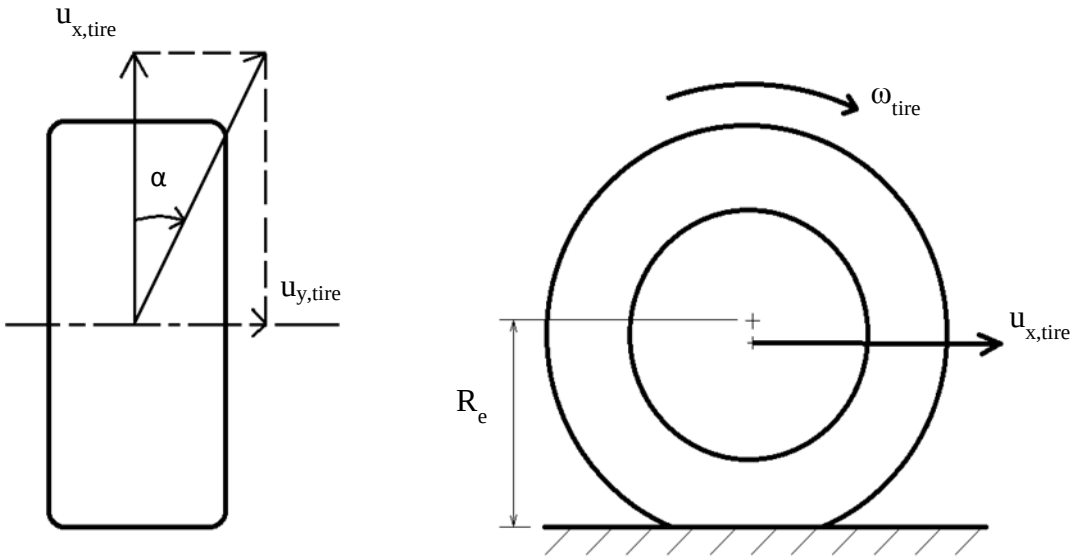

Figure 12: Tire slip kinematics

Therefore, the slip quantities can be calculated for each individual tire as:

$$\begin{cases} K_1 = \dfrac{R_e\omega_1}{\cos(\delta_1)\left(u_x + \omega\dfrac{B_f}{2}\right) + sin(\delta_1)\left(u_y + a\omega\right)} - 1 \\ K_2 = \dfrac{R_e\omega_2}{\cos(\delta_2)\left(u_x - \omega\dfrac{B_f}{2}\right) + sin(\delta_2)\left(u_y + a\omega\right)} - 1 \\ K_3 = \dfrac{R_e\omega_3}{u_x + \omega\dfrac{B_r}{2}} - 1 \\ K_4 = \dfrac{R_e\omega_4}{u_x - \omega\dfrac{B_r}{2}} - 1 \end{cases} \tag{74}$$

$$\begin{cases} \tan(\delta_1 - a_1) = \dfrac{a\omega + u_y}{u_x + \omega\dfrac{B_f}{2}} \\ \tan(\delta_2 - a_2) = \dfrac{a\omega + u_y}{u_x - \omega\dfrac{B_f}{2}} \\ tana_3 = \dfrac{b\omega - u_y}{u_x + \omega\dfrac{B_r}{2}} \\ tana_4 = \dfrac{b\omega - u_y}{u_x - \omega\dfrac{B_r}{2}} \end{cases} \tag{75}$$

For this simulation, the semi-empirical 1996 Pacejka's Magic Formula is used and more specifically, with incorporation of the similarity method introduced by Pacejka in 2002 [13]. In this modeling, two series of parameters are extracted using pure longitudinal and lateral slip separately. The combined longitudinal and lateral situations are determined by a theoretical slip analysis. The theoretical longitudinal slip σ_x, lateral slip σ_y and equivalent slip σ are used for this purpose. Neglecting camber angle effects, these can be calculated from the slip ratio and slip angle as:

$$\sigma_x = \frac{K}{|1+K|} \tag{76}$$

$$\sigma_y = \frac{tana}{|1+K|} \tag{77}$$

$$\sigma = \sqrt{{\sigma_x}^2 + {\sigma_y}^2} \tag{78}$$

It should be noted that, for $90°<\alpha<180°$, a negative sign should be added in eq. (77).

The resulting longitudinal and lateral forces can then be found using the Magic Formula expressions, neglecting camber angle effects:

$$F_x = \frac{\sigma_x}{\sigma} F_z D_x sin\left[C_x Arctan\left((1-E_x)B_x\sigma + E_x Arctan(B_x\sigma)\right)\right] \quad (79)$$

$$F_y = \frac{\sigma_y}{\sigma} F_z D_y sin\left[C_y Arctan\left((1-E_y)B_y\sigma + E_y Arctan(B_y\sigma)\right)\right] \quad (80)$$

For the longitudinal parameters:

$$\mathrm{C}_x = \mathrm{pC}_{x1} \quad (81)$$

$$\mathrm{D}_x = \lambda_x \left(\mathrm{pD}_{x1} + \mathrm{pD}_{x2} \frac{\mathrm{F}_z - \mathrm{F}_{z0}}{\mathrm{F}_{z0}}\right) \quad (82)$$

$$\mathrm{E}_x = \mathrm{pE}_{x1} \quad (83)$$

$$\mathrm{B}_x = \frac{K_x}{\mathrm{C}_x \mathrm{D}_x \mathrm{F}_z} \quad (84)$$

where F_{z0} is a reference tire normal load and

$$K_x = \mathrm{pK}_{x1} F_z exp\left(\mathrm{pK}_{x3} \frac{\mathrm{F}_z - \mathrm{F}_{z0}}{\mathrm{F}_{z0}}\right) \quad (85)$$

is the slope for K=0.

For the lateral parameters:

$$\mathrm{C}_y = \mathrm{pC}_{y1} \quad (86)$$

$$\mathrm{D}_x = \lambda_y \left(\mathrm{pD}_{y1} + \mathrm{pD}_{y2} \frac{\mathrm{F}_z - \mathrm{F}_{z0}}{\mathrm{F}_{z0}}\right) \quad (87)$$

$$\mathrm{E}_y = \mathrm{pE}_{y1} \quad (88)$$

$$\mathrm{B}_y = \frac{K_y}{\mathrm{C}_y \mathrm{D}_y \mathrm{F}_z} \quad (89)$$

where

$$K_y = \mathrm{pK}_{y1} \mathrm{F}_{z0} sin\left[2 Arctan\left(\frac{\mathrm{F}_z}{\mathrm{pK}_{y2} \mathrm{F}_{z0}}\right)\right] \quad (90)$$

is the slope for α=0.

The fitting of the Magic Formula equations was performed so that, for pure slip conditions:

$$F_{x,max} = F_z D_x \quad (91)$$

$$F_{y,max} = F_z D_y \quad (92)$$

Therefore, the tires coefficients of friction can be expressed as:

$$\Phi_x = D_x \quad (93)$$

$$\Phi_y = D_y \quad (94)$$

A summary of the parameters required for the Magic Formula can be seen in table 4.

Parameter	Description
F_{z0}	Reference normal load
λ_x	Max longitudinal friction scaling factor
λ_y	Max longitudinal friction scaling factor
pK_{x1}	Max longitudinal stiffness coefficient
pK_{y1}	Max cornering stiffness coefficient
pK_{x3}	Max longitudinal stiffness coefficient
pK_{y2}	Max cornering stiffness coefficient
pC_{x1}	Longitudinal shape factor
pC_{y1}	Lateral shape factor
pD_{x1}	Max longitudinal friction coefficient
pD_{y1}	Max lateral friction coefficient
pD_{x2}	Longitudinal friction load dependency factor
pD_{y2}	Lateral friction load dependency factor
pE_{x1}	Longitudinal curvature factor
pE_{y1}	Lateral curvature factor

Table 4: Pacejka Magic Formula coefficients

3. Vehicle subsystems and driver modeling

3.1 Modeling of engine and transmission

The engine output torque has been measured in cooperation with GearTech Engineering L.T.D. at a Dynapack™ hydraulic dynamometer, connected to the driving wheels of the vehicle. The measurement was performed under slowly increasing engine speed, so as to render rotational mass acceleration effects negligible. Instead of directly using the measured torque, the end result was fitted with a polynomial equation as:

$$T_{(n)} = t_0 + \sum_{j=1}^{4} t_j \left(\frac{n}{1000}\right)^j \tag{95}$$

This fitting was performed so that the simulation results would not be influenced by any localized anomalies on the output torque.

The differential that distributes the torque to the rear wheels is a Limited Slip type one. This means that an internal torque is exerted between the two outputs of the differential. There are two states in the operation of the differential:

- If the torque difference between the two outputs of the differential is bellow a specified value called bias torque T_{bias}, then the two outputs rotate with the same speed, therefore $\omega_3=\omega_4$.
- If the bias torque is reached, then the two outputs are allowed to rotate with different speeds. In this case, the differential cage rotational speed is:

$$\omega_{diff} = \frac{\omega_3 + \omega_4}{2} \tag{96}$$

The limited slip differential that is fitted in Prom Racing's vehicle is a Salisbury type Limited Slip Differential and in such an application, the bias torque is:

$$T_{bias} = T_p + |T_{in}| \cdot L.U.T. \tag{97}$$

where T_{in} is the input torque to the differential cage, T_p is a constant preload and L.U.T. is the lock up torque constant. Usually, a constant named torque bias ratio (T.B.R.=T_{max}/T_{min}) is used instead of L.U.T. The relationship between lock up torque constant and torque bias ratio is:

$$L.U.T. = \frac{T.B.R. - 1}{T.B.R. + 1} \tag{98}$$

The internal bias torque is applied by friction discs, placed symmetrically inside the differential. Due to friction, less output torque is applied on the faster rotating wheel and more torque is applied on the slower rotating wheel. Therefore, the equation for torque delivered to the two wheels under the differential slip condition is:

$$\left.\begin{aligned} T_3 &= \frac{T_{in} + sign(\omega_4 - \omega_3)T_{bias}}{2} \\ T_4 &= \frac{T_{in} - sign(\omega_4 - \omega_3)T_{bias}}{2} \end{aligned}\right\} \Rightarrow$$

$$\Rightarrow \begin{cases} T_3 = \dfrac{1 + sign(\omega_4 - \omega_3)sign(T_{in})L.U.T.}{2} T_{in} + \dfrac{sign(\omega_4 - \omega_3)}{2} T_p \\ T_4 = \dfrac{1 - sign(\omega_4 - \omega_3)sign(T_{in})L.U.T.}{2} T_{in} - \dfrac{sign(\omega_4 - \omega_3)}{2} T_p \end{cases} \quad (99)$$

The transmission of the vehicle consists of three distinct drive ratios:

- the primary drive ratio from the engine crankshaft up to the clutch i_p
- the gearbox drive ratio i_g
- the final drive ratio from the gearbox to the wheels

A schematic of the system can be seen in figure 13.

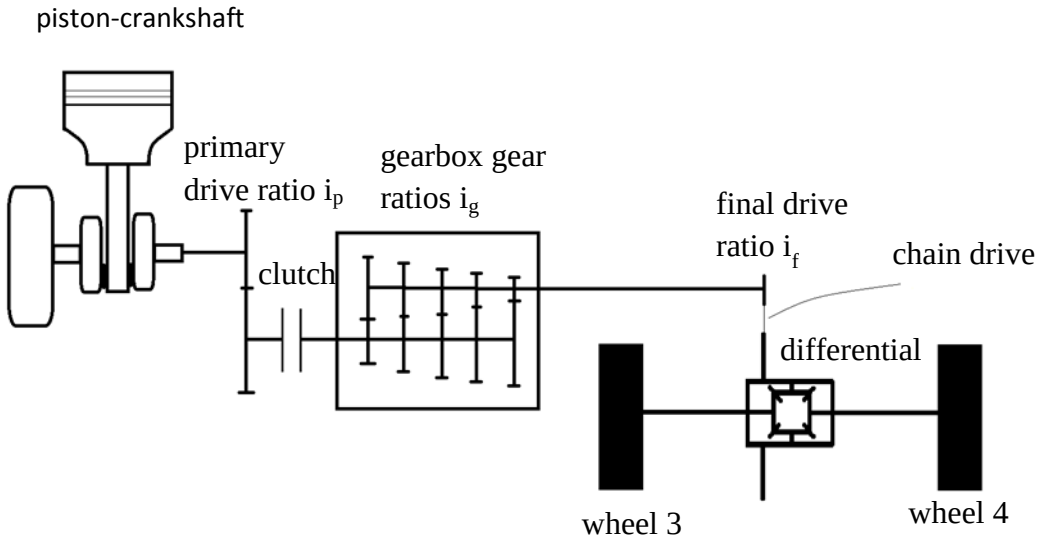

Figure 13: Schematic representation of the transmission

The total drive ratio of each gear (k) is

$$i_k = i_p i_{g,k} i_f \quad (100)$$

Considering that, the speed of the engine can be calculated as:

$$n = \frac{30}{\pi} i_k \omega_{diff} \overset{(96)}{\Longrightarrow} n = \frac{30}{\pi} i_k \frac{\omega_3 + \omega_4}{2} \overset{(74)}{\Longrightarrow}$$

$$\Rightarrow n = \frac{30}{\pi} \frac{i_k}{R_e} \frac{(1 + K_3)\left(u_x + \omega \frac{B_r}{2}\right) + (1 + K_4)\left(u_x - \omega \frac{B_r}{2}\right)}{2} \tag{101}$$

Since the engine torque has been measured as the effective torque delivered to the wheels, neglecting any difference to the mechanical efficiency of each gear of the gearbox, the torque delivered to the differential is:

$$T_{in} = T i_k - i_k J_{eng} \frac{\pi}{30} \dot{n} \tag{102}$$

where J_{eng} is the equivalent moment of inertia of the rotational parts of the engine, calculated at the crankshaft speed.

Finally, the longitudinal force delivered to the wheels during acceleration is:

$$\begin{cases} F_{x1} = \dfrac{-J_{w1}\dot{\omega}_1}{R_e} \\ F_{x2} = \dfrac{-J_{w2}\dot{\omega}_2}{R_e} \\ F_{x3} = \dfrac{T_3 - J_{w3}\dot{\omega}_3}{R_e} \\ F_{x4} = \dfrac{T_4 - J_{w4}\dot{\omega}_4}{R_e} \end{cases} \tag{103}$$

where J_w is the moment of inertia of the wheels.

In general, the slip ratios that correspond to tire longitudinal forces bellow the maximum tire force, can be considered relatively small. However, if rotational speeds ω_3 and ω_4 of the rear wheels are left unconstrained, extreme wheelspin can occur, should the torque of the engine provide the tires with force exceeding the tires maximum longitudinal force. In order to prevent this wheelspin, a traction control strategy should be employed, limiting the engine torque.

The rotational speed of the wheels affects the torque delivered to them, due to acceleration of their moment of inertia. This torque difference is usually small, assuming that excessive wheel spin does not occur. For this reason, instead of implementing a traction control strategy, the force delivered to the wheels will be limited by the maximum longitudinal force of the tires. The rotational speeds of the wheels will not be considered as separate variables. Instead, the slip ratios will be calculated using the torque applied to the wheels and the tire model.

Considering small slip ratios, the engine speed can be found by altering eq. (101) as:

$$n = \frac{30}{\pi}\frac{i_k}{R_e}\frac{\left(u_x + \omega\frac{B_r}{2}\right) + \left(u_x - \omega\frac{B_r}{2}\right)}{2} \Rightarrow$$

$$n = \frac{30}{\pi}\frac{i_k}{R_e}u_x \tag{104}$$

During acceleration, the total x-coordinate of the force due to tire longitudinal forces can be calculated as:

$$F_{x,accel} = F_{x1}sin\delta_1 + F_{x2}sin\delta_2 + F_{x3} + F_{x4} \approx F_{x1} + F_{x2} + F_{x3} + F_{x4} \overset{(103)}{\Longrightarrow}$$

$$\overset{(103)}{\Longrightarrow} F_{x,accel} = \frac{T_3 + T_4 - J_{w1}\dot{\omega}_1 - J_{w2}\dot{\omega}_2 - J_{w3}\dot{\omega}_3 - J_{w4}\dot{\omega}_4}{R_e} \Rightarrow$$

$$\Rightarrow F_{x,accel} = \frac{T_{in} - J_{w1}\dot{\omega}_1 - J_{w2}\dot{\omega}_2 - J_{w3}\dot{\omega}_3 - J_{w4}\dot{\omega}_4}{R_e} \tag{105}$$

Considering that the slip ratios of the wheels are relatively small, therefore $\omega_i \approx \frac{u_{x,i}}{R_e}$ for every wheel (i), substitution to eq. (105) yields:

$$F_{x,accel} = \frac{T_{in}}{R_e} - \dot{u}_x\frac{J_w}{{R_e}^2} \overset{(84)}{\Longrightarrow} F_{x,tot} = \frac{T}{R_e}i_k - i_k J_{eng}\frac{\pi}{30}\frac{\dot{n}}{R_e} - \dot{u}_x\frac{J_w}{{R_e}^2} \overset{(104)}{\Longrightarrow}$$

$$\Rightarrow F_{x,accel} = \frac{T}{R_e}i_k - \frac{{i_k}^2 J_{eng} + J_w}{{R_e}^2}\dot{u}_x \tag{106}$$

Finally, attributing all the acceleration force to the rear wheels as $F_{x,accel} \approx F_{x3} + F_{x4}$ yields:

$$F_{x3} + F_{x4} = \frac{T}{R_e}i_k - \frac{{i_k}^2 J_{eng} + J_w}{{R_e}^2}\dot{u}_x \tag{107}$$

$$\begin{cases} F_{x1} = 0 \\ F_{x2} = 0 \\ F_{x3} = \dfrac{T_3}{R_e} \\ F_{x4} = \dfrac{T_4}{R_e} \end{cases} \tag{108}$$

It should be noted that, during starting, considering the engine speed to be steady, eq. (107) should be transformed as:

$$F_{x3} + F_{x4} = \frac{T}{R_e}i_k - \frac{J_w}{{R_e}^2}\dot{u}_x \tag{109}$$

Therefore, for each distinct time moment, rear wheel forces will be calculated in the following manner:

- The sum of rear tires' forces is calculated from eq. (107) or (109).
- The differential is supposed to be in a non-slip state, therefore $\omega_3=\omega_4$. Combining this equality with eq. (74) yields:

$$(1+K_3)\left(u_x+\omega\frac{B_r}{2}\right)=(1+K_4)\left(u_x+\omega\frac{B_r}{2}\right) \tag{110}$$

  Using this relationship between slip ratios and the sum of the rear tires' forces from eq. (107) or (109), the force of each individual wheel can be calculated. The maximum total force $F_{x3}+F_{x4}$ can also be calculated, for the non-slip state of the differential.
- The required torque difference between the two wheels is calculated as $|F_{x3}-F_{x4}|R_e$. If it does not exceed the bias torque, found from eq. (97), then the differential will be considered to be in a non- slip state. Otherwise, the differential slips, and the torque values of the two rear wheels are calculated from eq. (99). The maximum total force $F_{x3}+F_{x4}$ can also be calculated from eq. (99), for the slip state of the differential.

3.2 Modeling of braking system

The braking system consists of two hydraulic circuits, one for the rear and one for the front wheels. These deliver the same amount of torque to the left and right wheels, but not to the front and rear axle. A steady distribution of brake force k_{bf} to the front wheels is attained and therefore, the torque delivered to each wheel is calculated as:

$$\begin{cases} T_1=-\frac{1}{2}\mathrm{k}_{bf}T_{brake}sign(\omega_1) \\ T_2=-\frac{1}{2}\mathrm{k}_{bf}T_{brake}sign(\omega_2) \\ T_3=-\frac{1}{2}(1-\mathrm{k}_{bf})T_{brake}sign(\omega_3) \\ T_4=-\frac{1}{2}(1-\mathrm{k}_{bf})T_{brake}sign(\omega_4) \end{cases} \tag{111}$$

where to torque

$$T_{brake}=|T_1|+|T_2|+|T_3|+|T_4| \tag{112}$$

is a positive value proportional to the force applied to the brake pedal.

As with the case of engine acceleration, if the wheels moment of inertia is considered to be small, then the same equations that apply for torque also apply for the tires forces during braking:

$$\begin{cases} F_{x1} = -\frac{1}{2}\mathrm{k}_{bf} F_{x,brake} sign(u_x + \omega \frac{B_f}{2}) \\ F_{x2} = -\frac{1}{2}\mathrm{k}_{bf} F_{x,brake} sign(u_x - \omega \frac{B_f}{2}) \\ F_{x3} = -\frac{1}{2}(1 - \mathrm{k}_{bf}) F_{x,brake} sign(u_x + \omega \frac{B_r}{2}) \\ F_{x4} = -\frac{1}{2}(1 - \mathrm{k}_{bf}) F_{x,brake} sign(u_x - \omega \frac{B_r}{2}) \end{cases} \quad (113)$$

where

$$F_{x,brake} = |F_{x1}| + |F_{x2}| + |F_{x3}| + |F_{x4}| \quad (114)$$

is again a positive quantity proportional to the force applied to the brake pedal.

Using eq. (113), the following calculation can take place:

$$\begin{cases} F_{x,brake} = \frac{|F_{x1}| + |F_{x2}|}{\mathrm{k}_{bf}} = \frac{|F_{x3}| + |F_{x4}|}{1 - \mathrm{k}_{bf}} \\ |F_{x1}| = |F_{x2}| \\ |F_{x3}| = |F_{x4}| \end{cases} \quad (115)$$

Requesting that none of braking forces exceeds the maximum tire longitudinal force capacity, it follows that:

$$F_{x,brake,max} = \\ = min\left(\frac{2min(|F_{x1,max}|, |F_{x2,max}|)}{\mathrm{k}_{bf}}, \frac{2min(|F_{x3,max}|, |F_{x4,max}|)}{1 - \mathrm{k}_{bf}}\right) \quad (116)$$

3.3 Modeling of shifting system

When a gear change is performed, either upshift or downshift, the engine output speed must be decoupled from the wheels, at least for a certain period of time. If (k) is the currently engaged gear, then eq. (104) states that:

$$n_{before\ gear\ change} = \frac{30}{\pi}\frac{i_k}{R_e} u_{x,before\ gear\ change} \quad (117)$$

$$n_{after\ gear\ change} = \begin{cases} \frac{30}{\pi}\frac{i_{k-1}}{R_e} u_{x,after\ gear\ change} \ \ for\ a\ downshift \\ \frac{30}{\pi}\frac{i_{k+1}}{R_e} u_{x,after\ gear\ change} \ for\ an\ upshift \end{cases} \quad (118)$$

During a gear upshift, the shifting system disables the engine output torque by seizing fuel delivery and ignition. The currently selected gear will therefore easily disengage and the next gear will subsequently easily engage. Because fuel injection and ignition have been disabled, due to engine friction, the engine speed will decrease during the

time elapsing between the current gear disengagement and the next gear engagement. As a result, the engine speed will approach the value of

$n = \frac{30}{\pi}\frac{i_{k+1}}{R_e}u_x$. This enables a near-smooth engagement of the next gear. In addition, any anomalies upon the engine speed not matching the value of $\frac{30}{\pi}\frac{i_{k+1}}{R_e}u_x$ can be smoothened by drivetrain compliance. Therefore, it can assumed that during the upshift of a gear, the vehicle speed remains constant:

$$u_{x,after\ gear\ change} = u_{x,before\ gear\ change} \tag{119}$$

During a gear downshift, the shifting system will make use of the clutch so as to disengage the engine torque. The previous gear will be engaged and the clutch will re-engage the engine to the rest of the transmission. Since no engine torque reduction is performed and considering the time needed for a gear change to be negligible, the momentum of the engine-wheels-vehicle system can be considered as unchanged:

$$mu_{x,after\ gear\ change} + \frac{J_w}{R_e}\omega_{w,after\ gear\ change} + \frac{i_{k-1}J_{eng}}{R_e}\frac{\pi}{30}n_{after\ gear\ change} =$$

$$= mu_{x,before\ gear\ change} + \frac{J_w}{R_e}\omega_{w,before\ gear\ change} + \frac{i_k J_{eng}}{R_e}\frac{\pi}{30}n_{before\ gear\ change}$$

$$\Rightarrow \left(m + \frac{{i_{k-1}}^2 J_{eng} + J_w}{{R_e}^2}\right)u_{x,after\ gear\ change} = \left(m + \frac{{i_k}^2 J_{eng} + J_w}{{R_e}^2}\right)u_{x,before\ gear\ change}$$

$$\Rightarrow u_{x,after\ gear\ change} = \frac{m + \frac{{i_k}^2 J_{eng} + J_w}{{R_e}^2}}{m + \frac{{i_{k-1}}^2 J_{eng} + J_w}{{R_e}^2}}u_{x,before\ gear\ change} \tag{120}$$

The shifting system performs a gear change when the engine speed reaches a lower or upper limit, the downshift and upshift engine speed respectively. For starting, an increased initial engine speed will be used, so as to improve launch acceleration time. As a result, the starting engine speed n_{start} is be maintained while starting, as calculated from eq. (27).

Following the analytical methodology presented in the previous chapter, the speeds $n_{2,k}$ calculated from eq. (14) are used as upshift engine speeds, potentially different for each gear (k).

As far as downshift engine speed is concerned, using eq. (11), it can be calculated that $n_{1,k} = n_{2,k-1}\frac{i_k}{i_{k-1}}$. However, if near constant speed is maintained, then should the engine speed be close to the downshift speed defined by eq. (11), a gear change will drive the engine speed back to the upshift speed. Then, if acceleration is to follow, a

gear shift will be again required. It is now evident that the first gear change was unnecessary and that a lower downshift engine speed should be chosen.

Let t_1 and t_2 be the elapsing times so as to accelerate from the downshift to the upshift engine speed, with and without a gear downshift respectively. Considering that any gear shift takes a specific time to complete, the times t_1 and t_2 can be calculated using eq. (8):

$$t_1 = \int_{n_{1,k}}^{n_{2,k}} \frac{dn}{f_k(n)} \tag{121}$$

$$t_2 = \int_{n_{1,k}\frac{i_{k-1}}{i_k}}^{n_{2,k-1}} \frac{dn}{f_{k-1}(n)} + \int_{n_{2,k-1}\frac{i_k}{i_{k-1}}}^{n_{2,k}} \frac{dn}{f_k(n)} + \Delta t_{shift} \tag{122}$$

It is evident now that the best engine shift speed is such that satisfies the equality:

$$t_1 = t_2 \Rightarrow \int_{n_{1,k}}^{n_{2,k}} \frac{dn}{f_k(n)} = \int_{n_{1,k}\frac{i_{k-1}}{i_k}}^{n_{2,k-1}} \frac{dn}{f_{k-1}(n)} + \int_{n_{2,k-1}\frac{i_k}{i_{k-1}}}^{n_{2,k}} \frac{dn}{f_k(n)} + \Delta t_{shift} \Rightarrow$$

$$\Rightarrow \Delta t_{shift} = \int_{n_{1,k}}^{n_{2,k-1}\frac{i_k}{i_{k-1}}} \frac{dn}{f_k(n)} - \int_{n_{1,k}\frac{i_{k-1}}{i_k}}^{n_{2,k-1}} \frac{dn}{f_{k-1}(n)} \tag{123}$$

It must be mentioned here that the shift time was included only once when calculating the acceleration time t_2. This is true in the case where the downshift from gear (k) to gear (k-1) is performed while not accelerating, for example while braking, and the no-acceleration state continues at least up until the end of the gear change. Usually, this is the most common scenario. However, if acceleration is present while deciding to downshift, then the shift time should be included twice as $2\Delta t_{shift}$.

In addition, due to the constraints of the track, the driver might not accelerate up to $n_{2,k}$, but to a lower engine speed. It is evident that the preceding analysis is valid if the maximum engine speed the driver would wish to accelerate to is at least $n_{2,k-1}\frac{i_k}{i_{k-1}}$. Due to the fact that the shifting system of the vehicle is not capable of predicting the aforementioned states, a set of steady and not altering engine downshift speeds will be used.

If $\Delta t_{shift} = 0$, then it can be easily found that $n_{1,k} = n_{2,k-1}\frac{i_k}{i_{k-1}}$. It will now be proven that for $\Delta t_{shift} > 0$ the resulting engine downshift speed is:

$$n_{1,k} < n_{2,k-1}\frac{i_k}{i_{k-1}} \tag{124}$$

By differentiation of eq. (121) and (122) with respect to $n_{1,k}$, it follows that:

$$\frac{\partial t_1}{\partial n_{1,k}} = -\frac{1}{f_k\left(n_{1,k}\right)} \tag{125}$$

$$\frac{\partial t_2}{\partial n_{1,k}} = -\frac{\frac{i_{k-1}}{i_k}}{f_{k-1}\left(n_{1,k}\frac{i_{k-1}}{i_k}\right)} \tag{126}$$

However, when mentioning about the valid solutions of eq. (14), it was stated that:

$$\frac{\partial \Delta T}{\partial n_{2,k}} < 0 \ \ for\ every\ n < n_{2,k} \overset{(13)}{\Longrightarrow}$$

$$\Rightarrow \frac{1}{f_k(n)} < \frac{i_{k+1}}{i_k}\frac{1}{f_{k+1}\left(\frac{i_{k+1}}{i_k}n_{2,k,s}\right)} \tag{127}$$

Performing the substitution $\begin{cases} k \to k-1 \\ n \to n\frac{i_{k-1}}{i_k} \end{cases}$ yields:

$$\frac{1}{f_{k-1}\left(n\frac{i_{k-1}}{i_k}\right)} < \frac{i_k}{i_{k-1}}\frac{1}{f_k(n)} \ for\ every\ n\frac{i_{k-1}}{i_k} < n_{2,k-1} \Rightarrow$$

$$\Rightarrow -\frac{\frac{i_{k-1}}{i_k}}{f_{k-1}\left(n\frac{i_{k-1}}{i_k}\right)} > -\frac{1}{f_k(n)} \ for\ every\ n < n_{2,k-1}\frac{i_k}{i_{k-1}} \tag{128}$$

Therefore $\frac{\partial t_2}{\partial n_{1,k}} > \frac{\partial t_1}{\partial n_{1,k}}$ for every $n_{1,k} < n_{2,k-1}\frac{i_k}{i_{k-1}}$. As it can be seen in figure 14, the direct outcome of this inequality, is that eq. (123) can only be satisfied for $n_{1,k} < n_{2,k-1}\frac{i_k}{i_{k-1}}$.

Additionally, it must be mentioned that there should be no gear downshift at intermediate engine loads. This is because the driver has not requested for full engine torque and a downshift so as to improve acceleration time by increasing wheel torque would be undesirable.

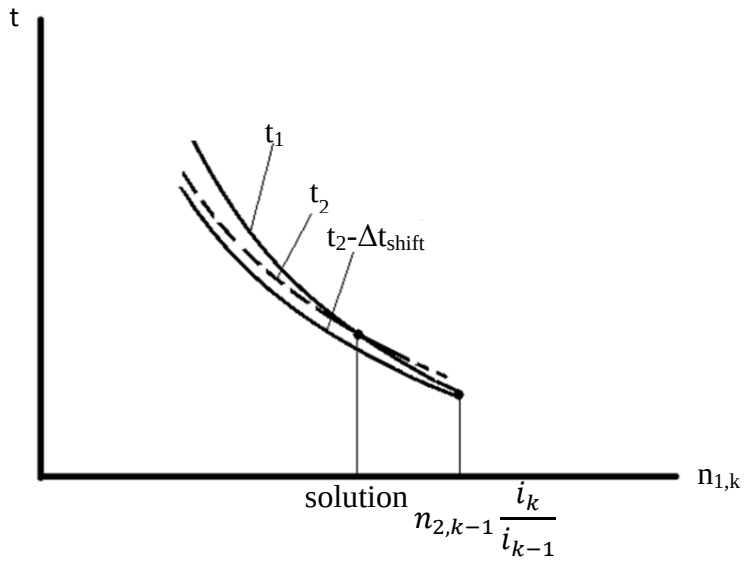

Figure 14: Downshift speed solution

Last but not least, should the engine speed reach very low values for the first gear, then there is no previous gear so as to increase engine speed. To eliminate this problem, the driver will re-enter into a starting mode using the clutch and increase the engine speed up to the starting engine speed n_{start}.

3.4 Driver Modeling

The driver controls all the inputs of the vehicle as a system. In this case, these inputs are the steering, the engine load and the braking force. To begin with, considering the physical abilities of the driver, all the driver inputs are limited by a maximum rate of change. Additionally, a time constant of Δt_{driver} is introduced as a reaction time. This time will be used for manipulating the driver's input to the pedals using a first order differential equation:

$$\Delta t_{driver}\frac{d}{dt}(pedal\ position) + pedal\ position = pedal\ position\ instructed \tag{129}$$

where the instructed pedal position is such that the force resulting for acceleration or braking, depending on the pedal used, is limited. For the throttle pedal only, if the instructed pedal position is 0% or 100%, then the maximum rate of change is applied. It should be noted that the same equation does not apply to the steering angle, as a different steer control method will be implemented later on.

The upper limit of the acceleration excreted on the vehicle is given by the tires' limits. A good approximation of the tires' limits in the case where longitudinal and lateral forces are present is the friction ellipse:

$$\left(\frac{F_x}{\Phi_x F_z}\right)^2 + \left(\frac{F_y}{\Phi_y F_z}\right)^2 \leq 1 \tag{130}$$

However, when the longitudinal force reaches this limit, the tires cornering stiffness decreases significantly, rendering the vehicle very difficult to control. For this reason, the driver always chooses a limited traction for the longitudinal and lateral acceleration:

$$\left(\frac{F_x}{(traction\ limit\ x)\Phi_x F_z}\right)^2 + \left(\frac{F_y}{(traction\ limit\ y)\Phi_y F_z}\right)^2 \leq 1 \tag{131}$$

where the x traction limit might be different for acceleration and braking. Considering that the loss of controllability mentioned due to decrease in cornering stiffness occurs when the two front, or the two rear tires, together reach the limit of traction, the final equation describing the acceleration or braking applied by the driver becomes:

$$F_{x,accel} = (traction\ limit\ x)\sum_{j=3}^{4}\left(\Phi_{xj}F_{zj}\right)\sqrt{1-\left(\frac{traction\ y}{traction\ limit\ y}\right)^2} \tag{132}$$

$$F_{x,brake} = (traction\ limit\ x)\sum_{j=1}^{4}\left(\Phi_{xj}F_{zj}\right)\sqrt{1-\left(\frac{traction\ y}{traction\ limit\ y}\right)^2} \tag{133}$$

where

$$(traction\ y)^2 = \min\left(\left(\frac{F_{y1}+F_{y2}}{\Phi_{y1}F_{z1}+\Phi_{y2}F_{z2}}\right)^2, \left(\frac{F_{y3}+F_{y4}}{\Phi_{y3}F_{z3}+\Phi_{y4}F_{z4}}\right)^2\right) \tag{134}$$

In order to decrease the complexity of the solution, the lateral forces F_{y1}, F_{y2}, F_{y3} and F_{y4} used in eq. (132), (133) and (134) are calculated using the slip ratios of the previous simulation time step.

3.5 Desired Trajectory

The problem of determining the best path the vehicle must follow so that it performs the best time on the race track is known as the racing line problem. Xiong [14] dealt with his problem by constraining the lateral acceleration of the vehicle as:

$$mU^2\kappa \leq \Phi mg \Rightarrow U \leq \sqrt{\frac{\Phi g}{\kappa}} \tag{135}$$

where Φ is the tires' coefficient of traction. The time spent in a racetrack will be:

$$t = \int_{track} dt = \int_{track} \frac{dt}{ds} ds = \int_{track} \frac{1}{U} ds \geq \frac{1}{\sqrt{\Phi g}} \int_{track} \sqrt{\kappa} ds \tag{136}$$

Therefore, an approach to minimize the integral $\int_{track} \sqrt{\kappa} ds$ could increase the potential of the driver to minimize lap-time. In [13], a nonlinear solver and an artificial intelligence approach were incorporated for solving this minimization problem. In the artificial intelligence approach, a dimensionless parameter defined as:

$$P = \min\left(max\left(\frac{\kappa_2 - \kappa_1}{\max(\kappa)}, -1\right), 1\right) \tag{137}$$

was used for deciding the deviation from the track centerline. The quantities κ_1 and κ_2 are the curvatures of a near and a more distant point on the track.

The optimization methods however did not always lead to desired results. In continuous turns, the methods seemed to produce a curve once heading to the inner and then to the outer limit of the track. Moreover, the computational time was not always satisfactory.

In general, many different methods have been used for determining the optimal racing line. However, in Formula Student, the tracks are usually narrow. Track widths of about 3.5m to 5m are more usual, while the car width is usually about 1.2m. This leaves little advantage for reducing times by using a better racing line.

Instead of dealing the problem with an optimization approach, a general method is employed, one that is usually preferred by racing drivers in practice. A typical racing line in a straight-turn-straight situation can be seen in figure 15. The driver evidently seems to be trying to maintain a high radius track. For doing so, he deviates towards the inside of the turn. Before and after the turn, he deviates towards the outside of the turn.

One way of achieving this is considering every part of the track that has a relatively large curvature abs(κ)>κ_{min} and can therefore be considered as a turn. For those track parts, the following equation can be chosen:

$$s_n = (corner\ cutting\ coefficient) sign(\kappa) \frac{track\ width - car\ width}{2} \tag{138}$$

where the corner cutting coefficient is a percentage of the maximum possible deviation from the track centerline the driver will chose, so as not to exit the limits of the track. Every other part of the track is close to a straight line and the deviation s_n can be chosen by linear interpolation. The negative of the values of the deviations of

the two most adjacent turns will be used for this interpolation. The resulting deviation will not be a continuous function. Therefore, smoothing of the results is required.

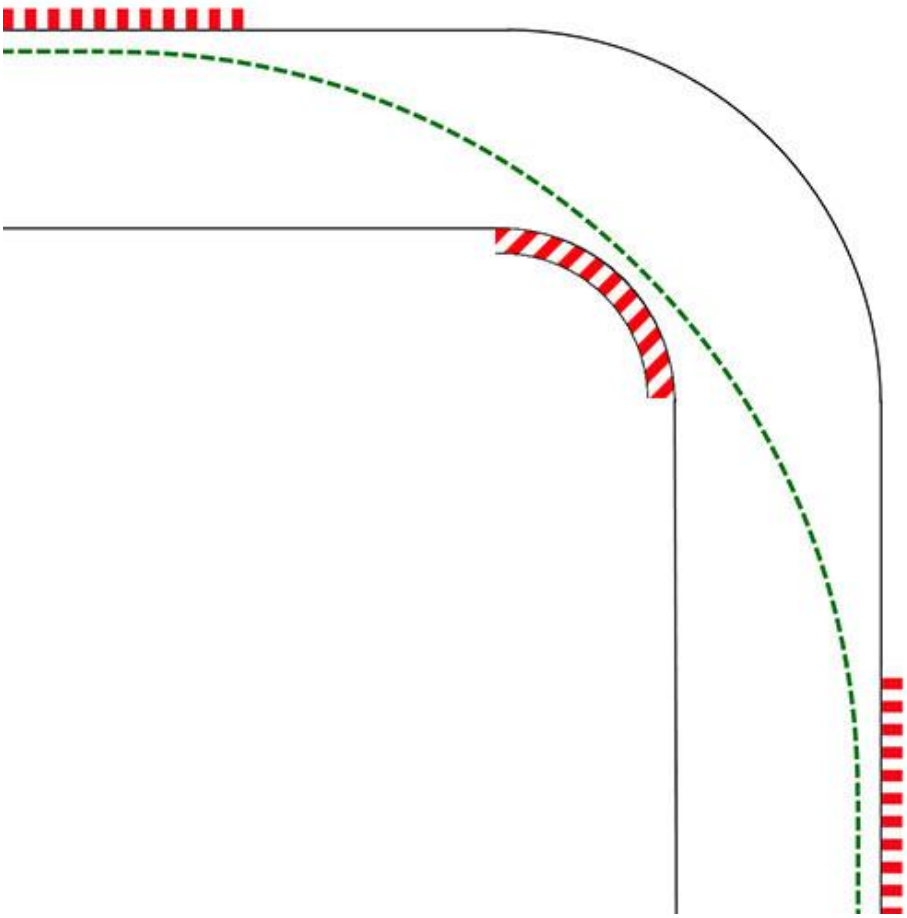

Figure 15: Typical racing line

Another method involves using the parameter defined eq. (137) instead of the sign function:

$$s_n = (corner\ cutting\ coefficient)P\frac{track\ width - car\ width}{2} \tag{139}$$

This method senses the increase or decrease in track radius and deviates accordingly.

However, the track itself might have a centerline that is not smooth. This means that, even if the deviation s_n is smoothened, the end result might be a curve of non-smooth radius. Therefore, after calculating the desired trajectory, additional smoothing is required so as to obtain a good result.

The final method used incorporates both eq. (138) and (139). Two different results are computed and then the average is taken. A flowchart describing each distinct step can be seen in figure 16.

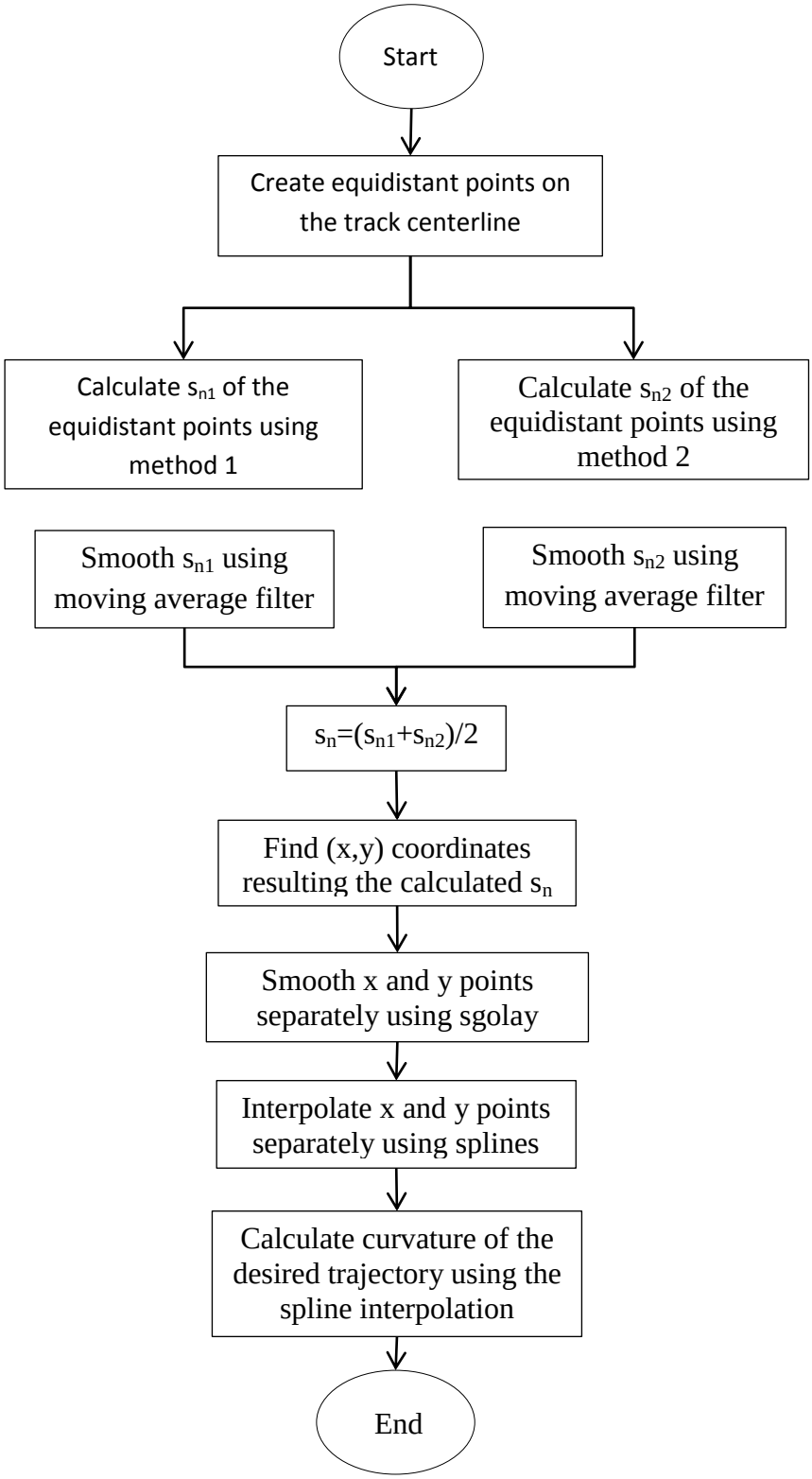

Figure 16: Racing line calculation flow chart

3.6 Velocity planning

Having specified the desired trajectory and considering that its curvature is a smooth function of the path length, it may be assumed that the maximum speed the driver should be attaining at every point in the track is the maximum steady state speed in a constant radius. This upper limit in speed can be easily determined by running the simulation in a constant radius turn, up to the point where the speed converges to a constant value.

However, performing a simulation for a large number of radii is a time consuming procedure. In order to avoid this method, the maximum speed is first analytically calculated. More specifically, taking the steady state for eq. (37), (38), (40) and (41), assuming zero lateral velocity, small steer angles and neglecting the vehicle width, for a turn of positive radius ρ, it follows that:

$$m\frac{u^2}{\rho} = F_{y1} + F_{y2} + F_{y3} + F_{y4} \tag{140}$$

$$0 = a\left(F_{y1} + F_{y2}\right) - b\left(F_{y3} + F_{y4}\right) \tag{141}$$

Taking the inner and outer wheel lateral forces to be the same $F_{y1} = F_{y2}$ and $F_{y3} = F_{y4}$ yields:

$$\begin{cases} F_{y1} = F_{y2} = \dfrac{1}{2}\dfrac{b}{L}m\dfrac{u^2}{\rho} \\ F_{y3} = F_{y4} = \dfrac{1}{2}\dfrac{a}{L}m\dfrac{u^2}{\rho} \end{cases} \tag{142}$$

The tire normal loads can be calculated from eq. (43) as:

$$\begin{cases} F_{z1} = 0.5\left(m\dfrac{b}{L}g + 2\xi\dfrac{h}{B_f}m\dfrac{u^2}{\rho} - F_D\dfrac{h_a}{L} + F_L\dfrac{b_a}{L}\right) \\ F_{z2} = 0.5\left(m\dfrac{b}{L}g - 2\xi\dfrac{h}{B_f}m\dfrac{u^2}{\rho} - F_D\dfrac{h_a}{L} + F_L\dfrac{b_a}{L}\right) \\ F_{z3} = 0.5\left(m\dfrac{a}{L}g + 2(1-\xi)\dfrac{h}{B_r}m\dfrac{u^2}{\rho} + F_D\dfrac{h_a}{L} + F_L\dfrac{a_a}{L}\right) \\ F_{z4} = 0.5\left(m\dfrac{a}{L}g - 2(1-\xi)\dfrac{h}{B_r}m\dfrac{u^2}{\rho} + F_D\dfrac{h_a}{L} + F_L\dfrac{a_a}{L}\right) \end{cases} \tag{143}$$

Wheels 2 and 4 have less vertical load and are therefore more prone to slippage. The maximum theoretical velocity so as to reach tire slippage for wheel 2 can be found as:

$$F_{y2} = \Phi_{y2} F_{z2} \xrightarrow{(142) and\ (143)} \frac{1}{2}\frac{b}{L} m \frac{u^2}{\rho} =$$

$$= 0.5\Phi_{y2}\left(m\frac{b}{L}g - 2\xi\frac{h}{B_f}m\frac{u^2}{\rho} - F_D\frac{h_a}{L} + F_L\frac{b_a}{L}\right) \Rightarrow$$

$$m\frac{u^2}{\rho} = \Phi_{y2}mg + \Phi_{y2}\frac{u^2}{\rho}\left(-2\xi\frac{h}{B_f}\frac{L}{b}m - \rho\left(\frac{1}{2}\rho C_D A\frac{h_a}{b} - \frac{1}{2}\rho C_L A\frac{b_a}{b}\right)\right) \Rightarrow$$

$$\frac{u^2}{\rho} = \frac{\Phi_{y2}g}{1 - \Phi_{y2}\left(\frac{\rho}{m}\left(\frac{1}{2}\rho C_L A\frac{b_a}{b} - \frac{1}{2}\rho C_D A\frac{h_a}{b}\right) - 2\frac{\xi}{b/_L}\frac{h}{B_f}\right)} \tag{144}$$

Likewise, for wheel 4:

$$\frac{u^2}{\rho} = \frac{\Phi_{y4}g}{1 - \Phi_{y4}\left(\frac{\rho}{m}\left(\frac{1}{2}\rho C_L A\frac{a_a}{a} + \frac{1}{2}\rho C_D A\frac{h_a}{a}\right) - 2\frac{1-\xi}{a/_L}\frac{h}{B_r}\right)} \tag{145}$$

Therefore, the theoretically approximated maximum, speed is:

$$u_{max,th} = = min\left\{\begin{array}{l}\sqrt{\dfrac{\rho\Phi_{y2}g}{1 - \Phi_{y2}\left(\frac{\rho}{m}\left(\frac{1}{2}\rho C_L A\frac{b_a}{b} - \frac{1}{2}\rho C_D A\frac{h_a}{b}\right) - 2\frac{\xi}{b/_L}\frac{h}{B_f}\right)}} \\ \sqrt{\dfrac{\rho\Phi_{y4}g}{1 - \Phi_{y4}\left(\frac{\rho}{m}\left(\frac{1}{2}\rho C_L A\frac{a_a}{a} + \frac{1}{2}\rho C_D A\frac{h_a}{a}\right) - 2\frac{1-\xi}{a/_L}\frac{h}{B_r}\right)}}\end{array}\right\} \tag{146}$$

Having defined the theoretical approximation, a traction fitting factor is used as a function of the radius:

$$\text{traction fitting factor}_{(\rho)} = \left(\frac{u_{max\,(\rho)}}{u_{max,th\ (\rho)}}\right)^2 \tag{147}$$

where the true maximum speeds u_{max} are found by running the simulation for a constant turn radii. A small number of different radii are used for the calculation of the traction fitting factor. Subsequently, maximum speeds are found for every point in the track as:

$$u_{max\,(\rho)} = u_{max,th\ (\rho)}\sqrt{\text{traction fitting factor}_{(\rho)}} \tag{148}$$

Having calculated the maximum speeds in the track, the points where braking is required can now be defined as such that the driver can marginally decelerate to the permitted speed. Those braking points are found while the simulation is running. More specifically, if the simulation comes to a point where $U > u_{max\,(\rho)}$, then a braking point must be defined at a previous position in the track. So as to reject any slight anomalies in maximum speed which the driver might ignore, the exceedance of maximum speed is being checked only if at least one of the following inequalities is satisfied:

$$|s_n| > s_{n.max} \tag{149}$$
$$|\psi| > max\ drift\ angle \tag{150}$$
$$|\beta + \psi| > \max track\ angle \tag{151}$$

where $s_{n.max}$ is a percentage of $\frac{track\ width - car\ width}{2}$. It should be mentioned that the quantities $s_{n.max}$, (max drift angle) and (max track angle) act as filters upon the maximum speed and should therefore be chosen small enough so that the driver does not completely ignore the maximum speed.

To find the previous track position where braking must commence, an initial braking attempt is performed. Deceleration is measured from that attempt and a new braking position is defined using steady deceleration approximation.

Both acceleration and braking deceleration are estimated in the following ways:

$$a_1 = \frac{U_{(t\_accel\_end)} - U_{(t\_accel\_end - \delta t_{sim})}}{\delta t_{sim}} \tag{152}$$

$$a_{2,u} = \frac{U_{(t\_brake\_start)} - U_{(t\_brake\_end)}}{t\_brake\_start - t\_brake\_end} \tag{153}$$

$$a_{2,s} = 2\frac{s_{(t\_brake\_start)} - s_{(t\_brake\_end)}}{(t\_brake\_start - t\_brake\_end)^2} + 2\frac{U_{(t\_brake\_start)}}{t\_brake\_start - t\_brake\_end} \tag{154}$$

where δt_{sim} is the simulation time step, a_1 is the acceleration approximation and $a_{2,u}$ and $a_{2,s}$ are the deceleration approximations using speed and length. The time moments (t_accel_end) and (t_brake_start) are not exactly the same, as there is always a transitional phase between acceleration and braking due to the time taken to release the throttle pedal.

Taking the time (t_brake_start) as the current braking starting point, a new point must be defined earlier or later in the track, depending upon whether the speed at the end of the previous braking attempt was greater or smaller than the desired maximum speed. Figure 17 illustrates the case where the new braking point must be after the current one. The driver will keep accelerating for an extra time of Δt_1 and then brake up to the desired speed u_{max}. The equations describing those motions are:

$$s_{pbs} - s_{be} = u_{pbs}\Delta t_1 + \frac{1}{2}a_1{\Delta t_1}^2 + u_{nbs}\Delta t_2 + \frac{1}{2}a_{2,s}{\Delta t_2}^2 \quad (155)$$

$$u_{nbs} = u_{max} - a_{2,u}\Delta t_2 \quad (156)$$

$$u_{nbs} = u_{pbs} + a_1\Delta t_1 \quad (157)$$

where s_{pbs} and u_{pbs} are the previous braking starting point length and speed, s_{be} is the required braking end point length and u_{nbs} is the new braking starting speed.

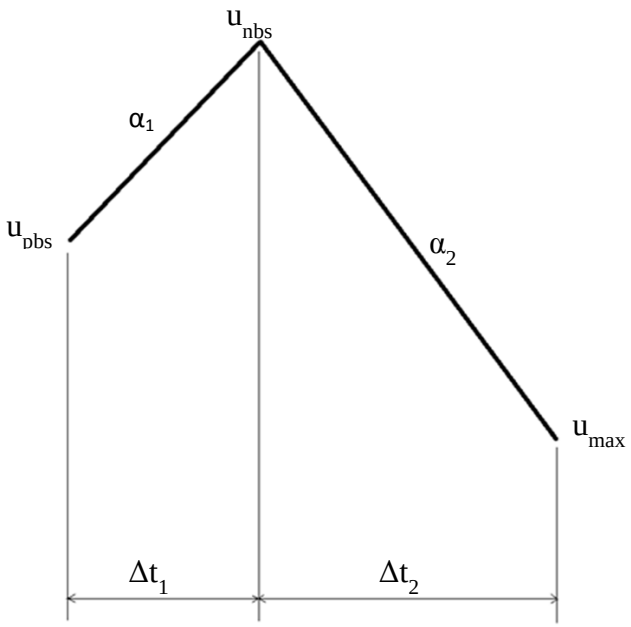

Figure 17: New braking point approximation

Eliminating the new braking start speed and braking time, eq. (155), (156) and (157) can be solved for Δt_1:

$$\begin{aligned} &\frac{1}{2}\left(1 - \frac{2a_{2,u} - a_{2,s}}{{a_{2,u}}^2}a_1\right){\Delta t_1}^2 \\ &+ \left[u_{pbs}\left(1 + \frac{a_1}{a_{2,u}}\right) - \frac{a_1}{a_{2,u}}\left(u_{pbs} - u_{max}\right)\left(1 - \frac{a_{2,s}}{a_{2,u}}\right)\right]\Delta t_1 \\ &- \frac{u_{pbs} - u_{max}}{a_{2,u}}\left[u_{pbs} - \frac{1}{2}\frac{a_{2,s}}{a_{2,u}}\left(u_{pbs} - u_{max}\right)\right] - \left(s_{pbs} - s_{be}\right) = 0 \end{aligned} \quad (158)$$

The time Δt_1 is added to the acceleration end time (t_accel_end) and a new braking procedure is performed. It must be mentioned that, in order for this method to converge, relaxation is required for the calculated time Δt_1, when the algorithm is not close to a solution.

3.7 Steering system and steering control

The steering system links the steering wheel angle δ_{steer} with the front wheel steer angles δ_1 and δ_2. Neglecting toe angles, for zero steering wheel angle, the front wheels should both align with the vehicle longitudinal axis. As a result, since the car is symmetric, it follows that:

$$\delta_{1\,(\delta_{steer})} = -\delta_{2\,(-\delta_{steer})} \tag{159}$$

Using this equation, the behavior of the steering system is modeled using a third order polynomial:

$$\delta_1 = c_3{\delta_{steer}}^3 + c_2{\delta_{steer}}^2 + c_1\delta_{steer} \tag{160}$$
$$\delta_2 = c_3{\delta_{steer}}^3 - c_2{\delta_{steer}}^2 + c_1\delta_{steer} \tag{161}$$

Implementing a steering control scheme that will enable the car to follow the desired trajectory is a difficult task. The approach used in this study, follows a technique for driverless vehicles introduced by Hoffmann et al. [15]. In an effort to exponentially decrease the deviation from the track centerline, a response would be desired that follows the equation:

$$\dot{s}_{n,d} = -k_{p,s}s_{n,d} \tag{162}$$

However, from eq. (32) it follows that $\dot{s}_n = Usin(\beta + \psi)$, where the angles β and ψ have been defined in figure 7. Therefore, the limit in the rate of change is $\dot{s}_n \leq U$. To account for this, the desired response equation is modified as:

$$\dot{s}_{n,d} = -\frac{k_{p,s}s_{n,d}}{\sqrt{1-\left(\frac{k_{p,s}s_{n,d}}{U}\right)^2}} \tag{163}$$

For a small deviation from the track centerline, eq. (163) can be approximated as an exponential decrease. Linking this result with eq. (32) yields:

$$Usin(\beta_d + \psi) = -\frac{k_{p,s}s_{n,d}}{\sqrt{1-\left(\frac{k_{p,s}s_{n,d}}{U}\right)^2}} \Rightarrow \sin(\beta_d + \psi_d) = -\frac{\frac{k_{p,s}s_{n,d}}{U}}{\sqrt{1-\left(\frac{k_{p,s}s_{n,d}}{U}\right)^2}} \Rightarrow$$

$$\Rightarrow tan(\beta_d + \psi_d) = -\frac{k_{p,s}s_{n,d}}{U} \tag{164}$$

Geometrically, this equation can be explained as the driver's wish to point the vehicle velocity to a desired direction. This direction is defined using a look ahead distance of $U/k_{p,s}$, as the adjacent side of the right triangle seen in figure 18.

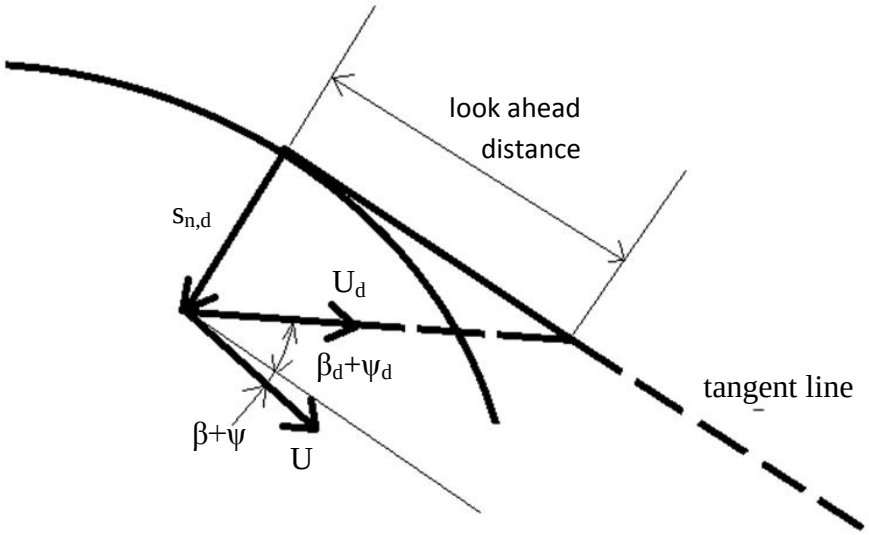

Figure 18: Desired vehicle direction

The steering will now be controlled based upon the error between the current and the desired angle:

$$(\beta + \psi) - (\beta_d + \psi_d) = \beta + \psi + Arctan\left(\frac{k_{p,s}s_n}{U}\right) \tag{165}$$

Maintaining the same result, the desired (β) angle is redefined as

$$\beta_d = -\psi - Arctan\left(\frac{k_{p,s}s_n}{U}\right) \tag{166}$$

and the angle error as:

$$\beta_e = \beta - \beta_d \tag{167}$$

The steering wheel angle will be controlled using a PID controller on the angle error:

$$\dot{\delta}_{steer} = -\left(k_i\beta_e + k_p\dot{\beta}_e + k_d\ddot{\beta}_e\right) \tag{168}$$

where k_i, k_p and k_d are the controller integral, proportional and derivative gains.

In order to tune those gains, a simple linearized bicycle car model is used. Taking eq. (38) and (41), assuming small velocity and steer angles and neglecting the vehicle width yields:

$$I_z\dot{\omega} = a\left(F_{y1} + F_{y2}\right) - b\left(F_{y3} + F_{y4}\right) \tag{169}$$

For the lateral tire forces, using the cornering stiffness coefficient, assuming small slip angles and neglecting lateral velocity, it follows that:

$$F_{y1} + F_{y2} = C_{a,f}\alpha_f \tag{170}$$
$$F_{y3} + F_{y4} = C_{a,r}\alpha_r \tag{171}$$
$$\delta - \alpha_f = -\frac{a\omega}{U} \tag{172}$$
$$\alpha_r = \frac{b\omega}{U} \tag{173}$$

where $C_{a,f}$ and $C_{a,r}$ are the cornering stiffnesses of the front and rear axle and δ is a mean steer angle between δ_1 and δ_2. In order for the slip angle a_f to adequately describe the sum of slip angles a_1 and a_2, as well as for the ratio δ_{steer}/δ, also called the steer ratio, to be a least fluctuating value, the angle δ is calculated using the following equation:

$$cot\delta = \frac{cot\delta_1 + cot\delta_2}{2} \tag{174}$$

Performing a substitution in eq. (169) using eq. (170) to (173), a single differential equation arises for the yaw rate:

$$\dot{\omega} + A\omega = B\delta \tag{175}$$

where the quantities A and B are calculated as:

$$A = \frac{a^2C_{a,f} + b^2C_{a,r}}{UI_z} \tag{176}$$
$$B = \frac{aC_{a,f}}{I_z} \tag{177}$$

Using eq. (32) and (33) the yaw rate and the error angle can be linked to the deviation from the track centerline:

$$\left.\begin{aligned}\dot{\beta} = \omega - kU\frac{\cos(\beta+\psi)}{1-\kappa s_n} = \omega - \omega_{ss}\\ \dot{s}_n = Usin(\beta+\psi) \approx U(\beta+\psi)\end{aligned}\right\} \Rightarrow$$

$$\left.\begin{aligned}\ddot{s}_n \approx U\dot{\beta} = U(\omega - \omega_{ss})\\ \beta_e = \beta - \beta_d \approx \beta + \psi + \frac{k_{p,s}s_n}{U}\end{aligned}\right\} \Rightarrow$$

$$\Rightarrow \begin{cases} \omega \approx \omega_{ss} + \dfrac{\ddot{s}_n}{U} \\ \beta_e \approx \dfrac{\dot{s}_n + k_{p,s} s_n}{U} \end{cases} \tag{178}$$

Substituting in eq. (168) and (175) yields:

$$\begin{cases} \dddot{s}_n + A\ddot{s}_n = BU\delta - U[\dot{\omega}_{ss} + A\omega_{ss}] \\ \dot{\delta}_{steer} = -\dfrac{1}{U}\left[k_d \dddot{s}_n + \left(k_p + k_{p,s}k_d\right)\ddot{s}_n + \left(k_i + k_p k_{p,s}\right)\dot{s}_n + k_i k_{p,s} s_n\right] \end{cases} \tag{179}$$

Considering that $\delta_{steer} = k_{steer}\,\delta$, where k_{steer} is the steer ratio, the two equations above can be combined so as to form the closed loop differential equation:

$$\begin{aligned} s^{(4)}{}_n + (A + Bk_d{}')\dddot{s}_n + B\left(k_p{}' + k_{p,s}k_d{}'\right)\ddot{s}_n + B\left(k_i{}' + k_p{}' k_{p,s}\right)\dot{s}_n \\ + Bk_i{}' k_{p,s} s_n = -U[\dot{\omega}_{ss} + A\omega_{ss}] \end{aligned} \tag{180}$$

where the constants:

$$\begin{cases} k_i' = {k_i}/{k_{steer}} \\ k_p' = {k_p}/{k_{steer}} \\ k_d' = {k_d}/{k_{steer}} \end{cases} \tag{181}$$

Therefore, the closed loop characteristic equation is:

$$\begin{aligned} S^4 + (A + Bk_d{}')S^3 + B\left(k_p{}' + k_{p,s}k_d{}'\right)S^2 + B\left(k_i{}' + k_p{}' k_{p,s}\right)S \\ + Bk_i' k_{p,s} = 0 \end{aligned} \tag{182}$$

Due to the high order of the system, it is difficult to predict its response for every arbitrary value of the gains. Instead, a certain response will be suggested and the gains are calculated so that this response is satisfied. Considering stability, the following form is proposed for the characteristic equation:

$$\begin{aligned} (S + \tau_1)(S + \tau)(S^2 + 2\zeta\omega_n S + \omega_n{}^2) = 0 \xrightarrow{choosing\ \tau = \zeta\omega_n} \\ S^4 + (\tau_1 + 3\tau)S^3 + \tau\left[3\tau_1 + \tau\left(2 + \frac{1}{\zeta^2}\right)\right]S^2 + \tau^2\left[\frac{\tau}{\zeta^2} + \tau_1\left(2 + \frac{1}{\zeta^2}\right)\right]S \\ + \frac{\tau_1\tau^3}{\zeta^2} = 0 \end{aligned} \tag{183}$$

Therefore, the system of equations relating the gains to the desired response constants are:

$$\begin{cases} A + Bk_d' = \tau_1 + 3\tau \\ B\left(k_p' + k_{p,s}k_d'\right) = \tau\left[3\tau_1 + \tau\left(2 + \dfrac{1}{\zeta^2}\right)\right] \\ B\left(k_i' + k_p'k_{p,s}\right) = \tau^2\left[\dfrac{\tau}{\zeta^2} + \tau_1\left(2 + \dfrac{1}{\zeta^2}\right)\right] \\ Bk_i'k_{p,s} = \dfrac{\tau_1\tau^3}{\zeta^2} \end{cases} \tag{184}$$

It can observed that A is the inverse of the time constant of the open loop eq. (175). Let $\lambda = A/\tau_1$. Then, requesting for the time $1/\tau$ to be the dominant time constant of the system, the following inequality applies: $1/\tau \geq 1/\tau_1 \Rightarrow \lambda \leq \lambda_{max} = A/\tau$. Substituting λ and λ_{max} to the equations for the gains yields:

$$\left.\begin{aligned} A + Bk_d' &= 3\tau + \frac{A}{\lambda} \\ B\left(k_p' + k_{p,s}k_d'\right) &= \tau\left[3\frac{A}{\lambda} + \tau\left(2 + \frac{1}{\zeta^2}\right)\right] \\ B\left(k_i' + k_p'k_{p,s}\right) &= \tau^2\left[\frac{\tau}{\zeta^2} + \frac{A}{\lambda}\left(2 + \frac{1}{\zeta^2}\right)\right] \\ Bk_i'k_{p,s} &= \frac{\tau^3}{\zeta^2}\frac{A}{\lambda} \end{aligned}\right\} \Rightarrow$$

$$\left.\begin{aligned} Bk_d' &= 3\tau + \left(\frac{1}{\lambda} - 1\right)A \\ Bk_p' + k_{p,s}\tau\left[3 + \lambda_{max}\left(\frac{1}{\lambda} - 1\right)\right] &= \tau\left[3\frac{A}{\lambda} + \tau\left(2 + \frac{1}{\zeta^2}\right)\right] \\ \frac{\tau^3}{k_{p,s}\zeta^2}\frac{A}{\lambda} + Bk_p'^{k_{p,s}} &= \tau^2\left[\frac{\tau}{\zeta^2} + \frac{A}{\lambda}\left(2 + \frac{1}{\zeta^2}\right)\right] \\ Bk_i' &= \frac{\tau^3}{k_{p,s}\zeta^2}\frac{A}{\lambda} \end{aligned}\right\} \Rightarrow$$

$$\Rightarrow \begin{cases} Bk'_d = 3\tau + \left(\frac{1}{\lambda} - 1\right)A \\ Bk'_p = \tau\left[3\frac{A}{\lambda} + \tau\left(2 + \frac{1}{\zeta^2}\right)\right] - k_{p,s}\tau\left[3 + \lambda_{max}\left(\frac{1}{\lambda} - 1\right)\right] \\ Bk'_p = \frac{\tau^2}{k_{p,s}}\left[\frac{\tau}{\zeta^2} + \frac{A}{\lambda}\left(2 + \frac{1}{\zeta^2}\right)\right] - \frac{\tau^3}{{k_{p,s}}^2\zeta^2}\frac{A}{\lambda} \\ Bk'_i = \frac{\tau^3}{k_{p,s}\zeta^2}\frac{A}{\lambda} \end{cases} \quad (185)$$

The two set of equations solved for the proportional gain k'_p can be combined and rearranged in terms of the look ahead distance gain $k_{p,s}$:

$$\left[3 + \lambda_{max}\left(\frac{1}{\lambda} - 1\right)\right]\left(\frac{k_{p,s}}{\tau}\right)^3 - \left(3\frac{\lambda_{max}}{\lambda} + 2 + \frac{1}{\zeta^2}\right)\left(\frac{k_{p,s}}{\tau}\right)^2 + \left[\frac{1}{\zeta^2} + \frac{\lambda_{max}}{\lambda}\left(2 + \frac{1}{\zeta^2}\right)\right]\frac{k_{p,s}}{\tau} - \frac{\lambda_{max}}{\lambda}\frac{1}{\zeta^2} = 0 \quad (186)$$

This third degree equation does not have trivial solutions for $\frac{k_{p,s}}{\tau}$. It can however be easily solved by factorization if λ=1. As the dominant time constant (1/τ) and damping ratio (ζ) of the response can still be chosen, letting λ=1 simplifies the selection of gains:

$$3\left(\frac{k_{p,s}}{\tau}\right)^3 - \left(3\lambda_{max} + 2 + \frac{1}{\zeta^2}\right)\left(\frac{k_{p,s}}{\tau}\right)^2 + \left[\frac{1}{\zeta^2} + \lambda_{max}\left(2 + \frac{1}{\zeta^2}\right)\right]\frac{k_{p,s}}{\tau} - \lambda_{max}\frac{1}{\zeta^2} = 0$$

$$\Rightarrow \left[\left(\frac{k_{p,s}}{\tau}\right) - \lambda_{max}\right]\left[3\left(\frac{k_{p,s}}{\tau}\right)^2 - \left(2 + \frac{1}{\zeta^2}\right)\left(\frac{k_{p,s}}{\tau}\right) + \frac{1}{\zeta^2}\right] = 0 \quad (187)$$

Therefore, three valid solutions can be obtained:

$$\left.\begin{array}{r} \left(\frac{k_{p,s}}{\tau}\right) = \lambda_{max} \\ \left(\frac{k_{p,s}}{\tau}\right) = \frac{\left(2 + \frac{1}{\zeta^2}\right) \pm \sqrt{4 + \frac{1}{\zeta^4} - \frac{8}{\zeta^2}}}{6} \end{array}\right\} \Rightarrow$$

$$\Rightarrow \begin{cases} k_{p,s} = A \\ k_{p,s} = \tau\dfrac{\left(2 + \frac{1}{\zeta^2}\right) \pm \sqrt{4 + \frac{1}{\zeta^4} - \frac{8}{\zeta^2}}}{6} \; for\; \zeta > 1.366 \end{cases} \quad (188)$$

Requesting for the look ahead distance gain to be independent of the speed of the vehicle, the following final solution arises:

$$\begin{cases} k_d = \dfrac{3\tau}{B} k_{steer} \\ k_{p,s} = \tau \dfrac{\left(2 + \dfrac{1}{\zeta^2}\right) \pm \sqrt{4 + \dfrac{1}{\zeta^4} - \dfrac{8}{\zeta^2}}}{6} \; for\; \zeta > 1.366 \\ k_i = \dfrac{A}{B} \dfrac{\tau^3}{k_{p,s}\zeta^2} k_{steer} \\ k_p = \dfrac{\tau}{B}\left[3(A - k_{p,s}) + \tau\left(2 + \dfrac{1}{\zeta^2}\right)\right] k_{steer} \end{cases} \tag{189}$$

4. The optimization technique

The primary step into creating an optimization technique is defining the objective function. As mentioned earlier, in general, the maximization of the Acceleration, Autocross and Endurance scores using the gear ratios is the combination that improves the overall performance of the vehicle in Formula Student competitions. However, following the outcomes from the analytical examination of gear ratios performed, it is reasonable that a change in gear ratios which may be beneficial for one event will probably impair the vehicle performance in another. In the Acceleration event for example, the optimal gear ratios are dependent only upon the performance of the engine and the tire grip for the starting gear ratio. In the Endurance race however, results will be greatly influenced by the speeds attained in the track. The same should apply for the Autocross race, with the slight difference that, since only a single lap is run, the initial part of the track will be closer to an acceleration run.

It is now evident that optimizing the scores of each event individually will probably lead to a different result than optimizing the sum of the scores. As examined later, while reviewing the results of the simulation and the optimization procedure, finding a global optimum is a difficult task for a single event. Therefore, the combination of multiple events might easily lead to a localized optimum, increasing the performance in a single event only. Additionally, this is not the only setback, as the Autocross and Endurance tracks vary from a competition to another.

In order to overcome the problems mentioned, the improvement to the total score resulting a change in gear ratios can be examined. From eq. (1) to (3) describing the scores, it can be observed that the total score of the Autocross and Endurance events is much greater than that of the Acceleration event. Furthermore, the type of engine of the vehicle should also be considered. A single cylinder engine has a low power output compared to multi-cylinder engines. Even though it allows the design of a lighter vehicle with overall improved cornering performance, the total power to weight ratio is decreased. As a result, it is a fact that most single cylinder vehicles have higher acceleration times that multi-cylinder ones. Having a low T_{min}/T_{team} ratio in eq. (1), where T_{min} is the time of the fastest vehicle and T_{team} is the team's time recorded for the event, renders the acceleration score considerably difficult to increase. This fact points out that the optimization method should include the Acceleration event, but should be directed towards improving the performance in Autocross and Endurance.

Considering now the difference between Autocross and Endurance events, usually the two respective tracks have minor differences, if not any at all. However, in the Autocross event, a single lap is run starting from a very low speed, rendering the first part of the track similar to an acceleration run. In contrast, in the Endurance event, almost 90% of the laps are run successively. This repetition in laps also enables the

driver to improve his/her performance. The similarity of the tracks of the two events implies that both can be satisfactory improved at the same time, but the difference between them renders the Endurance event more stable, as it is not prone to initial conditions and due to the driver's capability of attaining more consistent lap-times. As a result, for the available tracks, only the times of intermediate laps will be examined.

Last but not least, a strategy should be employed so as to combine the results of multiple tracks from different competitions. For a single track, it is evident that an objective function to be minimized can contain just the lap-time:

$$F = Lap\ Time \tag{190}$$

Even though all Formula Student tracks are similar, unfortunately they are not identical. Some might involve a less amount of tight corners and others longer straight lines. Considering eq. (2) and (3), both Autocross and Endurance scores are linear in comparison to the scoring factor:

$$s.f. = {}^{T_{min}}/_{T_{team}} \tag{191}$$

Therefore, when comparing the data of multiple competitions, a combination of the resulting scoring factors is necessary so as to decide upon the final result. One method involves forming the objective function to be maximized as the sum of the scoring factors:

$$F_{(s.f._j)} = \sum_j s.f._j \tag{192}$$

If the simple case of two tracks is now examined, when the objective function is optimized, the following relation applies:

$$dF = 0 \Rightarrow d(s.f._1) = -d(s.f._2) \tag{193}$$

This means that, at the optimal solution, a change in gear ratios that increases the score of competition 1 by one point will decrease the score of competition 2 by one point as well. However, if at the optimal solution $s.f._1 \neq s.f._2$, then that might not be a desirable situation. For example, if 200 and 300 points are achieved at the Endurance events of competitions 1 and 2 respectively, then it is logical that an addition of some points in competition 1 would be desirable, even though more points would be subtracted from competition 2. In this sense, a new objective function can be introduced that follows the relationship:

$$dF = \frac{d(s.f._1)}{s.f._1} + \frac{d(s.f._2)}{s.f._2} \Rightarrow$$

$$\Rightarrow F = ln(s.f._1) + ln(s.f._2) = ln(s.f._1 \cdot s.f._2) \tag{194}$$

or equivalently:

$$F = s.f._1 \cdot s.f._2 \tag{195}$$

Generalizing the solution for more tracks:

$$F_{(s.f._j)} = \prod_j s.f._j \tag{196}$$

Another advantage with this objective function is that the best times T_{min} need not be included in the optimization criteria.

The constraints of the gear ratios optimization problem are obviously such that a decreasing sequence in gear ratios is preserved. So as to not allow two sequential gear ratios to be exactly the same, a critical gear ratio slightly over one is introduced so that:

$$\frac{i_k}{i_{k+1}} \geq ratio_{crit} \Rightarrow$$

$$i_{k+1} ratio_{crit} - i_k \leq 0 \tag{197}$$

Letting the equation above be valid for k=1,2,…,m-1 the following system of m-1 constraints is obtained:

$$\begin{bmatrix} -1 & ratio_{crit} & 0 & \dots & 0 \\ 0 & -1 & ratio_{crit} & \dots & 0 \\ \vdots & \vdots & \vdots & \vdots & \vdots \\ 0 & 0 & \cdots & -1 & ratio_{crit} \end{bmatrix} \begin{bmatrix} i_1 \\ i_2 \\ \vdots \\ i_m \end{bmatrix} \leq \begin{bmatrix} 0 \\ 0 \\ \vdots \\ 0 \end{bmatrix} \tag{198}$$

Having defined the objective function and the constraints, a method to solve the optimization problem must be employed. Since the entire simulation is realized and performed in Matlab, one method would be using the optimization algorithms already existing in the software. The most common application performing a constrained optimization of multiple variables is ‘fmincon’. Several algorithms can be chosen in this function, most of them relying upon the gradient of the objective function.

However, upon making a change in gear ratios, a new gear might suddenly engage during acceleration that did not engage before. In the same manner, another gear might not engage at all. In addition, due to the time step of the simulation, there might

be slight differences in the braking points between a gear ratio set and another. All these factors result in a sudden change in lap-time, rendering the objective function non-differentiable at some points. Setting the differentiation step appropriately can solve this problem, but not consistently.

In order to overcome the problems resulting from the non-smooth nature of the objective function, an approach of testing a number of different gear ratios is be used, similar to a Monte Carlo simulation. Let $i_{0,k}$ for k=1,2,…,m be the initial gear ratios. A random set of gear ratios will now be produced and tested. At first, performing a rough investigation, the random numbers will be selected with the following maximum, mean and minimum values:

$$i_{min,k} = (1 - range) i_{mean,k} \quad (199)$$

$$i_{mean,k} = i_{0,k} \quad (200)$$

$$i_{max,k} = (1 + range) i_{mean,k} \quad (201)$$

where the value of the range is a percentage of the mean gear ratio.

After a certain number of runs, determined so as the method cannot improve the objective function significantly relatively to the number of runs performed, a new mean point $i_{best,k}$ is set, as being the value of the best performing gear ratios so far. This mean point will from now on be renewed after every run is performed. The algorithm now enters a more precise search, with the new maximum, mean and minimum values being symmetrically defined as:

$$i_{min,k} = i_{mean,k} - \min\left(\frac{i_{mean,k-1} - i_{mean,k}}{2}, \frac{i_{mean,k} - i_{mean,k+1}}{2}\right) \quad (202)$$

$$i_{mean,k} = i_{best,k} \quad (203)$$

$$i_{max,k} = i_{mean,k} + \min\left(\frac{i_{mean,k-1} - i_{mean,k}}{2}, \frac{i_{mean,k} - i_{mean,k+1}}{2}\right) \quad (204)$$

The symmetric placement using the equations above aids in not rejecting any of the random numbers, due to violation of the constraints when $ratio_{crit}$=1.

The most common distribution using an upper and lower limit is the beta distribution. This distribution is used for generating the random numbers and its parameters can be calculated as:

$$a = 1 + 2 \cdot exponent \cdot \frac{i_{max} - i_{mean}}{i_{max} - i_{min}} \quad (205)$$

$$\beta = 1 + 2 \cdot exponent \cdot \frac{i_{mean} - i_{min}}{i_{max} - i_{min}} \quad (206)$$

where the exponent is a quantity affecting the variance of the distribution. Greater exponent results to decreased variance. An exponent of 1 is used for the first rough search and an exponent of 2 for the final search.

Having considered all of the facts mentioned above, the optimization procedure will involve the following steps:

- Examination of the times in the acceleration event. The analytical method is used as an initial point. The best number of gear ratios to be used is determined manually, by evaluation of the results.
- The result for best acceleration time is taken as an initial point for the lap-time optimization. The optimal result is found for each track individually. The best number of gear ratios to be used is again determined manually, by evaluation of the results.
- The different results are examined as to how close their gear ratios are. By trial and error, an attempt is performed for moving a gear ratio resulting the optimization of one track, towards the set of gear ratios better for another track. New intermediate gear ratios might be introduced.
- All the tracks are simultaneously examined using an objective function
- The end result is compared to the gear ratios set for best acceleration. Modifications so as to improve acceleration time might be examined.

5. Results

5.1 Vehicle and driver constants

The different parameters involved in the analysis of the preceding chapters are part of the specifications of the race car designed. The majority of the parameters describing the vehicle and its systems are presented in Table 5.

Description	Symbol	Value
Total vehicle mass, including driver	M	250 kg
Vehicle yaw moment of inertia	I_z	80 kgm^2
Vehicle roll moment of inertia around the roll axis	I_{roll}	31 kgm^2
Vehicle pitch moment of inertia around the pitch axis	I_{pitch}	190 kgm^2
Equivalent moment of inertia of the rotational parts of the engine	J_{eng}	0.01 kgm^2
Equivalent moment of inertia of all tires, including coupled drivetrain	J_w	0.87 kgm^2
Rear weight distribution	Rd	53%
Wheelbase	L	1.53 m
C.O.G. height from ground	H	0.286 m
Front track width	B_f	1.238 m
Rear track width	B_r	1.115 m
Front suspension vertical stiffness	$k_{susp,front}$	2*36 N/mm
Front tires vertical stiffness	$k_{tire,front}$	2*115 N/mm
Front anti-roll bar stiffness	$k_{rollbar,front}$	400 Nm/deg
Rear suspension vertical stiffness	$k_{susp,rear}$	2*21 N/mm
Rear tires vertical stiffness	$k_{tire,\ rear}$	2*121 N/mm
Rear anti-roll bar stiffness	$k_{rollbar,\ rear}$	1100 Nm/deg
Suspension total damping ratio	Z	0.8
Aerodynamic center of pressure rear distribution	rd_a	51%
Aerodynamic center of pressure height from ground	h_a	0.65 m
Aerodynamic drag constant	C_DA	1.45 m^2
Aerodynamic lift constant	C_LA	3.65 m^2
Differential Lock up Torque constant for acceleration	$L.U.T._{\ acceleration}$	0.6
Differential Lock up Torque constant for deceleration	$L.U.T._{\ deceleration}$	0.42
Differential preload	T_p	25 Nm
Front brake distribution	k_{bf}	61%
Shifting system shift time constant	Δt_{shift}	0.2 sec
Engine max speed	n_{max}	9500 rpm

Table 5: Main parameters of the race car

Concerning the performance of the engine, the output torque and power, as well as the fitment of the polynomial proposed in eq. (95) can be seen in figure 19. Due to the fact that data are not available for low engine speeds, a linear interpolation is performed up to a zero torque engine speed of n_{min}. The fitting constants are included in table 6.

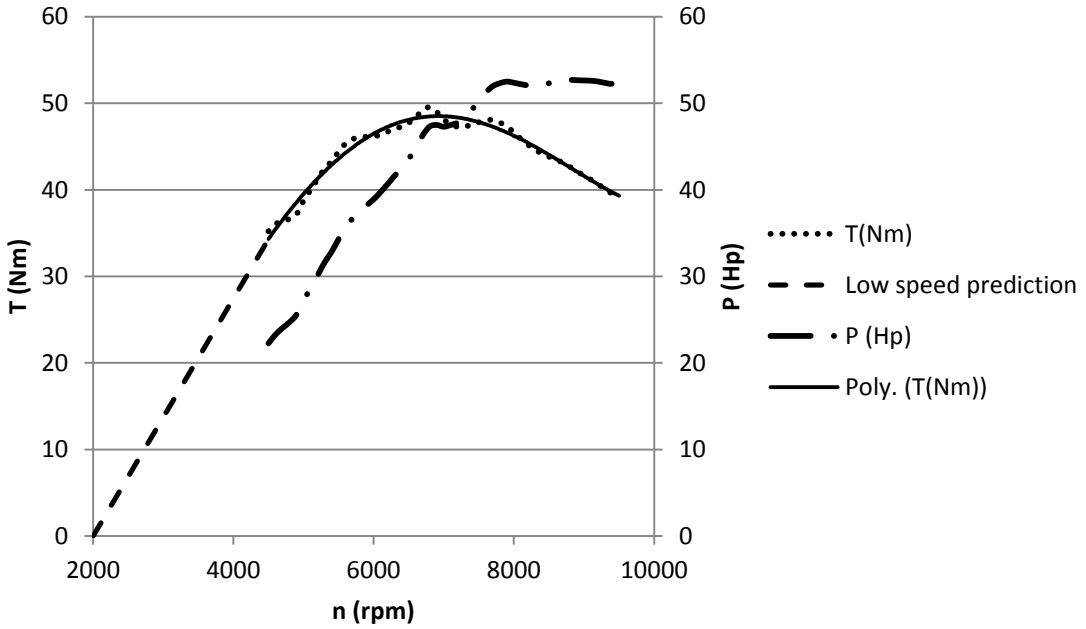

Figure 19: Dynamometer data and fitment

Parameter	Value
t_0	0.0516918197632723 Nm
t_1	-1.23488590256679 Nm/1000rpm
t_2	8.54112836523757 Nm/(1000rpm)^2
t_3	-9.29629686749032 Nm/(1000rpm)^3
t_4	-5.47925706182441 Nm/(1000rpm)^4
n_{min}	2000 rpm

Table 6: Engine torque fitting parameters

A plot of the steering system behavior and the steering system constants can be seen in figure 20 and table 7 respectively.

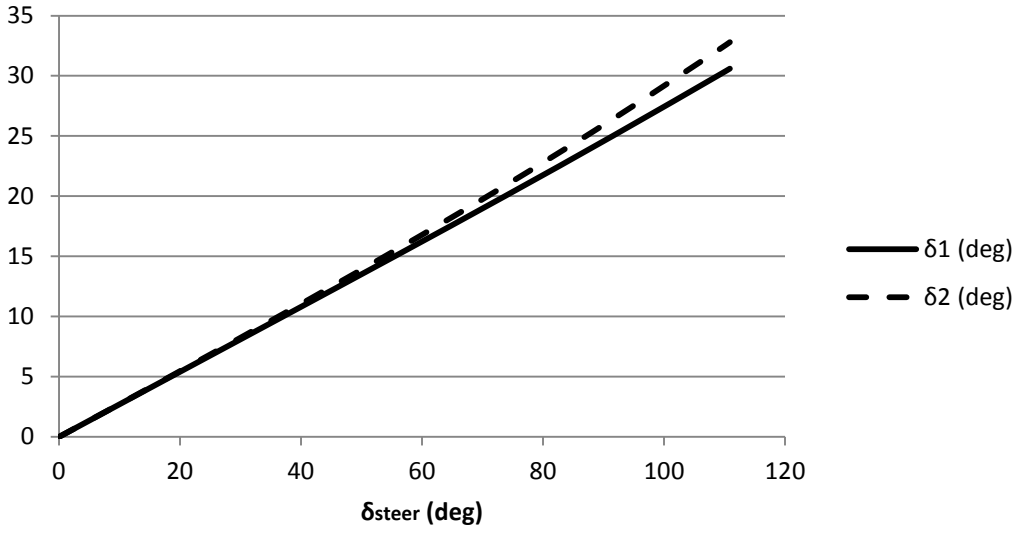

Figure 20: Wheel steer angles

Parameter	Value
c_1	0.270812004247308 deg/deg
c_2	0.000087022604859 deg/(deg)^2
c_3	0.00000121824745 deg/(deg)^3
$\delta_{steer,max}$	110°

Table 6: Steering system parameters

The data used for the tires fitted in the 2018 race car are obtained from the Formula SAE Tire Test Consortium (FSAE TTC) and are analyzed in the software OptimumTire [16]. The fluctuation of the results for pure lateral and pure longitudinal slip conditions is illustrated in figure 21. The final values of the parameters are included in table 7.

Parameter	Value
F_{z0}	780 N
pK_{x1}	47
pK_{y1}	45
pK_{x3}	-0.4
pK_{y2}	1.5
pC_{x1}	1.5
pC_{y1}	1.4
pD_{x1}	2.626
pD_{y1}	2.472
pD_{x2}	-0.3063
pD_{y2}	-0.5544
pE_{x1}	-0.4
pE_{y1}	0

Table 7: Tire model coefficient values

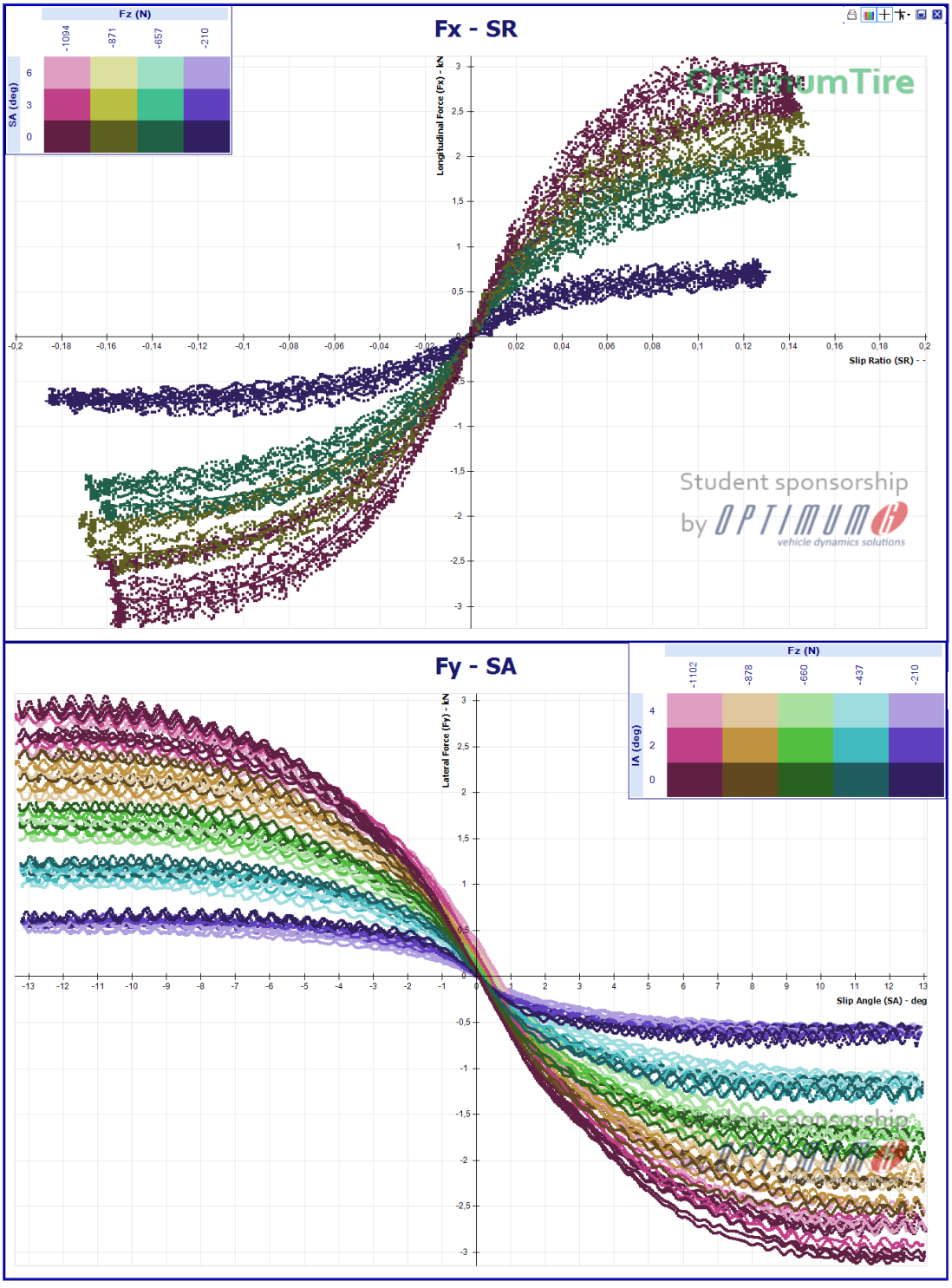

Figure 21: Tire data in OptimumTire

The data presented above are extracted from tests performed in a high friction surface. It is generally recommended that a friction scaling factor of $\lambda=\lambda_x=\lambda_y=2/3$ is used for a well-paved road.

The tires fitted in the 2019 project race car are a version of the ones modeled, from the same manufacturer, but with a lower profile. After a series of test runs, it was determined that the vehicle performance was significantly benefitted by this change. Unfortunately, data for these low-profile tires are not available to the team. So as to account for the increased performance of the new tires, the friction scaling factor was raised to a value of $\lambda=\lambda_x=\lambda_y=0.75$. This value was determined accordingly to the change in lap-times recorded during the test runs. The loaded rolling radius of these tires is approximately $R_e=0.199$ m.

Last but not least, the parameters needed to model the driver are determined appropriately, following measured data. Traction limit factors are tuned so that the measured vehicle speed profile during deceleration or acceleration, as well as the speeds attained in turns of known radius, match the outputs of the simulation. Using the values measured for throttle position and steering wheel angle, the driver's response constant as well as the maximum rate of change of his inputs can be determined. These values are placed in table 8. It should be noted that, during the acceleration event, the traction limit x factor should be raised to 80%.

Parameter	Value
traction limit x, acceleration	70%
traction limit x, braking	70%
traction limit y	92%
Δt_{driver}	0.3 sec
Max steering wheel rate	300 deg/sec
Max steering throttle rate	3 sec^{-1}

Table 8: Driver parameters

5.2 Gear ratios resulting from the analytical method

For performing the analytical optimization, two parameters are required. The first one is the rear wheels maximum torque due to tire traction $T_{r,max.}$ For a rear wheel drive vehicle, this value can be easily calculated in the steady-state, considering weight transfer:

$$T_{r,max} = rd\frac{\frac{mg}{1-\frac{h}{L}\Phi_x(traction\ limit\ x)}}{}\Phi_x(traction\ limit\ x) \tag{207}$$

The second parameter is the top speed expected at the end of the acceleration. Following measured data from competitions, a typical top speed for a combustion racecar in the acceleration event is about $U_{max}=100$ km/h.

Considering that the gearbox to be designed should replace the manufacturer's 6 speed solution for the engine, it would be difficult to exceed the number of 6 gear ratios. Therefore, different setups from 3 up to 6 different gear ratios are examined. The resulting gear ratios, engine starting speed, engine upshift speeds and theoretically calculated acceleration time are presented in table 9.

Gear number	**3 speed**		**4 speed**		**5 speed**		**6 speed**	
	$\mathbf{i_k}$	$\mathbf{n_{start}/n_2}$ **(rpm)**	$\mathbf{i_k}$	$\mathbf{n_{start}/n_2}$ **(rpm)**	$\mathbf{i_k}$	$\mathbf{n_{start}/n_2}$ **(rpm)**	$\mathbf{i_k}$	$\mathbf{n_{start}/n_2}$ **(rpm)**
1	13.3	8280/ 9500	13.7	8560/ 9500	13.9	8640/ 9500	13.9	8660/ 9500
2	9.37	9500	10.7	9500	11.6	9500	12.1	9500
3	7.13	-	8.59	9500	9.74	9500	10.5	9500
4	-	-	7.13	-	8.27	9500	9.20	9470
5	-	-	-	-	7.13	-	8.08	9420
6	-	-	-	-	-	-	7.13	-
Accel. Time (sec)	3.70		3.67		3.66		3.66	

Table 9: Gear ratios, engine start and shift up speeds resulting from the analytical optimization

It is evident that a greater number of gearbox gear ratios results to decreased acceleration time. This is logical since more tractive power is available when the gear ratios are placed in higher proximity one to the other. However, the shift time was not considered in this analytical approach, a factor that actually increases the overall acceleration time as the number of gear ratios increases, as it will be seen later on in the next chapter.

As far as the upshift engine speed is concerned, the calculated values reach the maximum engine speed the most of the times, while dropping slightly lower than that only when the ratio of successive gear ratios i_{k-1}/i_k is low. It can be also noted that the resulting ratio i_{k-1}/i_k is constantly decreasing as the gear number k increases. This can also be seen in figure 22. As a result, the engine speed drop between $n_{2,k}$ and $n_{1,k+1} = n_{2,k}\, {i_{k+1}}/{i_k}$ decreases for higher gear numbers. This is a significant outcome and is a common practice in gearbox design.

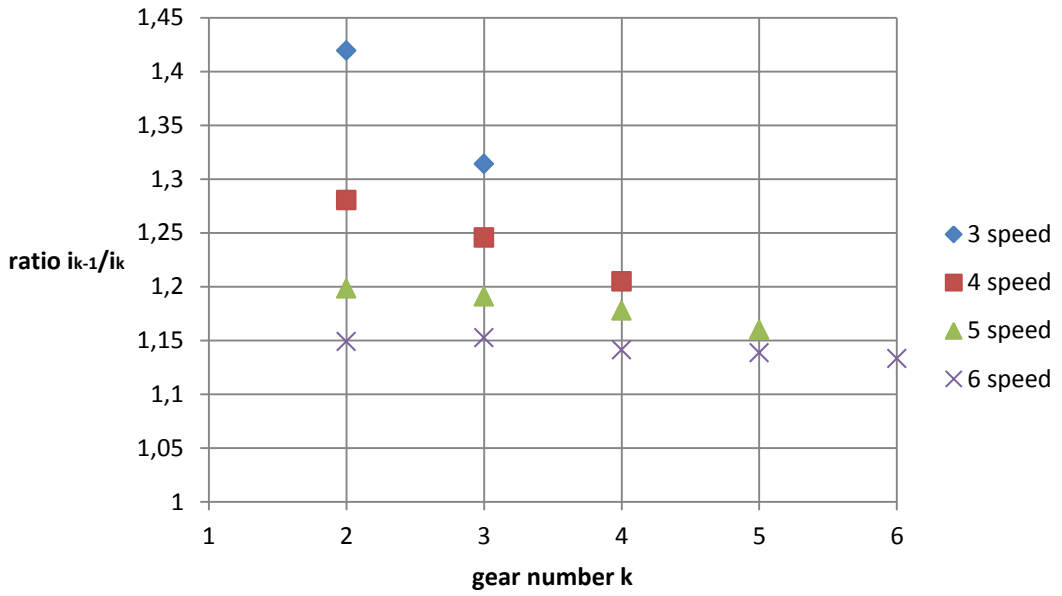

Figure 22: Ratio of successive gear ratios i_{k-1}/i_k

5.3 Vehicle simulation results and comparison with measured data

Besides the total lap-time, which is the final result of the simulations, several other outputs can be presented so as to prove the validity of the overall results. To begin with, it should be mentioned that three different tracks are used in the simulations. The most recent data available and the competitions where the team has plans in participating were considered. The aforementioned tracks are all Endurance race tracks of the competitions of Germany (F.S.G.) in 2016, Austria (F.S.A.) in 2015 and Hungary (F.S. East) in 2018. The track layout as well as the racing line computed are both illustrated in figures 23 to 25.

The speeds in the longitudinal and lateral axis can be seen in figure 26. As expected, the y-coordinate of the speed is significantly lower than the x-coordinate one.

The deviation from the desired trajectory is depicted in figure 27. With a proper choice of the time constant used in the gains of the steering PID controller, this tracking error is kept low at all times.

Lap-time convergence is examined in figure 28. It is evident that all laps after the first one share very similar lap-times. This is logical since, after the first lap, the speed reached before the first turn of the lap exceeds the traction limited maximum in-turn speed.

The data presented in figures 27 and 28 result runs performed in the race track of Germany. The first lap is included only.

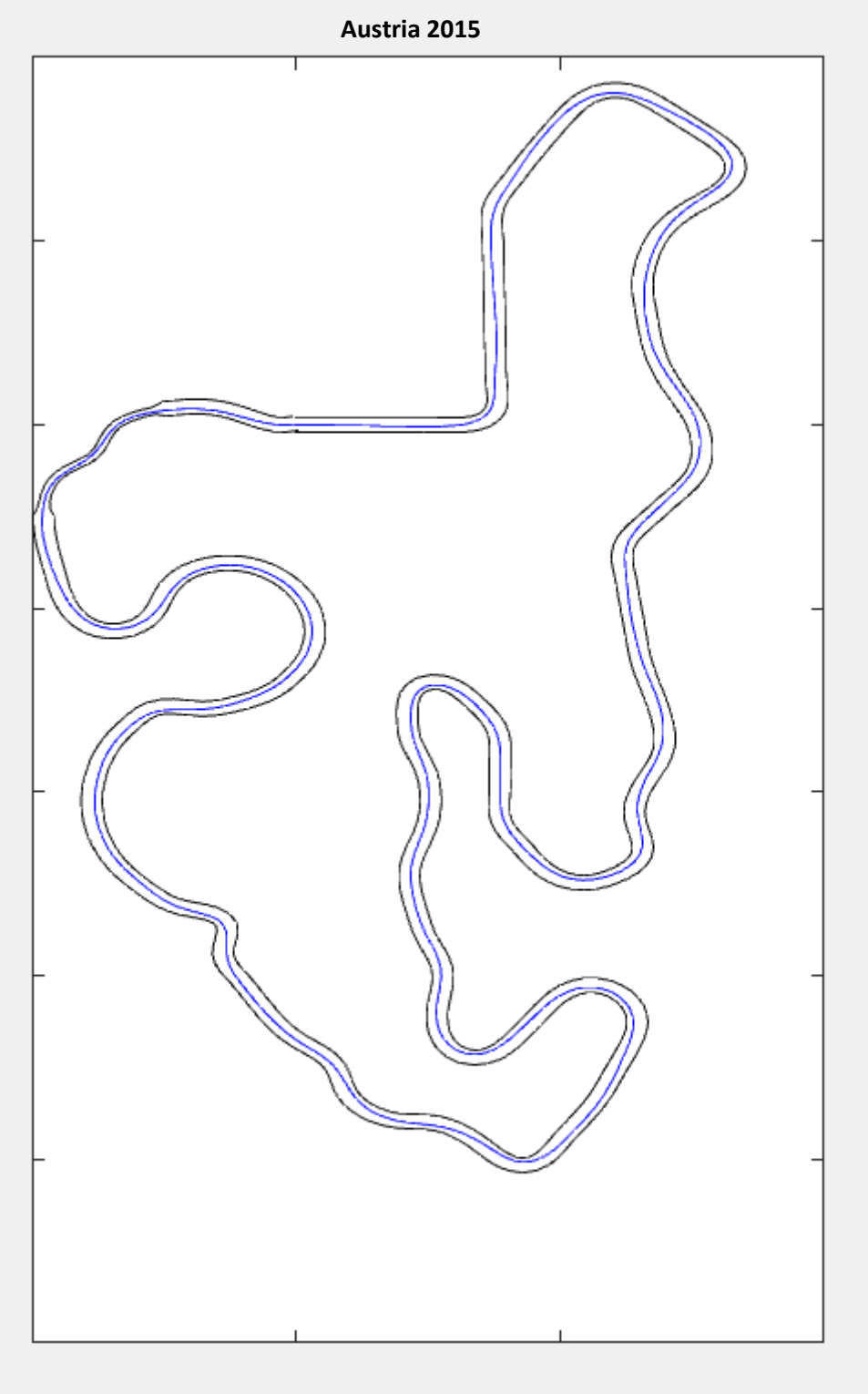

Figure 23: Austria 2015 Endurance track and racing line

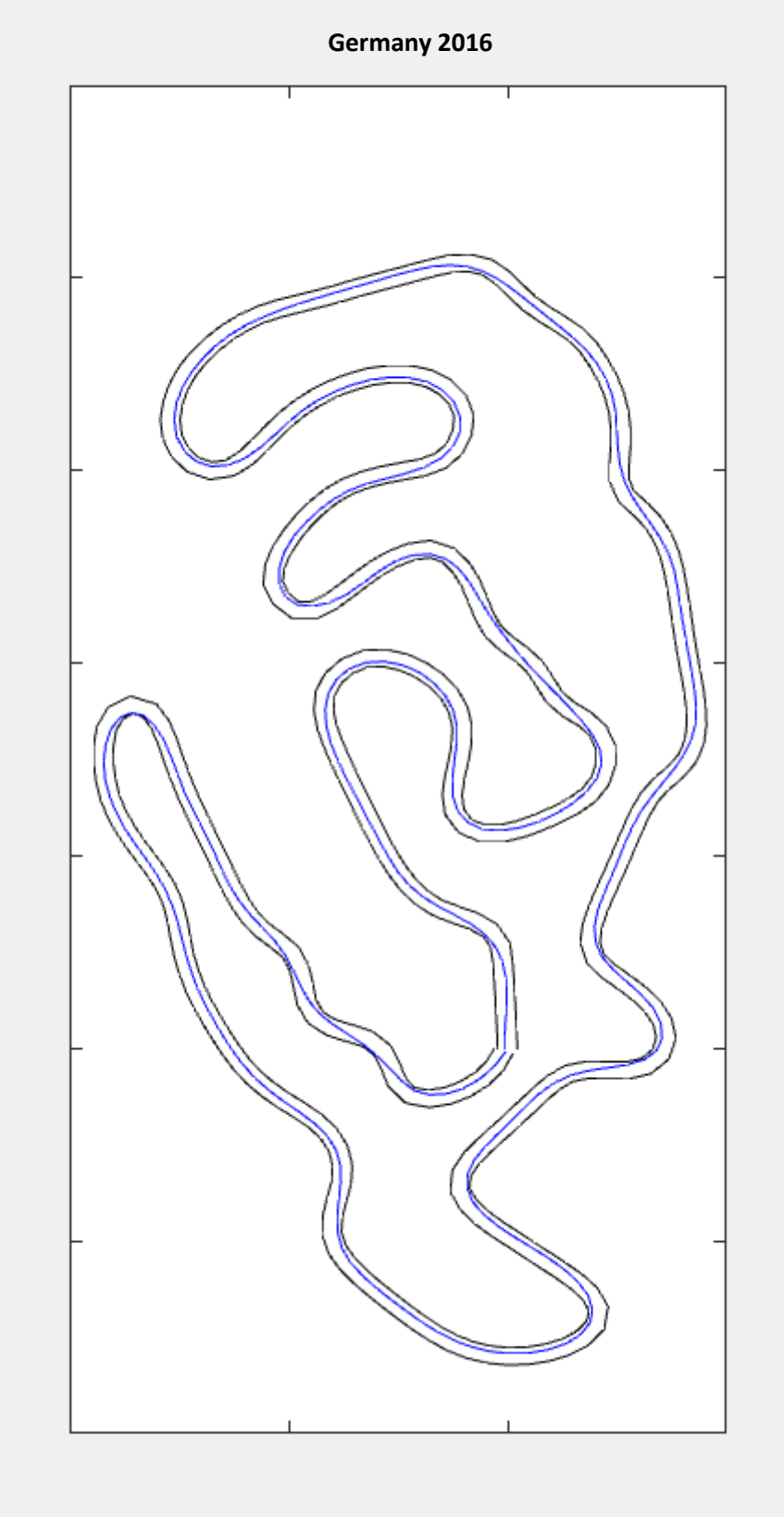

Figure 24: Germany 2016 Endurance track and racing line

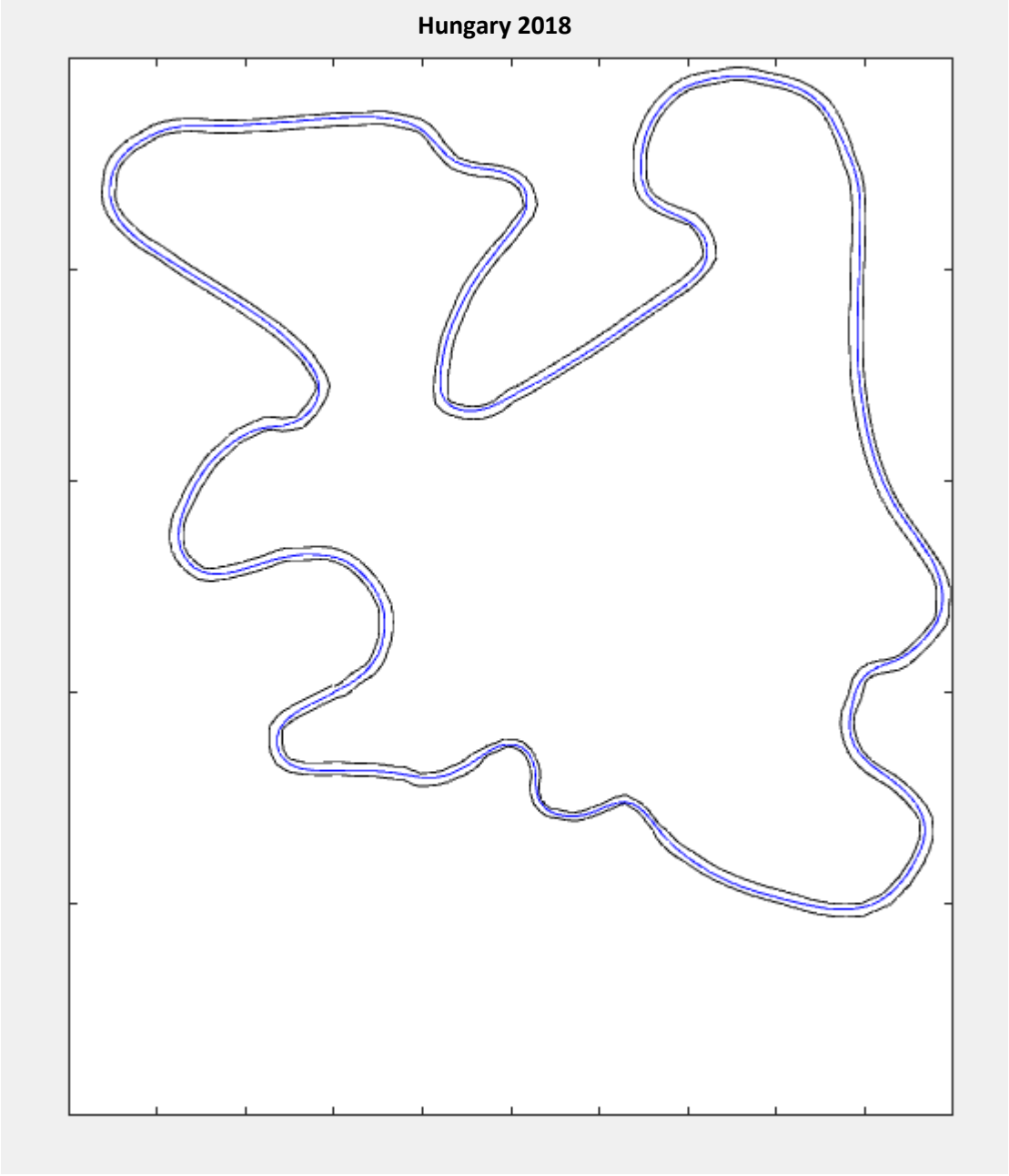

Figure 25: Hungary 2018 Endurance track and racing line

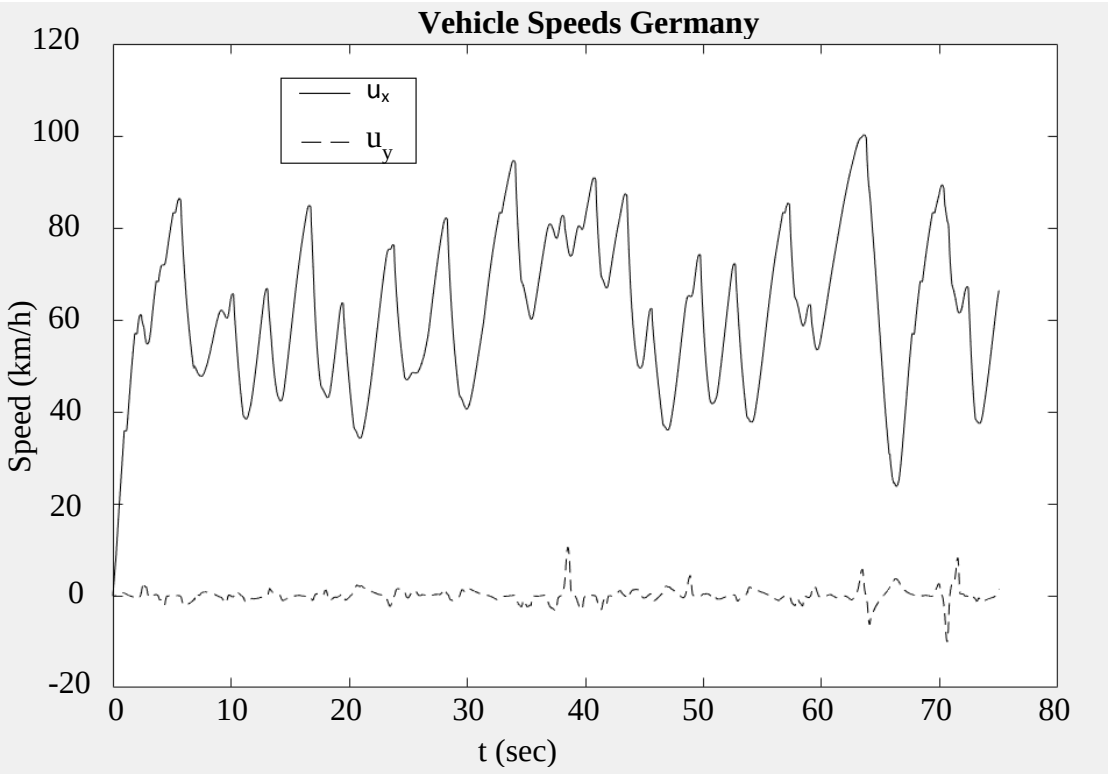

Figure 26: Vehicle speeds

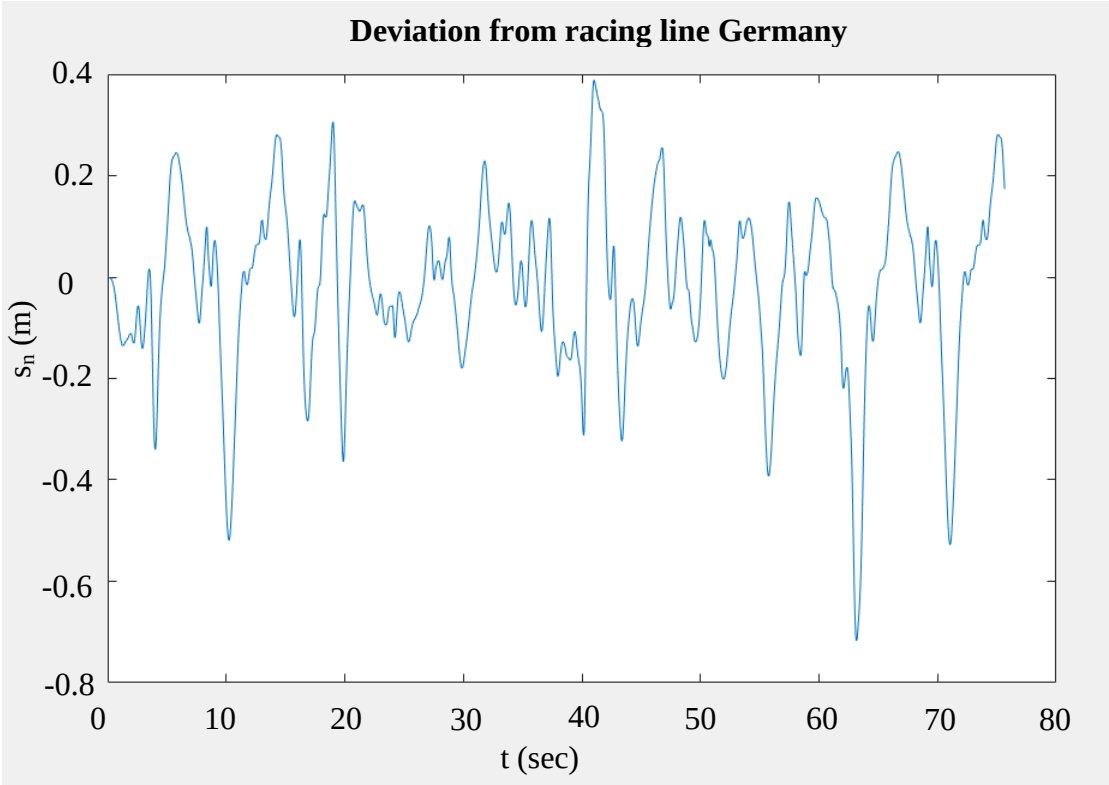

Figure 27: Deviation from racing line

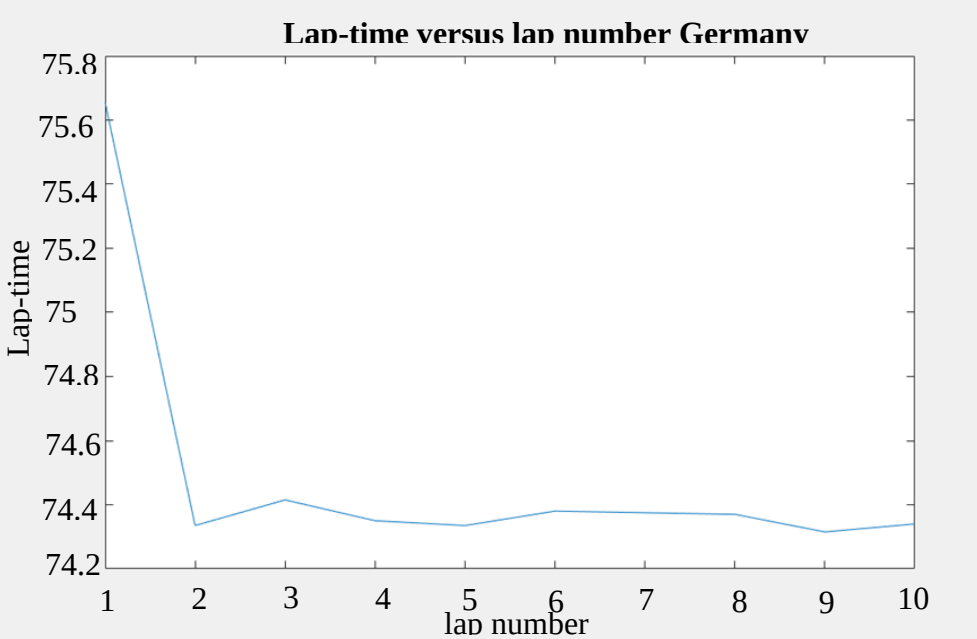

Figure 28: Lap-time versus lap number

Last but not least, a comparison between measured and simulated in-track speeds for the Hungarian competition can be seen in figure 29. This comparison was performed using input data that correspond to the setup of the racecar in that specific competition. A representative lap was isolated from the available data and aligned with the simulation data. It should be noted that differences are expected in this graph, as the tarmac was relatively damp.

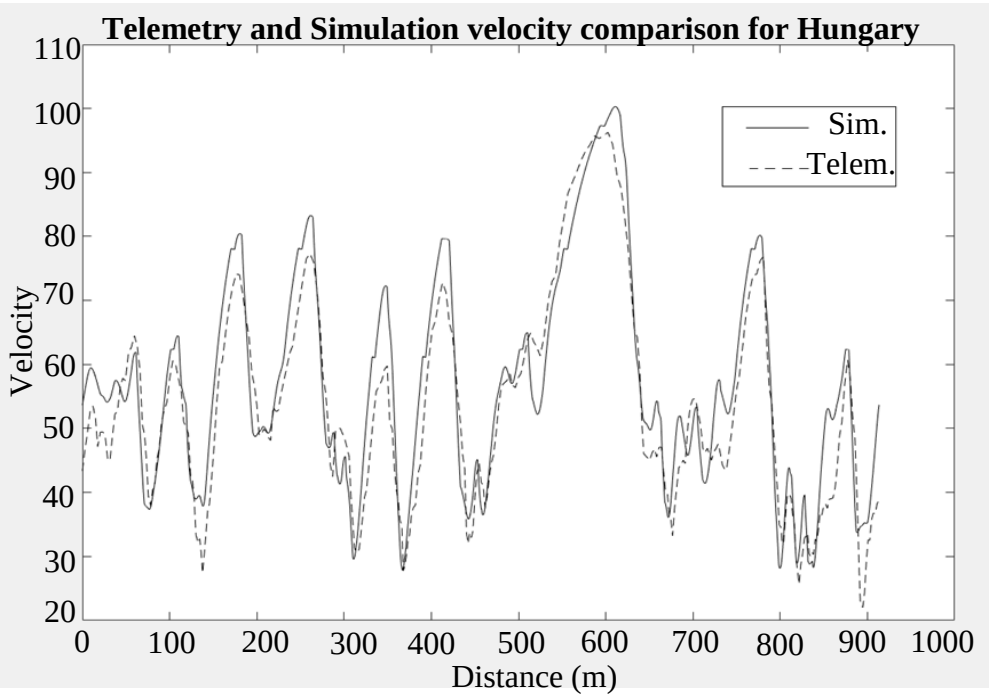

Figure 29: Simulation and telemetry speed comparison

5.4 Gear ratios optimization for acceleration

When examining the solutions of the analytical optimization for straight line acceleration, it was noted that an increase in the number of gear ratios results to decreased acceleration time. However, when adding the gear shift time in the analysis, this observation no longer holds. The times and maximum speeds resulting a 75m acceleration event for the calculated gearboxes are presented in table 10.

	3 speed	4 speed	5 speed	6 speed
Acceleration time (sec)	4.46	4.50	4.56	4.60
Maximum speed (km/h)	96.7	95.26	93.7	92.0

Table 10: Simulation results of the gearboxes calculated using the analytical optimization

A further investigation into the acceleration response of the simulation yielded the following three assumptions for the acceleration time:

- It is difficult to decrease the acceleration time lower than the results obtained for a 3-speed gearbox, when a greater number of gear ratios are used.
- A decrease is observed as first the gear ratio decreases, up to the value matching the rear tires traction limited torque to the maximum output torque of the engine as $i_1=T_{r,max}/T_{(nTmax).}$
- A decrease is observed as final the gear ratio increases, up to the value matching vehicle maximum speed to the maximum speed of the engine, calculated using eq. (30).

After considering the factors mentioned above, a minimization of the acceleration time is attempted using the stochastic algorithm mentioned in the previous chapter. Starting from four gear ratios, the algorithm brought the last two gear ratios close one to the other. Merging those and continuing the optimization lead to the gearbox described in table 11. A diagram showing the best lap-time found versus the iteration number, with the 3-speed analytically found optimal gearbox as a starting point, can be seen in figure 30.

Finally, two observations should be noted:

- Acceleration time of the best performing 4-speed gearbox is 4.45sec, just 0.04sec apart from the 3-speed one.
- The acceleration time is generally insensitive close to the optimal solution. For example, the time does not change for the 3-speed solution shown in table 11, if the last gear ratio ranges between 6.9 and 7.3. This means that the solution

presented might not be the exact optimal, but is such that yields the optimal result.

Gear number	i_k	n_{start}/n_2 (rpm)
1	12.2	6800/ 9500
2	8.32	9500
3	7.05	-
Acceleration time (sec)	4.41	
Maximum speed (km/h)	96.5	

Table 11: Gearbox resulting stochastic optimization of 75m acceleration

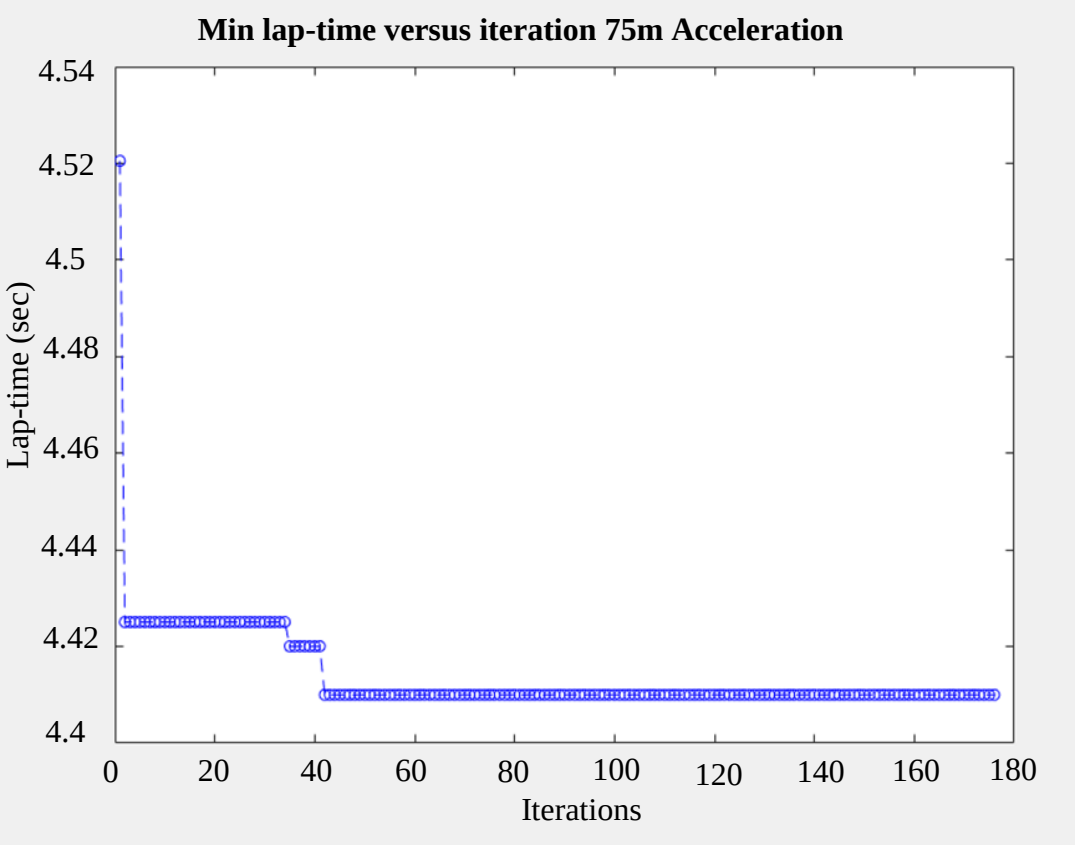

Figure 30: Best lap-time versus iteration number for 75m of acceleration

5.5 Gear ratios optimization for in-track performance

The stochastic algorithm is applied upon the tracks of Germany, Austria and Hungary. Four laps are run in total and the average of the three last lap-times is used as an objective function to be minimized, therefore excluding the first lap.

Before running the optimization algorithm, several observations are performed concerning the three tracks:

- The top speed in the track of Austria is about 85 km/h, whereas in both the tracks of Germany and Hungary is near 100 km/h.
- The lowest speeds attained vary between roughly 25 km/h and 35 km/h.
- The in-track local minimum and maximum speeds do not vary significantly with a change in gear ratios.
- The usage of gears varies between the tracks, given the same gearbox. For example, the first gear might be used in one track, but not at all in another.
- The usage of the shift time Δt_{shift} only once in eq. (123) calculating the engine downshift speed, is not necessarily the best assumption for all tracks.

In paragraph 2.2, it was mentioned that the optimal value of last gear ratio is such that matches the engine maximum speed with the vehicle top speed. This outcome was confirmed when simulating the acceleration event in the previous chapter. Considering that the top speeds reached in-track are known and that they occur in a straight line of significant length, the last gear ratio can be determined for all tracks. However, it is evident that no valuable result will emerge from doing so separately for each track, since the final gearbox design will include only one set of gear ratios common for all tracks.

In order to overcome this set back, the final gear ratio is set accordingly to the maximum speeds of the tracks of Germany and Hungary. It may also be observed that this speed is the same as the one attained at the end of the 75m acceleration run during the acceleration event. The localized maximum speed of the track of Austria may also be considered by proper calculation of the nearest prior gear to the final gear. However, this constraint would affect the performance in the rest of tracks and is therefore not being performed.

Last but not least, the choice of downshift engine speeds should be taken under consideration. Introducing these as extra variables to the optimization scheme would increase the complexity of the system and the likelihood of finding a localized result. For this reason, for the first set of runs, the downshift speeds were chosen to be the same for all tracks. A quick investigation indicated that the usage of twice the shifting time as $2\Delta t_{shift}$ in eq. (123) resulted to improved lap-times. Therefore, this method was incorporated as a first approximation.

Following the 3-speed optimal result of the Acceleration event, three different gears are examined initially. The resulting gear ratios for each individual track can be seen in table 12 and the course of the optimization is illustrated in figures 31 to 33.

The resulting gear ratios vary significantly from one track to another. However, it may be observed that, besides the common last gear, three different gear ratios seem to appear amongst the results. Successively, these have the approximate values of 11.5, 10.5 and 9. However, not all appear in each result individually. In an attempt to create a design adequately performing in all tracks, a 4-speed solution is proposed, containing these three observed ratios and the fixed final gear ratio.

	Gear ratios		
Gear number	**Austria**	**Germany**	**Hungary**
1	Not used	11.6	10.6
2	10.4	8.68	9.11
3	6.82	6.82	6.82

Table 12: Results by examination of each track separately

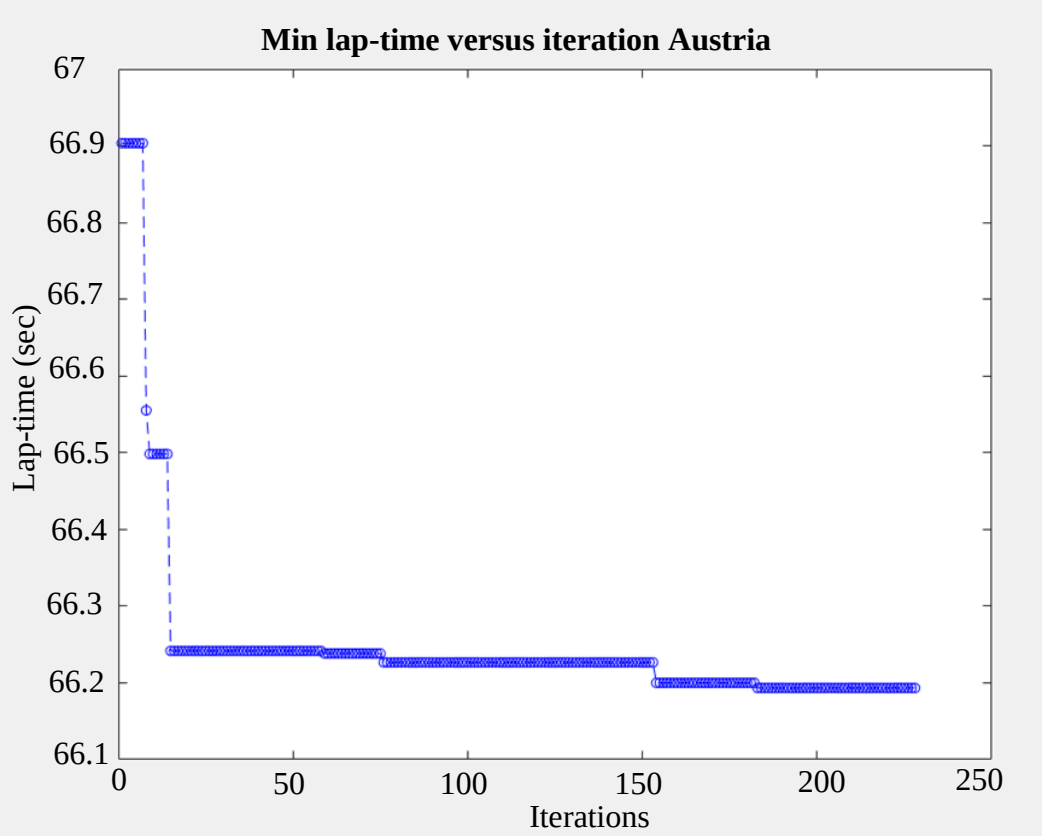

Figure 31: Best lap-time versus iteration number for the track of Austria

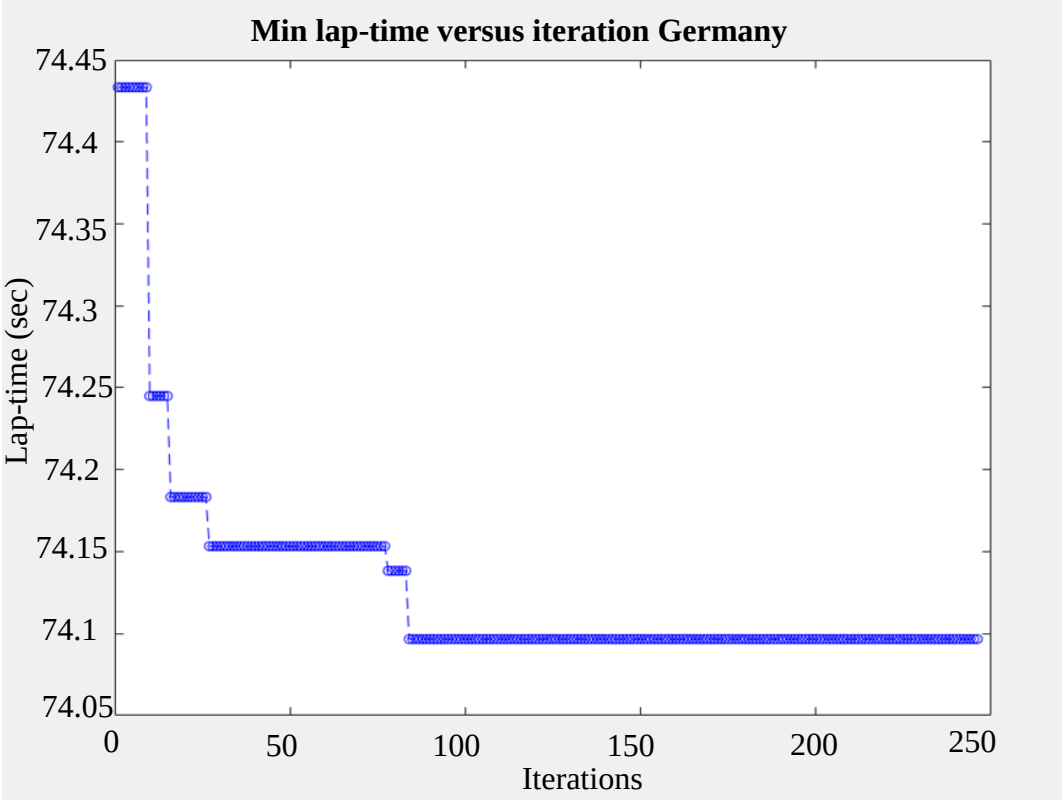

Figure 32: Best lap-time versus iteration number for the track of Germany

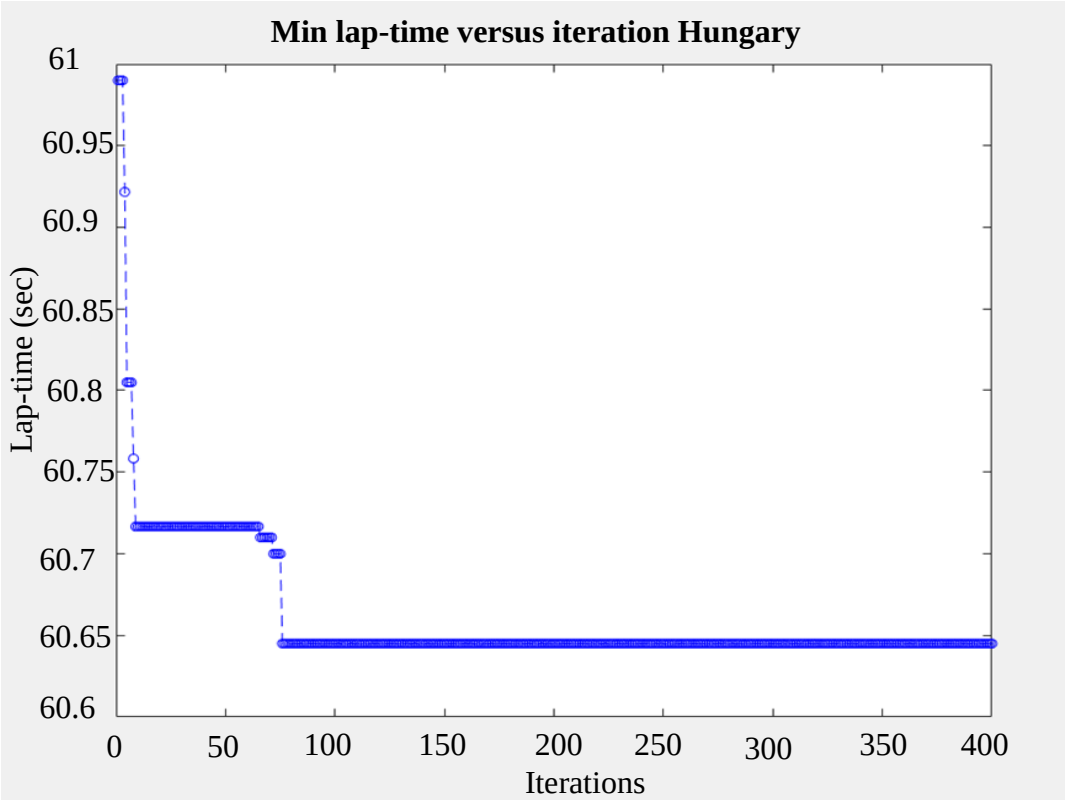

Figure 33: Best lap-time versus iteration number for the track of Hungary

After performing several runs so as to examine whether the proposed 4-speed gearbox has a satisfactory performance, it is determined that slightly higher lap-times of the per-track optimized results can be reached. Further refinement of the results by altering the engine downshift speeds differently per track, yields to additional improvement. Determining the gear ratios set $i = [12.5 \mid 10.5 \mid 8.5 \mid 6.82]$ as a decent starting point, all the tracks were examined and their lap-times were combined using an objective function. Two objective functions have been proposed in eq. (192) and (196). So as not to account for a minimum lap-time, used for the denominator of the scoring factors, eq. (196) is used. The resulting gear ratios, downshift engine speeds and the time used in eq. (123) for calculating them are included in table 13. A graph of the resulting lap-times versus the iteration number of the algorithm can be seen in figure 34.

		Downshift engine speeds/ Time used in eq. (123)		
Gear number	**Gear Ratios**	**Austria**	**Germany**	**Hungary**
1	12.6	-	-	-
2	10.3	3000/ $2\Delta t_{shift}$	3000/ $2\Delta t_{shift}$	3600/ $2\Delta t_{shift}$
3	8.67	4100/ Δt_{shift}	3800/ $2\Delta t_{shift}$	4100/ Δt_{shift}
4	6.82	5600/ Δt_{shift}	4800/ $2\Delta t_{shift}$	5600/ Δt_{shift}

Table 13: Results for the combination of three tracks

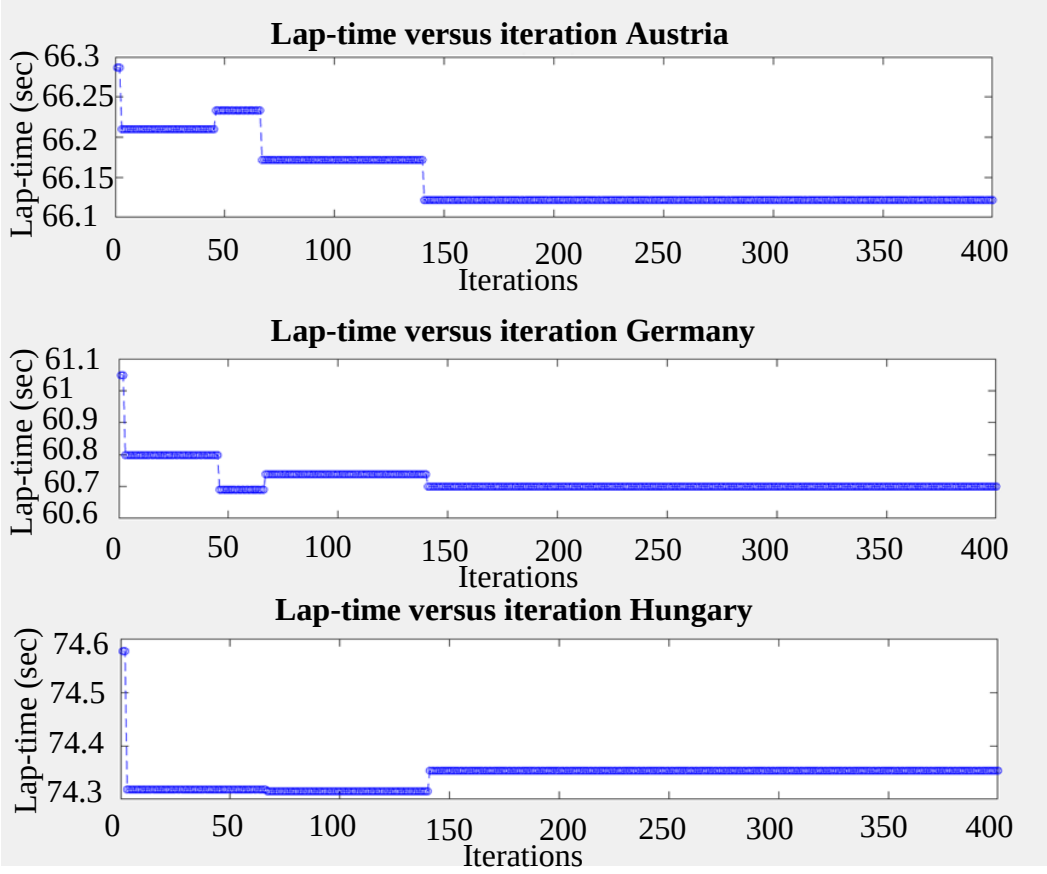

Figure 34: Best objective function lap-times versus iteration number for the combination of three tracks

5.6 Final results and modifications

At first, the acceleration event time is examined for the 4-speed gearbox, determined for best in-track performance. Running the respective simulation results to a time of 4.44 sec, just 30 msec above the 3-speed gearbox for optimal simulated acceleration time. This outcome is logical, should the two gearboxes be compared. The values of tables 11 and 13 indicate that the 4-speed solution nearly identical to the 3-speed one, with an intermediate gear added between the first and second gear. The constant decrease in the ratio between successive gears is no longer maintained, but the acceleration time does not increase significantly.

Therefore, the resulting 4-speed gearbox is a well performing solution for all of the dynamic events. However, it cannot be the final design due to two facts that have yet not been considered. To begin with, the first gear ratio is not adequately large for enabling the driver to start the vehicle easily. It may match the engine maximum output torque to the maximum tire limited torque, but that is beneficial in the case of an intense launch for acceleration. When a driver normally starts the vehicle, he or she rarely holds the clutch at the point of engagement for a long period of time. That being mentioned, the thrust provided by the engine is relatively low. If the momentum of the engine is not sufficiently large, then the engine stalls.

The operation of normally starting the vehicle can be easily modeled by considering the rate of change in momentum, between two distinguished time moments. At first, the clutch is disengaged, the engine is at an initial speed and the vehicle is stationary. After the clutch has been engaged, the vehicle is moving coupled to the engine. Using the thrust of the engine torque, conservation of momentum states that:

$$\int_{t_{engaged}}^{t_{disengaged}} T dt = \left(J_{eng} + \frac{mR_e^2 + J_w}{{i_1}^2}\right)\frac{\pi}{30} n_{engaged} - J_{eng}\frac{\pi}{30} n_{disengaged} \quad (208)$$

Using eq. (208), and considering the data measured from the 2018 vehicle, an initial engine speed of $n_{disengaged}$=5500rpm and a torque thrust of $\int_{t_{engaged}}^{t_{disengaged}} T dt = 5 Nms$ were determined as typical for the case of staring the vehicle. The resulting engaged engine speeds were typically close, or lower than, 2000rpm, lower than the selected idle speed of about 3000 rpm, therefore leading to frequently stalling the engine. Requesting for the engaged engine speed to be at least at the idle speed, results to a gear ratio of i_1=20.6.

The other fact that has not been considered is that gear ratios are inherently rational numbers. Not every set of the gear ratios calculated is possible to be implemented, as the number of teeth of the gear sets involved is limited. The total drive ratio is the product of the primary, the gearbox and the final drive ratios. Considering that both the gearbox and the final drive ratio can be altered, limiting the number of the teeth of their gear sets results to a set of possible gear ratios $i_{possible,k}$. After calculating those,

the most suitable set of gear ratios can be determined as such that minimizes the sum $\sum_k |i_{possible,k} - i_k|$. The limitations set to the teeth of the gearsets as well as the resulting gear ratios can be seen in tables 14 and 15 respectively.

	Gearbox		Final Drive	
Limitation	**Gear 1**	**Gear 2**	**Gear 1**	**Gear 2**
Maximum number of teeth	14	14	12	33
Minimum number of teeth	36	36	14	40

Table 14: Limitations on the number of gear teeth

Gear number	Desired Gear Ratios	Best achieved Gear Ratios	Teeth of gearbox gear 1	Teeth of gearbox gear 2
1	20.6	20,357	14	36
2	12.6	12,667	20	32
3	10.3	10,245	17	22
4	8.67	8,7083	20	22
5	6.82	6,8371	22	19

Table 15: Resulting gear ratios and number of gearbox gear teeth

Due to the fact that it is possible to select two and not just one gear set, the best gear ratios achieved are very close to the ones desired. In fact, the values differ by 1%, if not less. This justifies the examination of the gear ratios directly as real numbers and not performing a rational number conversion at every simulation.

Finally comparison between the simulated times of the calculated 4-speed gearbox and the already existing gearbox of the 2018 race car can be seen in table 16.

Designed gearbox				Former gearbox			
Acceleration	**Austria**	**Germany**	**Hungary**	**Acceleration**	**Austria**	**Germany**	**Hungary**
4.44	66.12	74.33	60.69	4.51	66.50	74.25	60.86

Table 16: Comparison between designed and already existing gearbox

6. Discussion and conclusion

Following the observations and the results presented in the previous chapter, several conclusions may be extracted, concerning the calculation of the gear ratios. At first, an examination of the single straight line acceleration problem yields the following:

- With an increase in the number of gears, the potential in decreasing acceleration time is enhanced, since more tractive power is available when the gear ratios are placed in higher proximity one to the other. However, when the shift time is considered, this observation is reversed.
- The best method to place the gear ratios is such that the ratio of successive gear ratios i_{k-1}/i_k is constantly decreasing as the gear number k increases. In this case, the engine speed drop between $n_{2,k}$ and $n_{1,k+1} = n_{2,k}\,{}^{i_{k+1}}/_{i_k}$ decreases as the gear number increases.
- The final gear ratio should match the expected maximum vehicle speed with the engine maximum speed.
- The first gear ratio should match the maximum driving tires torque limited due to traction with the maximum torque of the engine.
- The upshift engine speeds coincide with the engine maximum speed, unless the ratio of successive gear ratios is very close to one.

Concerning in-track performance now, the topology of the track determines the speeds attained, influencing the results of the best gear ratios:

- The resulting ratio of successive gear ratios i_{k-1}/i_k might not be a constantly decreasing number.
- As with the case of acceleration, the final gear ratio should match the expected maximum vehicle speed with the engine maximum speed.
- Obtaining a gearbox that performs well in a multiple number of tracks involves investigating which gear ratios are used on each track separately. The final solution may use all of those ratios so as to satisfy the needs of all the tracks.
- Decreasing the downshift engine speed lower than the value of $n_{1,k} = n_{2,k-1}\,{}^{i_k}/_{i_{k-1}}$ results to decreased lap-time. The downshift engine speeds should be chosen appropriately and potentially different in every track.

Finally, the improvement of in-track lap-time resulting the gearbox optimization is typically not more than half a second, or about 0.7%. This outcome might not seem adequately satisfactory. However, so as to attain a similar decrease, a weight reduction of 5% is necessary in the vehicle total mass. It should be noted that, in Formula Student applications, the overall weight of the car is considered very significant and design efforts are pushed to their limits. Therefore, achieving a 5% decrease, or roughly 10kg, is not a task easy to achieve.

Last but not least, the observations mentioned above are all coupled with the engine and the expected speeds of the vehicle. Typically, most race cars have double the maximum speed and triple the engine power of a Formula Student race car. As a result, the choice of a five speed gearbox for covering speeds of zero to 100km/h, would be entirely different in the speed range of zero to 200km/h. The ratio between successive gears would inevitably increase and the shift time would become less important compared to the total acceleration time.

7. Mechanical design and manufacturing of the gearbox

7.1 Design constraints and manufacturing method

As mentioned when posing the overall constraints of the project, the gearbox to be designed should replace the already existing solution of the manufacturer. Considering the additional limitation of budget for outsourced manufacturing, leads to adopting an approach of minimizing the number of parts to be redesigned and manufactured. More specifically:

- The first gear ratio, comprised out of a 36 and 14 teeth gear set, is implemented by the existing gearbox first gear ratio, which is identical. The ability of choosing a final drive ratio aided in pursuing this identicalness.
- The transmission shafts on which the gears are connected to are not changed. This selection was made possible by the fact that only one gear of the first gear ratio is attached with one axle, whereas the rest are removable.
- The original sequential 'dog-box' engagement type of the gears is used. This also enables the usage of most of the existing mechanical components of the shifting system.

The number of teeth of the gear sets of the calculated gearbox has been found after posing a maximum and a minimum limit. Considering that the center distance of the transmission shafts is fixed to the design of the engine, changing the number of gears alters the module and the contact ratio of the gearing. A large number of teeth results to a low module and therefore small sized teeth that lack in bending strength. On the other hand, a very small number of teeth leads to decreased contact ratio.

Last but not least, the manufacturing method must be decided. The most common way of producing gears is by means of hobbing. The material is then being case carburized around the tooth flank so as to increase local strength. The end result is ground so as to remove any warping introduced during the heat treatment and achieve a low surface roughness. The drawback of this method is that the module of the gearing must follow a standard size for which hobbs are available. Introducing a profile shift coefficient can remedy for this problem. However, it is possible that the required amount of profile shift cannot be achieved. Additionally, case hardening the material does not improve its properties anywhere but near the tooth flank.

Since the gears can be straight-cut, another manufacturing method is considered, as proposed by Bouquet et al. [17]. A near-net shape for the internal pockets and holes of the gear can be achieved at the beginning. The material is then being hardened and the shape of the teeth is formed after the heat treatment by a wire-EDM process. In this way, the material properties can be maintained throughout the gear by performing a through hardening, while a tooth shape of high accuracy can be achieved.

Additionally, any parameters of the tooth profile may be chosen, without any restrictions due to the limitations of the manufacturing process.

What must be considered is the surface quality of tooth flank. The wire-EDM process cannot achieve an adequate surface finish, such that a grinding method is capable of. However, since the overall shape of the tooth is accurate, the remaining unevenness of the surface can be removed by a running-in method. Ioakimidis (Ιωακειμίδης) [18] used a running-in method for correcting warping anomalies on a bevel 90 degrees gear set. By little or none at all net torque being transferred from one gear to another, the profile of the teeth was shifted by a maximum of 0.15mm, using appropriate speeds and grit of polishing paste.

7.2 Gear arrangement and shifting mechanism design

The engagement type and main shifting mechanism of the gears is illustrated in figure 35. Extruded pin-like geometries, commonly referred to as gear 'dogs', on a gear wheel that linearly slide, match a set of pockets on an adjacent gear wheel. The pockets are larger than the 'dogs', allowing for easier gear engagement. The linear movement of the sliding gear is accomplished by means of a retaining device, the shift fork, which follows a groove on a rotating cylinder, the shift drum.

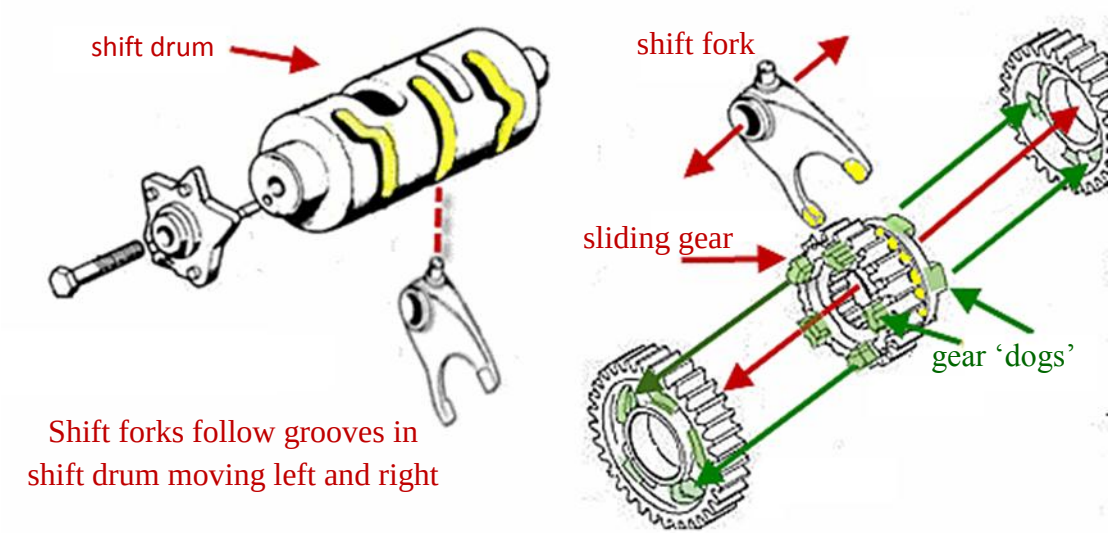

Figure 35: Engagement and shifting mechanism of gears

In some similar gearbox configurations, the sliding parts are not the gears themselves, but a set of separate 'dog'-carrying rings. Implementing this approach was not

pursued, as it would require the manufacturing of additional parts and the modification of the transmission axles so as to resolve spatial issues.

During each gear change, the shift drum will rotate by an angle Δφ. The resulting displacement of the shift fork that is coupled to the sliding gear should be:

$$\Delta x = dog\ length + initial\ clearance - final\ clearance \quad (209)$$

where the initial and final clearance distances are measured before and after the engagement.

So as to easily design the curve of the displacement (x) in relation to the angle (φ), for $0<\varphi<\Delta\varphi$ and $0<x<\Delta x$, instead of the angle, the proportional projected length of the outer diameter of the shift drum is used:

$$projected\ length = \varphi \frac{shift\ drum\ diameter}{2} \quad (210)$$

The curve designed is wrapped around the shift drum and embossed on its cylindrical surface. The resulting surface is then being offset evenly to both directions.

A Bezier curve was used for designing the gear displacement. For best gear shifting, the gear engagement and disengagement should be performed quickly. Therefore, so as to increase the derivative $dx/d\varphi$, the control points of the Bezier curve are set as close as possible. When the gear change is performed using a single sliding gear, the distance of the control points is limited by a minimum radius on the curve. In the case where two sliding gears are used, an intermediate point halfway through the total angle Δφ is defined. On that point, the previously engaged gear has disengaged and attains a certain clearance distance. The same clearance is attained by the new gear to be engaged. The derivative at the position where the gears are engaged is set to zero, so that no torque is transferred to the shift drum from transverse loads on the gear.

The arrangement of the gears of the original KTM gearbox and the custom gearbox can be seen in figures 36 and 37 respectively. It is evident that the gears utilizing a higher gear ratio, which induces greater loads to the system, are placed close to the ends of the transmission shaft, so as to reduce bending loads on the shaft.

The final positioning is also restricted by the fact that the grooves on the shift drum cannot intersect one another. This defines certain boundaries for the movement of the sliding gears and the size of their adjacent gears. For example, of the three sliding gears in figure 37, the rightmost position of the leftmost one cannot be very close to the leftmost position of the intermediate one. As a result, the leftmost sliding gear -5th gear of the custom gearbox- might have to interfere with the adjacent gear -2nd gear of the custom gearbox. To prevent this, the adjacent gear must have a large root diameter, while the rightmost gear a small tip diameter.

KTM configuration: 2 6 4 3 5 1

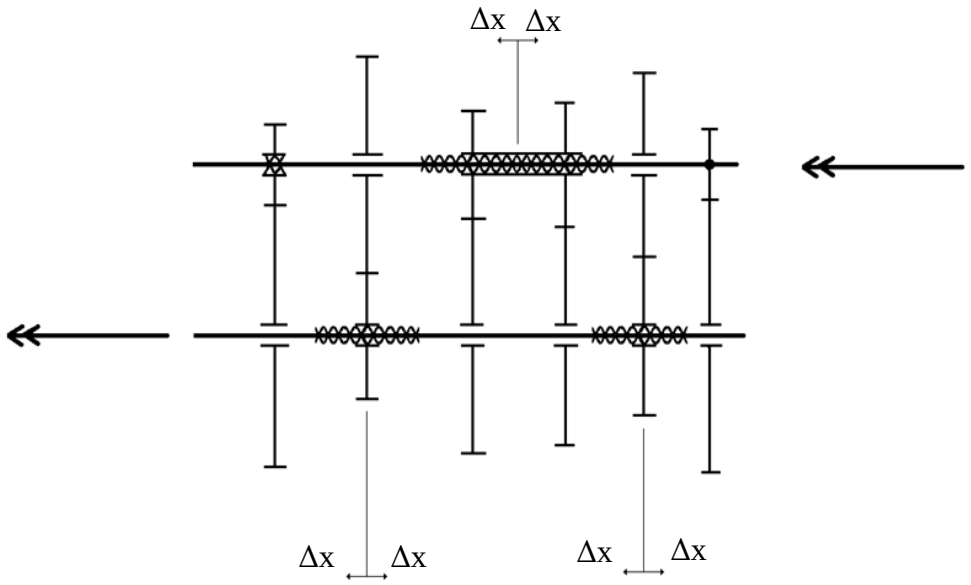

Figure 36: Original KTM gearbox configuration

Custom configuration: 2 5 3 4 1

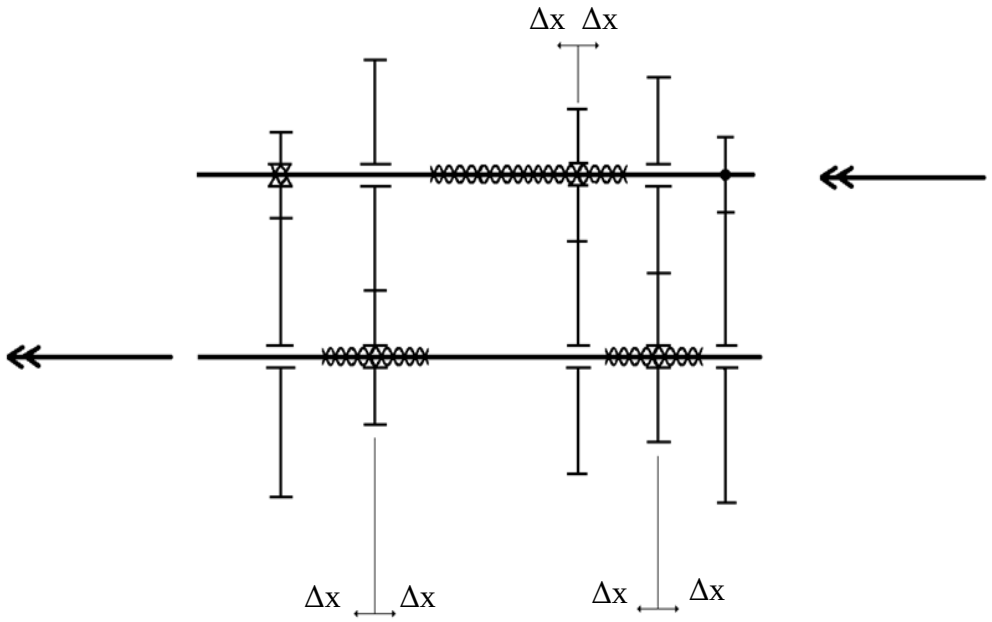

Figure 37: Custom gearbox configuration

7.3 Basic module and gear teeth strength calculations, choice of material

Since no restrictions are imposed to the tooth shape from the manufacturing method, the module of the gearing does not have to attain a specified value. Let 1 and 2 be the gears of the input and output transmission shafts respectively. Considering a zero profile shift coefficient, the module can be calculated as:

$$m = \frac{2a_{12}}{z_1 + z_2} \tag{211}$$

where α_{12} is the distance of the transmission shafts and z_1,z_2 are the number of teeth of gears 1 and 2 respectively.

In fact, if eq. (211) holds, then the profile shift coefficients X_1 and X_2 are not necessarily zero. Instead:

$$X_1 = -X_2 \tag{212}$$

Therefore, the profile shift coefficient is an unconstraint design variable. Other ones include the pressure angle of the gearing and the addendum and dedendum heights, defining the tip and root diameters. Considering that, the following approach is adopted:

- module is set according to eq. (211)
- the pressure angle is chosen to follow the standardized value of 20°
- the addendum and dedendum coefficients are chosen according to the standardized values of 1 and 1.25 respectively
- the profile shift coefficients that follow eq. (212) are determined so as to maximize tooth strength
- the addendum and dedendum coefficients are changed, if the resulting tip and root diameter need to change for spatial reasons in the gearbox design
- the pressure angle is changed, if problems such as undercutting or low contact ratio occur

All the respective calculations are performed with the aid of the KISSsoft gear calculation software [19]. The service life is found according to ISO 6336 method B [20], with incorporation of the graphical method as proposed by Obsieger [21]. The maximum engine output torque and respective speed are used for this calculation. The width of each gear set is determined from this analysis, by requesting a service range of approximately 2500km, estimated for 2 years of complete testing, competing and post-season testing of the racecar, using an additional factor of safety of 1.5. The percentage of usage of each gear over the distance traveled is calculated from the results of the simulation runs performed. The required life time and percentage of usage of each gear set are included in table 17.

Gear number	Usage (over distance) (%)	Required Lifetime (Hrs)
1	1	0,42
2	2	0,52
3	20	4,2
4	55	9,9
5	22	3,1

Table 17: Percentage of usage and required lifetime for each gear set over a range of 2500km

Last but not least, lifetime calculations depend upon the choice of material. An increased surface compression strength as well as an adequate fatigue strength are both necessary for obtaining high gear tooth strength. As mentioned previously, the manufacturing method employed allows for a through hardening of the material. Considering these parameters, a high-strength tool steel is selected.

For acquiring the material properties mentioned, high values of surface hardness should be achieved. However, as hardness increases dramatically, the material becomes brittle and difficult to machine. Accounting for those two factors, the tool steel chosen is the UDDEHOLM CALMAX® [22] tool steel. The stress-strain diagram measured by Brøndsted et al. [23] and illustrated in figure 38 indicates that this tool steel is more ductile than others.

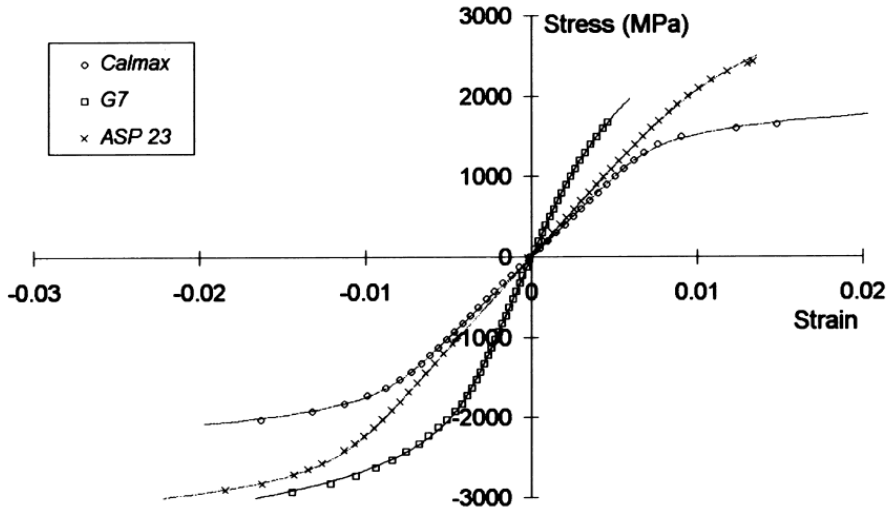

Figure 38: Stress-strain diagram for UDDEHOLM CALMAX® and other tool steels

A summary of the heat treated material mechanical properties, as given by the supplier, can be seen in table 18. It should be noted that the numbers used for the calculation of gear teeth strength are taken according to ISO 6336 figures 5 and 6 for

‘ME’ quality alloyed through hardened wrought steels and the maximum diagram-given surface hardness.

Hardness (HRC)	54-56
Yield strength $R_{p0.2}$ (MPa)	1400
Ultimate tensile strength R_m (MPa)	2100
Elongation at break (%)	4
Yield compressive strength $R_{p0.2}$ (MPa) @56HRC	1900
Ultimate compressive strength R_m (MPa) @56HRC	2300

Table 18: UDDEHOLM CALMAX® material data summary according to supplier

7.4 Finite element analysis

In order to design the main body of the gears, a F.E.A. model was developed in Solidworks [24] for the engaged position of each gear. The compliance of the transmission shafts is excluded from this analysis and replaced with appropriate radial or circumferential displacement constraints. A frictionless contact set is defined between the ‘dogs’ of one gear and the pockets of the respective mating gear.

So as to accurately calculate the contact stress around the gear tooth flank, a contact set combined with a significantly refined mesh should be employed between the teeth of the driving and driven gears. However, this combination would excessively increase the solution time. Therefore, since the contact stress and tooth bending stress have already been examined in KISSsoft, a bonded contact set is utilized in this analysis, so as to allow for a faster design and evaluation cycle, each time a change is performed in the design of the gear.

The resulting stress contour plots are illustrated in figures 39 to 43. In figure 39, only the designed gear that engages the first gear is depicted. Examination of the results reveals that an increased factor of safety is attained compared to the material’s yield strength. This is a result of three factors:

- A minimum gear rim thickness 4mm is used, for avoiding impaired tooth stiffness and stress concentration around the root fillet.
- The length of each internal spline was limited due to the spline strength
- A minimum pocket radius of 4mm is utilized, for easier machining.

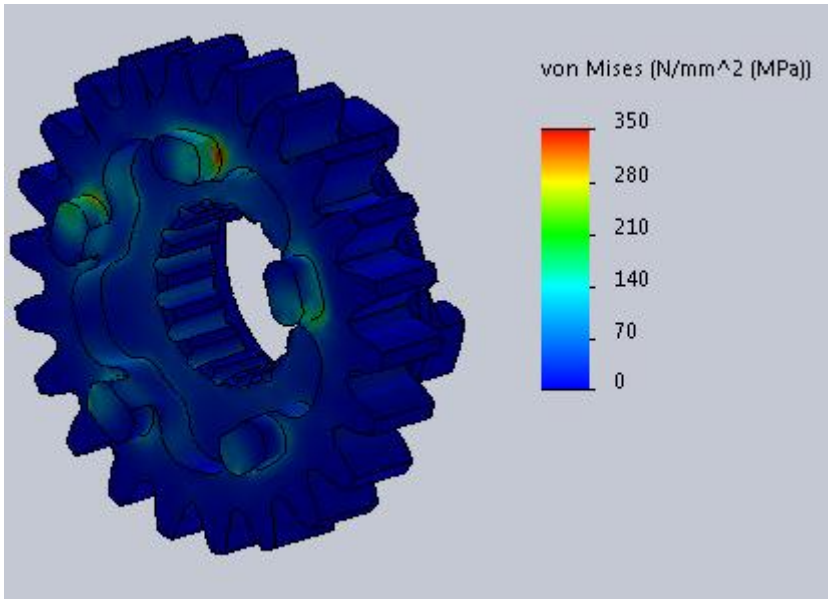

Figure 39: First gear engagement stress contour plot

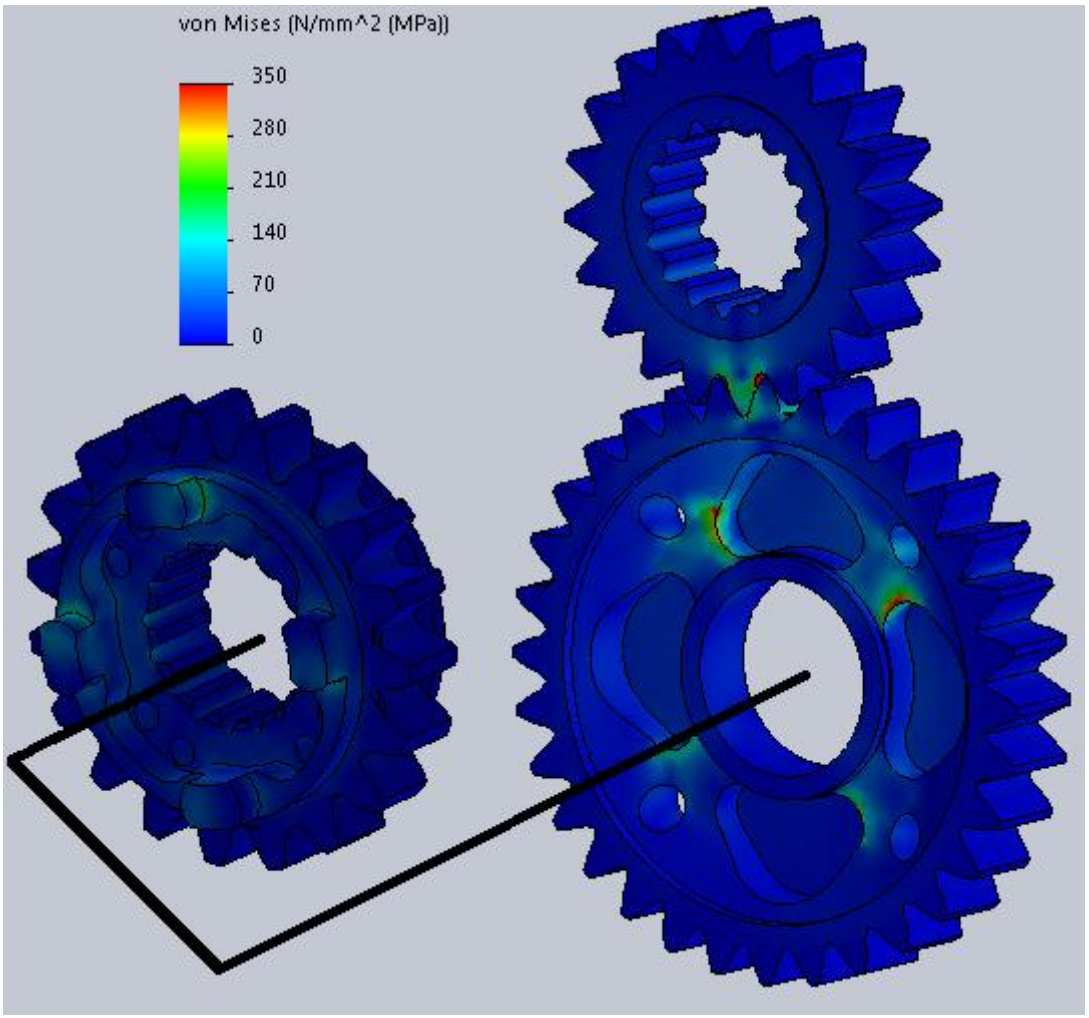

Figure 40: Second gear engagement stress contour plot

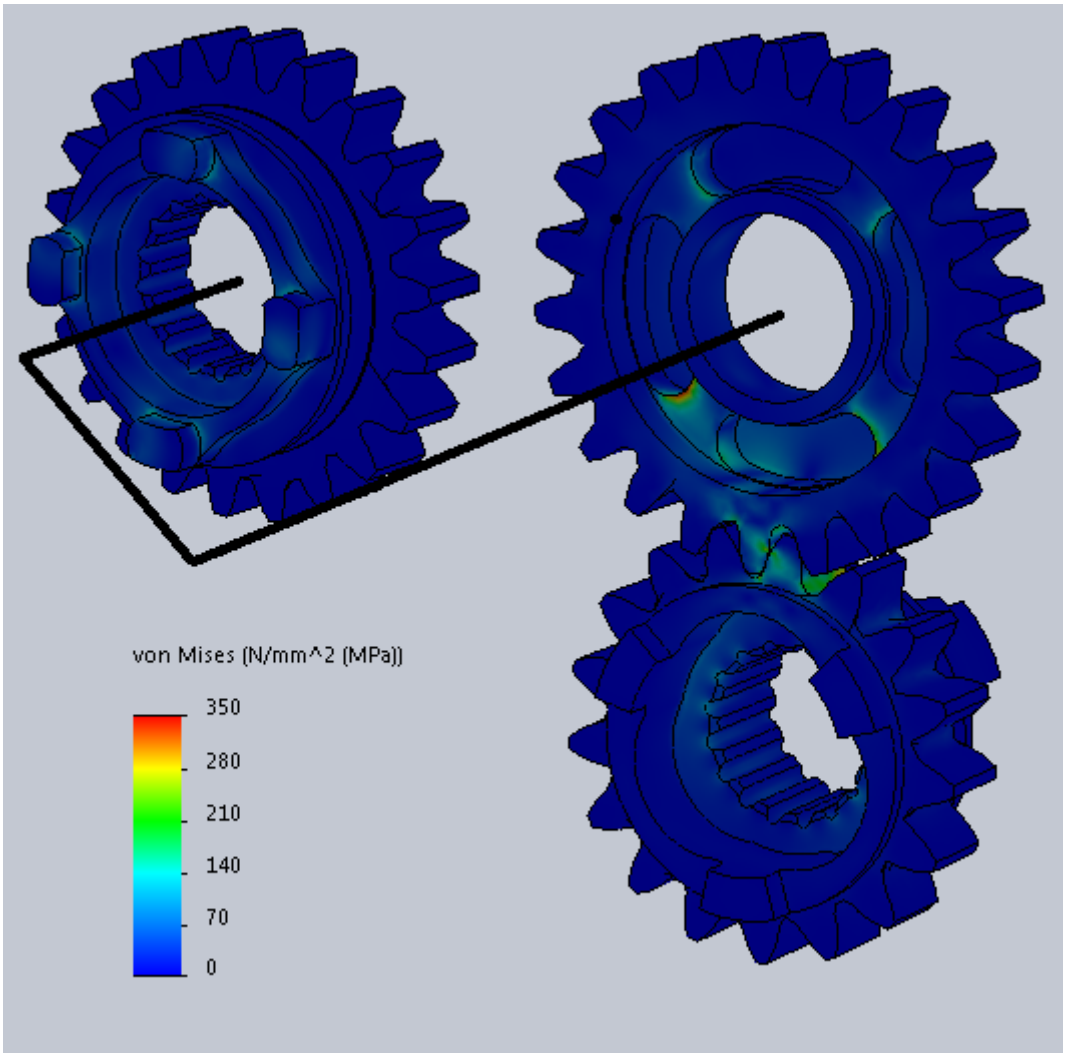

Figure 41: Third gear engagement stress contour plot

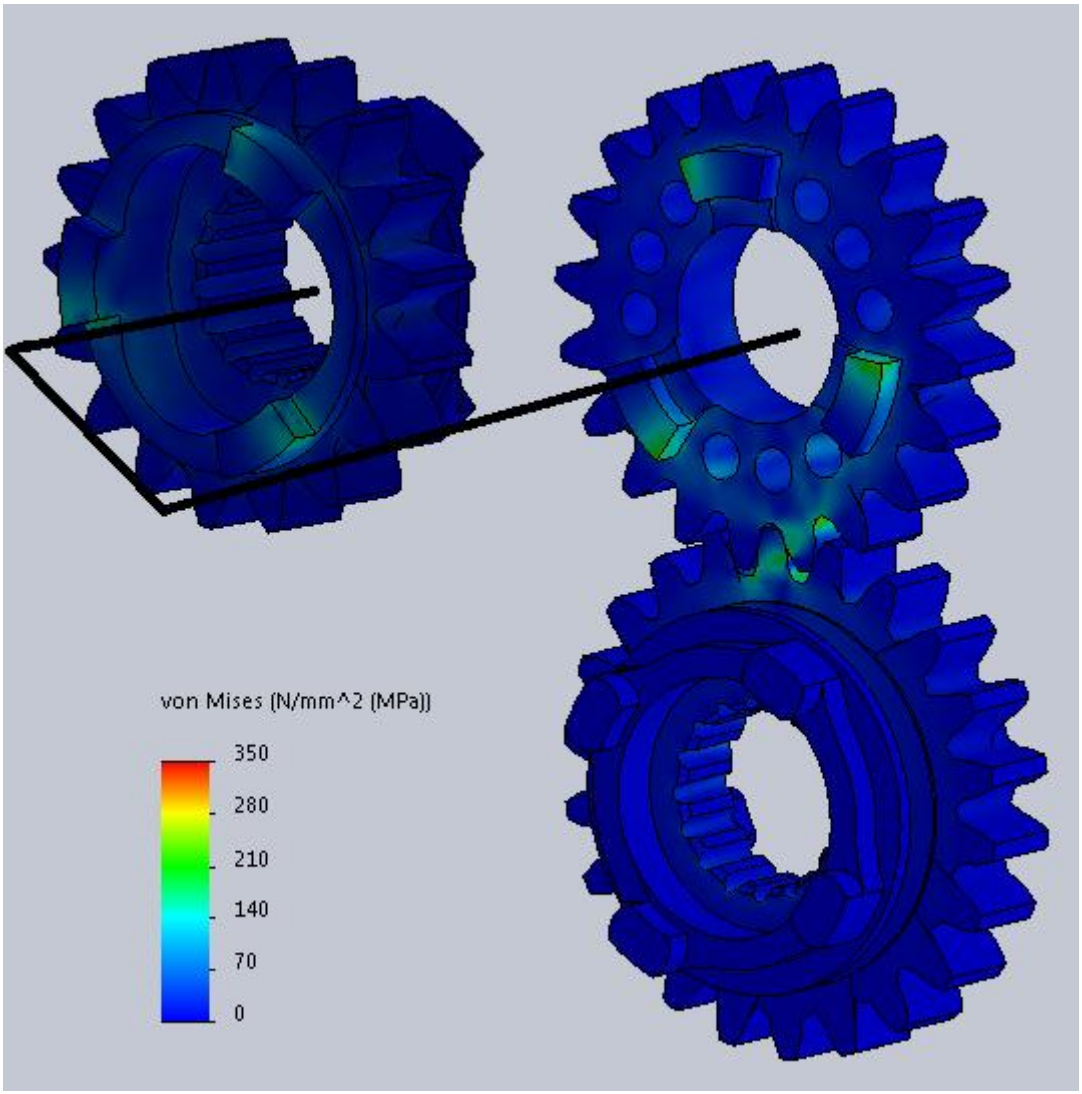

Figure 42: Fourth gear engagement stress contour plot

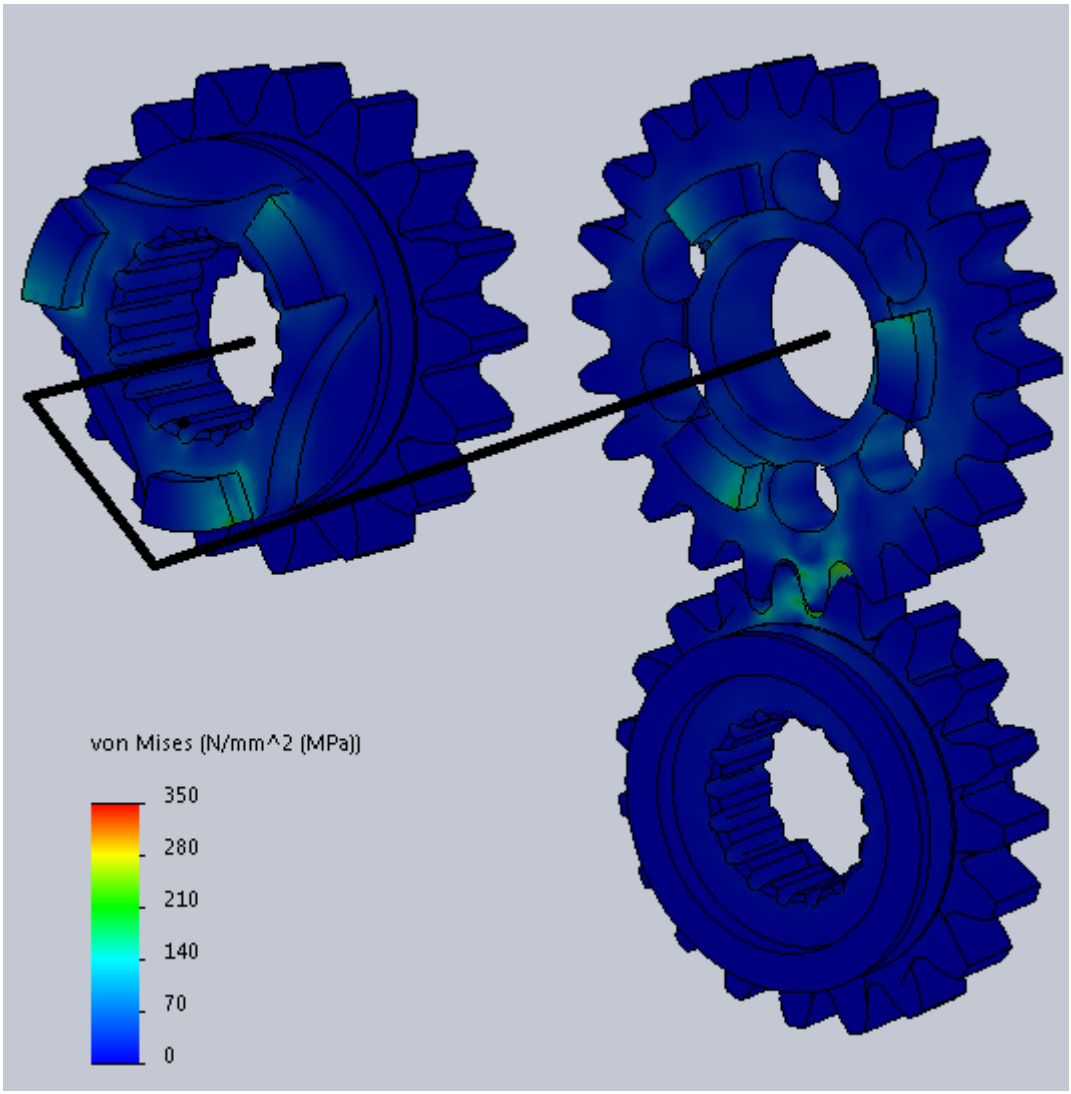

Figure 43: Fifth gear engagement stress contour plot

8. References

[1] Formula Student Rules 2019. (2018, October 07). Retrieved from https://www.formulastudent.de/fsg/rules/

[2] Savaresi, S. M., Ciotti, D., Sofia, M., Rosignoli, E., & Bina, E. (2006). Gear-set optimization of a race car. *11th IFAC Symposium on Control in Transportation Systems, Delft, Netherlands, 39*(12), 579-584. Retrieved from https://doi.org/10.3182/20060829-3-NL-2908.00100

[3] Avgerinos, C. [Αυγερινός, Χ.]. (2013). Μοντελοποίηση και βελτιστοποίηση κιβωτίου ταχυτήτων για χρήση σε μονοθέσιο τύπου Formula Student (Unpublished Diploma thesis). Aristotle university of Thessaloniki, Thessaloniki, Greece.

[4] IPG Automotive. (2017). *CAR MAKER: Tutorial*. Retrieved from https://ipg-automotive.com/fileadmin/user_upload/content/Specials/FormulaCarMaker_Tutorial_2017.pdf

[5] Matlab (Version R2016.a) [Computer software]. (2016). Retrieved from https://www.mathworks.com

[6] Tremlett, A. J., Massaro, M., Purdy, D. J., Velenis, E., Assadian, F., Moore, A. P., & Halley, M. (2015). Optimal control of motorsport differentials. *Vehicle System Dynamics, 53*(12), 1772-1794. Retrieved from http://dx.doi.org/10.1080/00423114.2015.1093150

[7] Criens, C. H. A., Dam, ten, T., Luijten, H. J. C., & Rutjes, T. (2006). Building a MATLAB based Formula Student simulator (DCT rapporten; Vol. 2006.069). Technische Universiteit Eindhoven, Eindhoven, Netherlands.

[8] Singh, C., & Palanivelu, S. (2018). Development of a lap-time simulator for a FSAE race car using multi-body dynamic simulation approach. *International Journal of Mechanical Engineering and Technology, 9*(7), 409-421. Retrieved from http://www.iaeme.com/IJMET/issues.asp?JType=IJMET&VType=9&IType=7

[9] dos Santos, R. D. (2014). Model and dynamic simulation program for vehicle analysis accounting suspension compliance (Unpublished Masters thesis). Instituto Superior Técnico, Lisbon, Potrugal.

[10] Brown, L. (2013). Improving performance using torque vectoring on an electric all-wheel-drive formula SAE race car (Unpublished Bachelor thesis). The University of Western Australia, Perth, Australia.

[11] Harsh, D. (2018) Full vehicle model of a Formula Student car (Unpublished Masters thesis). Delft University of Technology, Delft, Netherlands.

[12] Vilela, D., & Barbosa, R. S. (2011). Analytical models correlation for vehicle dynamic handling properties. *Journal of the Brazilian Society of Mechanical Sciences and Engineering, 33*(4), 438-439. Retrieved from http://dx.doi.org/10.1590/S1678-58782011000400007

[13] Pacejka, H. B. (2002). Semi-empirical tyre models. *Tyre and vehicle dynamics* (2nd ed., pp. 165-172). Retrieved from https://doi.org/10.1016/B978-075066918-4/50004-6

[14] Xiong, Y. (2010). Racing line optimization (Unpublished Masters thesis). Massachusetts Institute of Technology, Cambridge, USA.

[15] Hoffmann, G.M., Tomlin, C., Montemerlo, M., & Thrun, S. (2007). Autonomous automobile trajectory tracking for off-road driving: Controller design, experimental validation and racing. *2007 American Control Conference*, 2296-2301. Retrieved from http://ai.stanford.edu/~gabeh/papers/hoffmann_stanley_control07.pdf

[16] OptimumG. (2018). *OptimumTire: Help file*. Retrieved from http://www.optimumg.com/docs/OptimumTire_Help_File.pdf

[17] Bouquet, J., Hensgen, L., Klink, A., Jacobs, T., Klocke, F., & Lauwers, B. (2014). Fast production of gear prototypes - a comparison of technologies. *6th CIRP International Conference on High Performance Cutting,* 77-82. Retrieved from https://doi.org/10.1016/j.procir.2014.03.066

[18] Ioakimidis, T. [Ιωακειμίδης, Θ.]. (2015). Αποτύπωση σφαλμάτων εξειλιγμένης και εξέλιξη τους κατά τη διαδικασία στίλβωσης με χρήση τεχνικών αντιστρόφου σχεδιασμού σε βαθμίδα τοξοτών κωνικών τροχών (Unpublished Diploma thesis). National Technical University of Athens, Athens, Greece.

[19] KISSsoft (Version 03-2011G) [Computer software]. (2011). Retrieved from https://www.kisssoft.ch

[20] International Organization for Standardization. (2003). Calculation of load capacity of spur and helical gears —Part 5: Strength and quality of materials (ISO Standard No. 6336-5:2003). Retrieved from https://www.iso.org/standard/32503.html

[21] Obsieger, B. (1980). Zahnformfaktoren von Aussen- und Innenverzahnungen bei der Herstellung im Abwaelzverfahren mit Schneidraedern. *Konstruktion, 32*(11). 443-447.

[22] Uddeholm. (2012). *Uddeholm Calmax: Specifications sheet*. Retrieved from https://www.uddeholm.com/files/PB_Uddeholm_calmax_english.pdf

[23] Brøndsted, P., & Skov-Hansen, P. (1997). Fatigue properties of high-strength materials used in cold-forging tools. *International Journal of Fatigue, 20*(5), 373-381. Retrieved from https://doi.org/10.1016/S0142-1123(98)00006-1

[24] Solidworks (Version 2016) [Computer software]. (2016). Retrieved from https://www.solidworks.com/